

ENVIRONMENTAL REGULATION OF CYCLIC DI-GMP TURNOVER IN  
*VIBRIO CHOLERAE*

By

Benjamin J. Koestler

A DISSERTATION

Submitted to  
Michigan State University  
in partial fulfillment of the requirements  
for the degree of

Microbiology and Molecular Genetics - Doctor of Philosophy

2014

## ABSTRACT

### ENVIRONMENTAL REGULATION OF CYCLIC DI-GMP TURNOVER IN *VIBRIO CHOLERAE*

By

Benjamin J. Koestler

3', 5'-cyclic diguanylic acid (c-di-GMP) is an intracellular bacterial second messenger that mediates the transition between a sessile, biofilm forming lifestyle to a motile, virulent lifestyle. Diguanylate cyclase (DGC) enzymes synthesize c-di-GMP, whereas c-di-GMP specific phosphodiesterase (PDE) enzymes hydrolyze the second messenger. Although numerous bacterial behaviors are regulated by c-di-GMP, the regulatory inputs of this system remain mostly undefined.

Here, I examine how the marine bacterium and human pathogen *Vibrio cholerae* utilizes c-di-GMP signaling to interpret and respond to environmental cues. The central hypothesis that underpins my research is that *V. cholerae* senses environmental signals with DGCs and PDEs to modulate c-di-GMP concentrations in different environments. As c-di-GMP is a widely conserved second messenger utilized by many different bacteria, the mechanisms by which *V. cholerae* utilizes c-di-GMP in different environments can be applied to other bacterial systems to further comprehend how they behave in and adapt to various surroundings.

To examine the influence of environmental factors on c-di-GMP synthesis and hydrolysis, I have developed a novel method named The *Ex vivo* Lysate c-di-GMP Assay (TELCA) that systematically measures total DGC and PDE cellular activity.

I have shown that *V. cholerae* grown in different environments exhibits distinct intracellular levels of c-di-GMP, and using TELCA have determined that these differences correspond to changes in both c-di-GMP synthesis and hydrolysis. These findings highlight that modulation of both total DGC and PDE activity alters the intracellular concentration c-di-GMP.

While searching for specific environmental cues that regulate c-di-GMP, I have found that bile acids, a prevalent constituent of the human proximal small intestine, increase intracellular c-di-GMP in *V. cholerae*. This bile-mediated increase in c-di-GMP is quenched by bicarbonate, the intestinal pH buffer secreted by intestinal epithelial cells. These findings lead me to propose that *V. cholerae* senses distinct microenvironments within the small intestine, using bile and bicarbonate as chemical cues, and responds by modulating intracellular c-di-GMP.

In addition to its function as a bacterial second messenger, c-di-GMP has potent immunostimulatory properties in eukaryotes; these properties make c-di-GMP a prime candidate for use as a vaccine adjuvant. Here, I present a novel method of delivering c-di-GMP into eukaryotic cells using adenovirus. I have demonstrated that c-di-GMP can be synthesized *in vivo* by delivering DGC DNA into the cell, and that this c-di-GMP increases the secretion of numerous cytokines and chemokines. This novel adenovirus c-di-GMP delivery system offers a more efficient and cost-effective method to administer c-di-GMP as an adjuvant to stimulate innate immunity.

## ACKNOWLEDGEMENTS

I would like to acknowledge and thank C.M. Waters for providing mentorship and guidance. I would also like to acknowledge T.M. Schmidt, R.A. Britton, and S.H. Shiu for their guidance. I thank E.L. Reynolds and J.P. Massie for assistance in data collection (Chapter 4). I also acknowledge A. Amalfitano for guidance and S.S. Seregin, Y.A. Aldhamen, D.P.W. Rastall, S. Godbehere, J. Collins, and A.M.A. Hunt for assistance in collecting data (Chapter 5). I am grateful for assistance from L. Chen and A.D. Jones from the mass spectrometry facility. I would also like to thank K. Whitehead for providing the mixture for SHB, B.R. Pursley for constructing pBRP2, and C. Chan for constructing pANDA2. I thank S.M. Butler for help proofreading and formatting this dissertation. And finally, I would like to acknowledge the Rudolph Hugh Fellowship, the Russell B. DuVall Scholarship, and the Marvin Hensley Fellowship.

## TABLE OF CONTENTS

LIST OF TABLES.....	viii
LIST OF FIGURES.....	ix
LIST OF ABBREVIATIONS .....	xii
CHAPTER 1 – Background .....	1
The bacterial second messenger cyclic di-GMP .....	1
<i>Vibrio cholerae</i> : marine bacterium and human pathogen.....	3
Innate Immune response to c-di-GMP .....	5
Summary .....	8
CHAPTER 2 - Exploring Environmental Control of Cyclic di-GMP Signaling in <i>Vibrio cholerae</i> by Using the <i>Ex Vivo</i> Lysate Cyclic di-GMP Assay (TELCA).....	10
Preface .....	10
Bacterial strains and growth conditions .....	12
Synthesizing [ <sup>13</sup> C]-c-di-GMP .....	13
Generation of lysates .....	14
Detection and quantification of c-di-GMP.....	15
TELCA quantification of whole cell DGC activity .....	17
TELCA quantification of whole cell PDE activity .....	22
The local environment alters the intracellular concentration of c-di-GMP in <i>V. cholerae</i> .....	23
Growth environments modulate both c-di-GMP synthesis and hydrolysis .....	26
QS controls both total DGC and PDE activity in <i>V. cholerae</i> .....	29
CdgA contributes to the increased DGC activity at low cell density .....	31
Discussion.....	32
CHAPTER 3 – Bile Acids and Bicarbonate Inversely Regulate Intracellular Cyclic di-GMP in <i>Vibrio cholerae</i> .....	37
Preface .....	37
Growth conditions and molecular methods .....	38
Detection and quantification of intracellular c-di-GMP.....	40
Systematic screen of DGC and PDE activity .....	41
Systematic screen of DGC and PDE expression .....	41
Biofilm quantification .....	42
Bile increases the intracellular concentration of c-di-GMP in <i>V. cholerae</i> .....	43

The bile mediated increase of intracellular c-di-GMP is growth-phase dependent .....	44
Three DGCs are more active in the presence of bile .....	45
The activity of PDEs in <i>V. cholerae</i> is not altered by bile .....	48
The three bile-inducible DGCs are inner membrane proteins .....	50
Three DGCs increase c-di-GMP synthesis in the presence of bile acids.....	52
A <i>toxR</i> deletion mutant partially loses bile-mediated c-di-GMP increase ...	53
Transcription of VC1295 is inhibited by bile acids.....	55
Three DGCs and one HD-GYP account for bile-mediated c-di-GMP induction.....	59
Deletion of the bile-responsive DGCs and PDE reduces bile induction of <i>V. cholerae</i> biofilm formation.....	61
Bicarbonate decreases the bile-mediated increase of c-di-GMP in <i>V. cholerae</i> .....	62
Discussion.....	65
Future directions.....	71
CHAPTER 4 – Intracellular c-di-GMP Negatively Correlates with the Growth Rate and Ribosomal RNA of <i>V. cholerae</i> .....	76
Preface .....	76
Measuring growth rate of <i>V. cholerae</i> .....	77
RNA extractions and quantification.....	78
Intracellular c-di-GMP and growth rate of <i>V. cholerae</i> are correlated.....	78
Growth rate inhibition caused by ectopic DGC expression is dose-dependent.....	79
Intracellular c-di-GMP concentration required for growth inhibition varies for different DGCs.....	83
Increased intracellular c-di-GMP reduces the expression of rRNA.....	86
Discussion.....	88
Future directions.....	91
CHAPTER 5 - A novel Adenovirus Adjuvant Stimulates Innate Immunity by <i>in vivo</i> cyclic di-GMP Synthesis .....	95
Preface .....	95
DNA manipulation and virus construction.....	96
HeLa cell transformation.....	97
Animal protocols .....	98
Quantitative PCR.....	99
Cytokine and chemokine quantification .....	100
ELISPOT analysis.....	101
<i>C. difficile</i> challenge .....	101
Generating an adenovirus harboring a <i>V. cholerae</i> DGC .....	102
Synthesis of c-di-GMP in a murine system.....	105

C-di-GMP synthesized <i>in vivo</i> stimulates innate immunity in a mouse model .....	106
C-di-GMP synthesized <i>in vivo</i> lowers the effective antigen dose of Ad5-TA.....	110
Ad5-VCA0956 does not significantly enhance protection of Ad-TA against <i>C. difficile</i> .....	114
Discussion.....	119
Future directions.....	122
CHAPTER 6 – Conclusions .....	124
APPENDICES.....	127
REFERENCES .....	138

## LIST OF TABLES

Table 1	Description of DGC expression strain intracellular c-di-GMP levels and growth inhibition .....	82
Table 2	Cytokine and chemokine secretion of mice infected with Ad5 vectors after 6 hours .....	111
Table 3	Cytokine and chemokine secretion of mice infected with Ad5 vectors after 24h hours .....	112
Table A1	Bacteria strain list .....	128
Table A2	Plasmid list .....	129
Table A3	Primer list .....	134

## LIST OF FIGURES

Figure 1	LC-MS/MS differentiation of [ <sup>12</sup> C]-c-di-GMP and [ <sup>13</sup> C]-c-di-GMP ....	19
Figure 2	TELCA of [ <sup>13</sup> C]-c-di-GMP synthesis of DGC and PDE ectopic expression strains .....	21
Figure 3	TELCA of [ <sup>13</sup> C]-c-di-GMP hydrolysis of DGC and PDE ectopic expression strains .....	23
Figure 4	Growth curves of <i>V. cholerae</i> grown in different media.....	25
Figure 5	Intracellular c-di-GMP concentrations of <i>V. cholerae</i> grown in different media.....	26
Figure 6	TELCA of <i>V. cholerae</i> grown in different media .....	28
Figure 7	TELCA of <i>V. cholerae</i> QS mutants .....	30
Figure 8	Intracellular c-di-GMP concentrations of <i>V. cholerae</i> grown with different bile additives.....	44
Figure 9	Intracellular c-di-GMP concentrations of <i>V. cholerae</i> during the course of growth with bile .....	46
Figure 10	High-throughput screen of the <i>in vivo</i> activity of each of the 40 <i>V. cholerae</i> DGCs with bile .....	48
Figure 11	High-throughput screen of the <i>in vivo</i> activity of each of the 40 <i>V. cholerae</i> PDEs with bile .....	50
Figure 12	The amino acid sequence hydrophobicity and predicted signaling domains of the bile-responsive DGCs .....	51
Figure 13	Intracellular c-di-GMP concentrations of <i>V. cholerae</i> DGC expression strains in the presence and absence of SHB .....	54

Figure 14	Intracellular c-di-GMP concentrations of <i>V. cholerae</i> $\Delta$ <i>toxR</i> and $\Delta$ <i>toxT</i> deletion mutants in the presence of bile.....	55
Figure 15	Relative transcription of DGCs and PDEs in the presence and absence of bile .....	57
Figure 16	Intracellular c-di-GMP concentrations of <i>V. cholerae</i> DGC and PDE mutant strains in the presence and absence of bile .....	60
Figure 17	Biofilm formation of <i>V. cholerae</i> DGC and PDE mutants in the presence of bile.....	63
Figure 18	Intracellular c-di-GMP concentrations of <i>V. cholerae</i> grown in the presence of bile and bicarbonate .....	64
Figure 19	Proposed model of <i>V. cholerae</i> c-di-GMP regulation in the human small intestine .....	70
Figure 20	Linear regression of intracellular c-di-GMP concentrations on growth rates of <i>V. cholerae</i> grown in different media .....	79
Figure 21	Growth rates of <i>V. cholerae</i> DGC expression strains.....	81
Figure 22	Linear regression of intracellular c-di-GMP concentrations on growth rates of <i>V. cholerae</i> DGC expression strains .....	84
Figure 23	Intracellular c-di-GMP concentrations of <i>V. cholerae</i> DGC expression strains .....	86
Figure 24	Growth rates of <i>V. cholerae</i> DGC expression strains.....	87
Figure 25	Relative rRNA abundance of <i>V. cholerae</i> DGC expression strains ..	89
Figure 26	C-di-GMP synthesized <i>in vivo</i> by VCA0956 in HeLa cells.....	104
Figure 27	Infection of Ad5-VCA0956 in a murine model system .....	107
Figure 28	qRT-PCR of mouse liver gene transcripts 24 hours after infection with Ad5 vectors.....	109

Figure 29	IFN $\gamma$ ELISPOT analysis of mice vaccinated with Ad5-TA and Ad5 vectors .....	115
Figure 30	<i>C. difficile</i> challenge of BALB/c mice .....	116
Figure 31	<i>C. difficile</i> challenge of BALB/c mice vaccinated with Ad5-TA and Ad5-VCA0956.....	118

## LIST OF ABBREVIATIONS

Ad5 .....	Adenovirus type 5-derived
AI .....	Quorum sensing autoinducer
<i>Bd</i> .....	Below detection
BiC .....	Sodium bicarbonate
BV .....	Bovine bile
CDAD .....	<i>C. difficile</i> associated diarrhea
c-di-AMP .....	Cyclic dimeric adenosine 3',5'-monophosphate
c-di-GMP .....	Cyclic dimeric guanosine 3',5'-monophosphate
cfu .....	Colony forming unit
CHAPS .....	3-[(3-Cholamidopropyl)dimethylammonio]-1-propanesulfonate
CV .....	Crystal violet
CT .....	Cholera enterotoxin
DGC .....	Diguanylate cyclase enzyme
GTP .....	Guanosine-5' triphosphate
h.p.i. ....	Hours post injection
IM .....	Intramuscular
IPTG .....	Isopropyl $\beta$ -D1-thiogalactopyranoside
IV .....	Intravenously
LB .....	Luria-Bertani media
LC-MS/MS .....	Liquid chromatography coupled with tandem mass spectrometry

M.O.I.....	Multiplicity of infection
<i>m/z</i> .....	Mass to charge ratio
OD.....	Optical density
ORF .....	Open reading frame
PBS.....	Phosphate buffered saline
PDE .....	Phosphodiesterase enzyme
ppGpp .....	Guanosine 3',5'-bispyrophosphate
pppGpp .....	Guanosine 3'-diphosphate, 5'-triphosphate
QS.....	Quorum sensing
R.L.U .....	Relative luminescence units
rRNA .....	Ribosomal RNA
SDS.....	Sodium dodecyl sulfate
SFCs .....	Spot forming cells
SHB .....	Synthetic human bile
TELCA.....	The <i>Ex vivo</i> Lysate c-di-GMP Assay
TCP.....	Toxin co-regulated pilus
TLR.....	Toll-like receptor
Tris .....	2-Amino-2-hydroxymethyl-propane-1,3-diol
Vp .....	Viral particles
WT .....	Wild type

## CHAPTER 1 – Background

### *The bacterial second messenger cyclic di-GMP*

Nucleotide small molecules are utilized by organisms from across the tree of life to relay signals from sensor proteins to target receptor proteins within the cell; known bacterial second messengers include cyclic adenosine 3',5'- monophosphate (cAMP), cyclic guanosine 3',5'-monophosphate (cGMP), guanosine 3',5'-bispyrophosphate (ppGpp), guanosine 3'-diphosphate, 5'-triphosphate (pppGpp), cyclic dimeric adenosine 3',5'-monophosphate (c-di-AMP), and cyclic dimeric guanosine 3',5'-monophosphate (c-di-GMP). C-di-GMP was first discovered in 1985 by Benzimen *et al.* [1], and since has been predicted to be utilized in >75% of all bacteria in representatives from every major bacterial phyla [2].

Diguanylate cyclase enzymes (DGCs) synthesize c-di-GMP from two GTP molecules. These enzymes contain a conserved C-terminal GGDEF domain with a GG[D/E]EF active site motif and a highly variable N-terminus that often encodes conserved signal recognition domains such as GAF, PAS, or receiver domains [3-6]. Conversely, c-di-GMP specific phosphodiesterase enzymes (PDEs) hydrolyze c-di-GMP and contain either a conserved C-terminal EAL or HD-GYP domain [7, 8]. Similar to DGCs, PDE domains are often linked to N-terminal signal recognition domains.

C-di-GMP regulates numerous phenotypes in different bacteria (for a comprehensive review of c-di-GMP controlled phenotypes, please refer to Romling *et*

*al.* [9]). Motility, the ability of a bacterial cell to move, has been shown to be negatively regulated by c-di-GMP in many organisms [10-13]. Conversely, biofilm formation, the bacterial behavior where cells excrete exopolysaccharides to form a three-dimensional surface-associated community [14], is positively regulated by c-di-GMP. Biofilm-forming communities have been shown to play important roles in environmental persistence and virulence [15]. C-di-GMP has been shown to positively regulate biofilm formation in several pathogens including *Pseudomonas aeruginosa* [11], *Salmonella enterica* [11], and *Vibrio cholerae* [16]. The differential regulation of motility and biofilm formation by c-di-GMP indicates that c-di-GMP mediates the transition between sessile and motile, virulent lifestyles.

A characteristic feature of c-di-GMP signaling networks is the relatively large number of DGCs and PDEs encoded in individual bacterial genomes that theoretically contribute to changes in the intracellular concentration of c-di-GMP. For example, the bacteria *V. cholerae* encodes 61 distinct proteins predicted to modulate c-di-GMP [17]. Because of this complexity, c-di-GMP signaling systems are typically redundant, and it is challenging to understand on a systems level how the concentration of c-di-GMP is controlled. Changes in c-di-GMP could be mediated by modulation of total DGC activity, PDE activity, or both. It is not well understood why some bacteria encode so many DGCs and PDEs, and the functions of the variable N-terminal domains for most of these enzymes have not been characterized. One hypothesis is that each DGC or PDE senses and responds to a

specific environmental signal by altering c-di-GMP synthesis or degradation activity in the C-terminal domain.

A handful of environmental cues have been shown to influence intracellular c-di-GMP in various bacteria. For example, specific environmental signals that interact with DGCs and PDEs have been identified such as zinc in *E. coli* [18], amino acids in *P. aeruginosa* [19], nitric oxide in *Legionella pneumophila* [20], and norspermidine in *V. cholerae* [21]. Additionally, a DGC from *Bordetella pertussis* and a DGC/PDE complex from *E. coli* bind oxygen to alter c-di-GMP turnover [22, 23]. There is also evidence that phototrophic bacteria utilize c-di-GMP to modulate intracellular c-di-GMP in different light conditions [24, 25]. DGCs and PDEs have also been identified in *Xanthomonas campestris* and *Vibrio parahaemolyticus* that bind molecules associated with quorum sensing networks to modulate c-di-GMP turnover [8, 26, 27]. However, these enzymes with known ligands represent only a small fraction of the known DGCs and PDEs, and the environmental signals recognized by the vast majority of DGCs and PDEs remain unidentified.

#### *Vibrio cholerae: marine bacterium and human pathogen*

One bacterium in which c-di-GMP signaling has been studied is *V. cholerae*. *V. cholerae*, a gram-negative marine bacterium, is the causative agent of the human diarrheal disease cholera. In aquatic environments, *V. cholerae* favors a sessile lifestyle by preferentially forming biofilms on chitinous surfaces [28-30]. Upon ingestion into a human host, *V. cholerae* expresses virulence and colonization

factors that lead to severe diarrhea, subsequently reseeding the bacteria back into the environment. The pathogenesis of *V. cholerae* is dependent on two virulence factors, cholera enterotoxin (CT) and the toxin c-regulated pilus (TCP) [31]. The expression of both CT and TCP is controlled by the transcriptional regulators ToxR/S, which coordinate with the transcriptional regulator ToxT to optimize virulence expression in the human host [32, 33].

The transition of *V. cholerae* between aquatic environments and the human host is mediated by c-di-GMP, which regulates biofilm formation, motility, and virulence gene expression [16, 34-36]. It has been proposed that the intracellular c-di-GMP concentration in *V. cholerae* is relatively high in aquatic environments leading to a sessile biofilm forming lifestyle, whereas in the human host, reduced c-di-GMP concentrations stimulate virulence factor expression [34]. Due to the technical limitations of measuring intracellular c-di-GMP, this model has not been directly tested, and the specific environmental cues that regulate the transition between these two niches remain unknown.

Upon entering the human host, it is imperative that *V. cholerae* recognizes environmental signals to mediate the transition from an aquatic bacterium to a human pathogen. One signal prevalent in the small intestine is bile. Bile is an antimicrobial substance secreted from the liver into the proximal small intestine that aids in digestion by emulsifying lipids. The composition of secreted bile is heterogeneous and includes inorganic salts, cholesterol, phospholipids, pigments, and bile acids [37]. Bile acids are derived from cholesterol in the liver and are

processed by hepatic cells to produce a mixture dominated by taurine and glycine conjugates [37, 38]. Bile acids have detergent properties that enable the interaction between bile and digestive lipids. For a complete review on the properties of bile, refer to Begley *et al.* [39].

The interplay between enteric bacteria and bile is extensive. In bacteria, there is evidence that bile causes oxidative stress, DNA damage, and perturbs the cell membrane [40-42]. To counteract this stress, *V. cholerae* upregulates the porin protein *ompU* in a *toxR*-dependent manner to increase bile resistance [43]. *V. cholerae* also employs six resistance-nodulation-division family efflux pumps that have been implicated in bile resistance [44-46]. Additionally, *V. cholerae* increases biofilm formation in a *vpsR* dependent manner in the presence of bile acids, presumably to increase resistance to the deleterious effects of bile [47]. It is clear that the sensing of bile by *V. cholerae* leads to distinct physiological changes, but a connection between bile and c-di-GMP has not been described in *V. cholerae* or any other bacterium.

#### *Innate Immune response to c-di-GMP*

In addition to its role regulatory role as a bacterial second messenger, c-di-GMP is a potent stimulator of innate immunity in eukaryotic organisms. Presumably, as c-di-GMP is an intracellular second messenger unique to bacteria, it is recognized by eukaryotic organisms as a signal of bacterial invasion. This stimulation of innate immunity occurs at least in part through the eukaryotic

protein STING, which senses pathogen derived nucleic acids in the cytoplasm and subsequently activates a signaling cascade to stimulate a type-I interferon response [48, 49]. Studies show that the presence of c-di-GMP can trigger the production of IL-2, IL-4, IL-5, IL-6, IL-8, IL-12p40, IL-17, IP-10, TNF- $\alpha$ , KC, MIP-1 $\alpha$ , MIP-1 $\beta$ , MIP-2, MCP-1, RANTES, IFN- $\beta$ , IFN- $\gamma$ , stimulate the NLRP3 inflammasome pathway, and promote the recruitment and activation of macrophages, NK-cells,  $\alpha\beta$  conventional T-cells, and enhance DC maturation [49-57]. Furthermore, *in vivo* studies have shown that co-administration of purified c-di-GMP with an antigen confers increased protection of animals in several different murine challenge models, including those utilizing *Staphylococcus aureus*, *Klebsiella pneumoniae*, and *Streptococcus pneumoniae* [53-55, 58].

Because c-di-GMP activates a robust immune response, there has been ongoing focus on using c-di-GMP as an adjuvant to improve vaccine efficacy [59]. Adjuvants are compounds administered alongside vaccine antigens for the purpose of enhancing the longevity, potency, or reducing the effective dose of the antigen without introducing toxic side effects. This is accomplished by stimulating the innate arm of the immune system, resulting in increased cytokine and chemokine production and upregulation of proinflammatory genes [60], which then enhances antigen recognition and response [61]. The development of novel adjuvants may be critical to the success of vaccines targeting diseases for which vaccinations have previously failed such as *Clostridium difficile*, human immunodeficiency virus, malaria, and cancer. Despite the demand, currently there are few adjuvants

approved for human use. The most commonly used adjuvants are aluminum-salt (Alum)-based; however, these adjuvants suffer drawbacks including local reactions to administration, inadequate T-cell responses, allergic IgE-type responses, and are ineffective with specific types of antigens [62]. Other less-commonly utilized adjuvants include oil and water emulsions, lipopolysaccharide derivatives, self-assembling viral nanoparticles, and cholera toxin B subunit [62]. While each adjuvant offers different advantages and disadvantages, there is a large demand for novel adjuvants that can be paired with and improve vaccine antigens. Because c-di-GMP has effective immunostimulatory properties, it makes an ideal candidate for a novel adjuvant [59].

Despite the properties that make c-di-GMP a promising adjuvant, there are currently practical limitations to using c-di-GMP as a vaccine adjuvant. The studies examining the adjuvant properties of c-di-GMP utilized mucosal, intramuscular (IM), or systemic administration of chemically synthesized c-di-GMP [53-55, 58]. While this method has been shown to effectively activate innate immunity, it lacks efficiency and the mechanism by which c-di-GMP enters the cytoplasm of cells to stimulate STING is unknown. Furthermore, chemical synthesis of pharmaceutical grade c-di-GMP in large quantities is currently cost prohibitive. There is a need for an efficient and cost effective method of delivering c-di-GMP *in vivo* for use as an adjuvant.

## *Summary*

The broad goal of this study is to understand how the model bacterium *V. cholerae* uses c-di-GMP signaling to interpret and respond to changing environmental signals. The central hypothesis that underlies my research is that *V. cholerae* senses environmental signals with different DGC and PDE proteins to modulate c-di-GMP concentrations in different environments. The rationale for this study is that c-di-GMP is a conserved second messenger utilized by a broad spectrum of bacteria, and the mechanisms by which *V. cholerae* utilizes c-di-GMP signaling in different environments can be applied to other bacterial systems to further comprehend how they similarly respond and adapt to their environments. Furthermore, as c-di-GMP has potent immunostimulatory properties, knowledge of this signaling system can be appropriated to develop new applications for clinical settings.

To show that a changing environment impacts c-di-GMP signaling globally, I have demonstrated that intracellular c-di-GMP concentrations of *V. cholerae* vary when *V. cholerae* is grown in different environments. I developed The Ex Vivo Lysate Cyclic di-GMP Assay (TELCA) to examine total cellular DGC and PDE activity, and used TELCA to show that these variations of c-di-GMP concentrations in different environments are due to changes in both c-di-GMP synthesis and hydrolysis. Using TELCA, I was also able to show that quorum sensing regulation of c-di-GMP levels in *V. cholerae* is due primarily to decreased DGC activity during transitions from low- to high-cell-density.

I have also begun to explore specific environmental cues that modulate c-di-GMP in *V. cholerae*, and I have shown that bile acids increase intracellular c-di-GMP in *V. cholerae*. I determined that this increase is due to multiple factors including altered c-di-GMP synthesis activity of three DGCs and reduced expression of one PDE. Additionally, this bile-mediated increase in intracellular c-di-GMP is quenched by bicarbonate, another common component of the human digestive tract.

Finally, I have applied the knowledge I have gained regarding active DGCs of *V. cholerae* to develop a novel adenovirus adjuvant that delivers DGC DNA into eukaryotic cells, resulting in c-di-GMP synthesis *in vivo* and a robust innate immune response. Additionally, this adenovirus construct harboring a DGC gene is able to reduce the effective dose of a *C. difficile* vaccine antigen to stimulate IFN $\gamma$  production of splenocytes. This novel method of *in vivo* c-di-GMP synthesis offers a more efficient and cost-effective alternative to using c-di-GMP as a vaccine adjuvant.

## CHAPTER 2 - Exploring Environmental Control of Cyclic di-GMP Signaling in *Vibrio cholerae* by Using the *Ex Vivo* Lysate Cyclic di-GMP Assay (TELCA)

### *Preface*

Quorum sensing (QS), the process of bacterial cell-cell communication mediated by AIs that are constitutively secreted and accumulate with cell density, is a fundamental chemical signaling system in bacteria. Sensing of AIs by bacteria provides information on the local population density and composition to appropriately regulate bacterial behaviors such as competence, biofilm formation, and virulence [63-68]. In *V. cholerae*, QS is mediated by two AI molecules (CAI-1 and AI-2) that are produced in tandem [67]. In the low-cell-density state, AI concentrations are low and their cognate receptors function as kinases ultimately leading to phosphorylation of the response regulator LuxO. Phosphorylated LuxO upregulates the transcription of four small regulatory RNAs, which subsequently suppress translation of the master QS regulator HapR [69, 70]. When the concentration of AIs increase, they bind the AI receptors switching them to phosphatases, leading to dephosphorylation of LuxO, deactivation of the sRNAs, and induction of HapR expression [71]. In *V. cholerae*, biofilm formation is repressed in the high-cell-density QS state via direct repression of extracellular polysaccharide synthesis genes by HapR [66, 72].

Both the QS and c-di-GMP signaling systems are inextricably linked in *V. cholerae* [73]. At low cell density, the intracellular c-di-GMP concentration of *V.*

*cholerae* is relatively high, promoting biofilm formation and inhibiting motility. Upon transition to the high-cell-density state the intracellular c-di-GMP concentration is suppressed, decreasing biofilm formation [66, 72]. In *V. cholerae* the transcription of 18 of the 61 predicted c-di-GMP turnover enzymes are differentially regulated at low and high cell density [66, 72, 74]. However, because of the complexity of this signaling system it remains unclear if the QS-mediated changes in c-di-GMP levels in *V. cholerae* are being driven by changes in c-di-GMP synthesis, hydrolysis or both.

To further the exploration of the environmental modulation of c-di-GMP and the regulatory connections between QS, c-di-GMP, and biofilm formation in *V. cholerae*, I have developed a novel approach, hereby named **The *Ex vivo* Lysate c-di-GMP Assay (TELCA)**, which enables the quantification of c-di-GMP synthesis and hydrolysis of a whole-cell lysate. I have shown that growing *V. cholerae* in divergent environments can lead to a 20-fold difference in the intracellular concentration of c-di-GMP, and these distinct c-di-GMP concentrations can be attributed to both changes in c-di-GMP synthesis and hydrolysis. I also used TELCA to show that alteration of both c-di-GMP synthesis and hydrolysis between the low- and high-cell density QS states contributes to the QS-mediated change of intracellular c-di-GMP. I further show that deletion of the DGC CdgA, which is transcriptionally regulated by HapR and has been predicted to be a key DGC in the induction of biofilm formation [72, 74-76], significantly reduces the elevated DGC activity associated with low cell density, highlighting the sensitivity of TELCA. TELCA provides a new

method to study complex c-di-GMP signaling networks from a systems perspective. The findings of this chapter have been published in the Journal of Applied and Environmental Microbiology [77].

### *Bacterial strains and growth conditions*

The *V. cholerae* El Tor biotype strain C6706str2 was used for all experiments [78]. All strains, plasmids, and primers used are listed in Tables A1-3. The construction of the expression plasmids for VCA0956 and VC1086 are described elsewhere [72, 79]. Unless otherwise specified, cultures were grown in Luria-Bertani media (LB, 1.0% tryptone, 0.5% yeast extract, 1.0% NaCl, Accumedica) at 35°C with shaking at 220 rpm. MOPS media was purchased from Teknova and prepared as per manufacturer's instruction. The composition of AKI, AB, ASW, and M9 media are described elsewhere [80-83]. MOPS, AB, and M9 were supplemented with glucose as a carbon source (0.2% for MOPS and AB, 0.4% for M9). For experiments involving the expression of DGCs or PDEs from plasmids, media was supplemented with kanamycin (Sigma) at 100 µg/mL and the inducer isopropyl β-D1-thiogalactopyranoside (IPTG) at 0.1 mM.

The construction of the  $\Delta hapR$  and  $\Delta luxO$  strains has been described previously [67, 68]. To generate the  $\Delta cdgA$  strain, natural transformation and homologous recombination were used. Briefly, Phusion DNA polymerase (NEB) was used to amplify approximately 500 bp upstream and downstream of *cdgA* (VCA0074) using the primers VCA0047KO-1 (upstream) and VCA0047KO-2

(downstream), and VCA0047KO-3 (upstream) and VCA0047KO-4 (downstream) (Table A3). Fusion PCR was then used to join these products upstream and downstream of a chloramphenicol resistance cassette (*cat*) bordered by FLP recombination target (FRT) sites from the plasmid pKD3 [84]. This DNA was introduced to *V. cholerae* by inducing natural transformation using a modified protocol from Marvig and Blokesch [85]. *V. cholerae* was grown on chitin flakes in modified M9 media [82]. This media (M9-T) contained the standard concentration of M9 salts supplemented with 5 mM CaCl<sub>2</sub>, 3.6 mM MgSO<sub>4</sub>, and 4.5 mM *N*-acetyl-D-glucosamine as a carbon source and was balanced to a pH of 6.0. Concentrated DNA was introduced to the culture, and homologous recombination events were selected by growing the culture on LB supplemented with 1 µg/mL chloramphenicol. The *cat* gene was excised by ectopically expressing the FLP recombinase from the vector pTL17 [86].

### *Synthesizing [<sup>13</sup>C]-c-di-GMP*

[<sup>13</sup>C]-c-di-GMP was synthesized from guanosine-[<sup>13</sup>C]-5' triphosphate ([<sup>13</sup>C]-GTP, Sigma) using the purified DGC WspR-R242A as previously described [87]. The reaction consisted of 56 µM WspR-R424A, 20 µM [<sup>13</sup>C]-GTP, 24 mM Tris-Cl, 5 mM MgCl<sub>2</sub>, 45 mM NaCl, and EnzCheck Phosphate Assay Kit reaction buffer mix (Invitrogen) at a total volume of 100 µL, hypothetically yielding 10 µM [<sup>13</sup>C]-c-di-GMP (two GTP molecules per molecule c-di-GMP). The reaction was run overnight followed by treatment for 30 minutes at 37°C with Antarctic phosphatase (NEB) in its corresponding reaction buffer to remove any excess [<sup>13</sup>C]-GTP. The reaction was

heated at 100°C for 10 minutes to inactivate the Antarctic phosphatase and precipitate protein. After cooling to room temperature, the reaction was centrifuged at max speed for 10 minutes to remove the precipitated protein, and the supernatants were removed and stored at -20°C until use. [<sup>13</sup>C]-c-di-GMP synthesis was confirmed using liquid chromatography with mass spectrometry as described below.

### *Generation of lysates*

Cell lysates for TELCA were generated by inoculating overnight cultures of *V. cholerae* 1:1000 into 30 mL of the specified media with the appropriate antibiotics or inducer. Cultures grown to the desired OD<sub>600</sub> as indicated were centrifuged at 7800 rpm to pellet the cells. The pellets were then resuspended in 15 mL TELCA reaction buffer, which consisted of 25 mM Tris, 5 mM MgCl<sub>2</sub>, and 5 mM NaCl balanced to a pH of 7.5. The cultures were then processed three times using a M110-P processor (Microfluidics) at 20,000 psi producing a clear lysate. A protein assay (Bio-Rad) was performed according to the manufacturer's instructions to quantify the total protein content, and each lysate was diluted to 0.1 mg/mL in TELCA reaction buffer. To measure c-di-GMP synthesis, 100 mM [<sup>13</sup>C]-GTP stock was added to a final concentration of 1 mM (10 μL [<sup>13</sup>C]-GTP stock in 990 μL lysate diluent for timecourse experiments, 1 μL [<sup>13</sup>C]-GTP stock in 99 μL lysate diluent for endpoint experiments). To measure c-di-GMP hydrolysis, 10 μM [<sup>13</sup>C]-c-di-GMP stock was added to a final concentration of 100 nM (10 μL [<sup>13</sup>C]-c-di-GMP stock in 990 μL lysate diluent for timecourse experiments, 1 μL [<sup>13</sup>C]-c-di-GMP stock in 99

$\mu\text{L}$  lysate diluent for endpoint experiments). The concentrations are within the physiological ranges of the natural concentrations of GTP and c-di-GMP found in a bacterial cell [79, 88]. The reactions were then mixed and incubated at 37°C until the experimental endpoint, and then the reaction was stopped by mixing 100  $\mu\text{L}$  reaction to 100  $\mu\text{L}$  of phenol:chloroform:isoamyl alcohol (25:24:1). The mixture was centrifuged at max speed for 5 minutes, and then the aqueous phase was removed and stored at -80°C until analysis.

#### *Detection and quantification of c-di-GMP*

For the quantification of intracellular c-di-GMP, overnight cultures grown in the corresponding media were used to inoculate 2 mL cultures (1:1000). Cultures were grown to the appropriate OD<sub>600</sub> (OD<sub>600</sub>, AKI: 0.5-1.0; LB: 0.5-0.8; ASW: 0.2-0.4; MOPS: 0.4-0.8; AB: 0.3-0.7; M9: 0.2-0.4), and a 1.5 mL aliquot of culture was centrifuged at maximum speed for 30 seconds. The supernatant was removed, and the pellet was resuspended in 100  $\mu\text{L}$  of cold extraction buffer (40% acetonitrile/40% methanol/0.1 N formic acid). The slurry was incubated at -20° C for 20 minutes, and then the insoluble fraction was pelleted by centrifugation for 10 minutes at maximum speed. The supernatant was collected and stored at -80°C. Prior to analysis, the extraction buffer was evaporated using a vacuum manifold, and the pellet was resuspended in 100  $\mu\text{L}$  water. [<sup>12</sup>C]-c-di-GMP and [<sup>13</sup>C]-c-di-GMP was quantified using an Acquity Ultra Performance liquid chromatography system (Waters) coupled with a Quattro Premier XE mass spectrometer (Waters) as previously described [79]. Chromatographic separation of 10  $\mu\text{L}$  sample was

accomplished using reverse phase separation on a Waters BEH C18 2.1 x 50 mm column and a flow rate of 0.3 mL/minute, using the following gradient: solvent A (10 mM tributylamine and 15 mM acetic acid in 97:3 water:methanol) to solvent B (methanol), 0 minutes; A=99%:B=1%, 2.5 minutes; A=80%:B=20%, 7.0 minutes; A=35%:B=65%, 7.5 minutes; A=5%:B=95%, 9.01 minutes; 99%:B=1%, 10 minutes; gradient ends.

After separation, the detection of c-di-GMP was carried out using electrospray ionization with multiple reaction monitoring in negative ion mode where [<sup>13</sup>C]-c-di-GMP was detected with a *m/z* of 709.16 → 354.31 and [<sup>12</sup>C]-c-di-GMP with a *m/z* of 689.16 → 344.31. The MS detection was optimized using the following parameters: capillary voltage, 3.5 KV; cone voltage, 50 V; collision energy, 34 V; source temperature, 120°C; desolvation temperature, 350°C; cone gas flow, 50 L/h (nitrogen), 800 L/h; collision gas flow (nitrogen), 0.15 mL/min; and multiplier voltage, 650 V. The concentration of c-di-GMP was determined by generating an 8-point standard curve (1:2 dilutions) of chemically synthesized c-di-GMP (Biolog) ranging from 1.9 nM to 250 nM. The intracellular c-di-GMP concentration was calculated by dividing the c-di-GMP concentration of the sample by the total intracellular volume of bacteria extracted. This was estimated by multiplying the average cell volume of the bacterial cell, determined by measuring individual cell dimensions using differential image contrast microscopy, and the number of bacterial cells in the extract.

### *TELCA quantification of whole cell DGC activity*

I sought to develop a systems approach to examine if changes in the levels of c-di-GMP in *V. cholerae* could be attributed to the modulation of net DGC and/or PDE activity. The rationale for developing this method is that current approaches to directly measure c-di-GMP primarily utilize liquid chromatography coupled with tandem mass spectrometry (LC-MS/MS) of cell extracts [89-91] or an *in vivo* FRET biosensor to quantify c-di-GMP at the single cell level [92]. While these methods allow accurate quantification of the average intracellular c-di-GMP in the cell, they cannot distinguish if differences in the intracellular c-di-GMP are being driven by changes in c-di-GMP synthesis or hydrolysis. Consider a case where the levels of c-di-GMP are elevated by growth in a different environment. This increase in c-di-GMP can be due to increased DGC activity, decreased PDE activity, or modulation of both. One cannot predict *a priori* solely based on the concentration of c-di-GMP how this change is mediated. My method, named TELCA, quantifies total DGC or PDE activity of cell lysates using [<sup>13</sup>C]-containing substrates to allow the differentiation of newly synthesized or degraded c-di-GMP from natural occurring c-di-GMP by mass spectrometry. The substrate for the DGC assay measures synthesis of [<sup>13</sup>C]-c-di-GMP from exogenous [<sup>13</sup>C]-GTP whereas the PDE assay monitors the degradation of exogenous [<sup>13</sup>C]-c-di-GMP.

To assess how effectively TELCA measures cellular DGC activity, extracts were generated from cultures of wild type (WT) *V. cholerae* ectopically expressing an active DGC (VCA0956), an active PDE (VC1086), or the vector control. Note that

WT *V. cholerae* has a relatively low intracellular concentration of c-di-GMP at the growth state used for these experiments (mid-exponential growth, OD<sub>600</sub> of 0.5-0.8) due to QS mediated reduction in c-di-GMP levels at high cell density. I hypothesized that lysates produced from cells expressing VCA0956 would more rapidly synthesize [<sup>13</sup>C]-c-di-GMP from [<sup>13</sup>C]-GTP than lysates with the empty vector control or overproducing the PDE VC1086. The cells from all three cultures were harvested and lysed using a Microfluidics M110-P Processor, which exposes the cells to high shear and impact force resulting in a uniform lysate. This process causes minimum disruption of protein conformation and thus is well suited to generate lysates for this assay. [<sup>13</sup>C]-GTP was added to 0.1 mg/mL total protein from each extract to a final concentration of 1.0 mM, and aliquots of the reaction were removed at specified timepoints followed by quenching with a phenol-chloroform extraction. The concentration of newly synthesized [<sup>13</sup>C]-c-di-GMP was quantified using LC-MS/MS. To differentiate [<sup>13</sup>C]-c-di-GMP from naturally occurring [<sup>12</sup>C]-c-di-GMP, I measured a mass to charge ratio (*m/z*) of 709.16 > 354.31 to detect [<sup>13</sup>C]-c-di-GMP and 689.16 > 344.31 for [<sup>12</sup>C]-c-di-GMP as previously described (Fig. 1A) [79]. The TELCA reaction generated a signal at the same retention time of chemically synthesized [<sup>12</sup>C]-c-di-GMP standards at a *m/z* of 709.16 > 354.31 with no signal at 689.16 > 344.31, indicating that this detection method is sufficient to discriminate between these two carbon isotope forms of c-di-GMP (Fig. 1B).

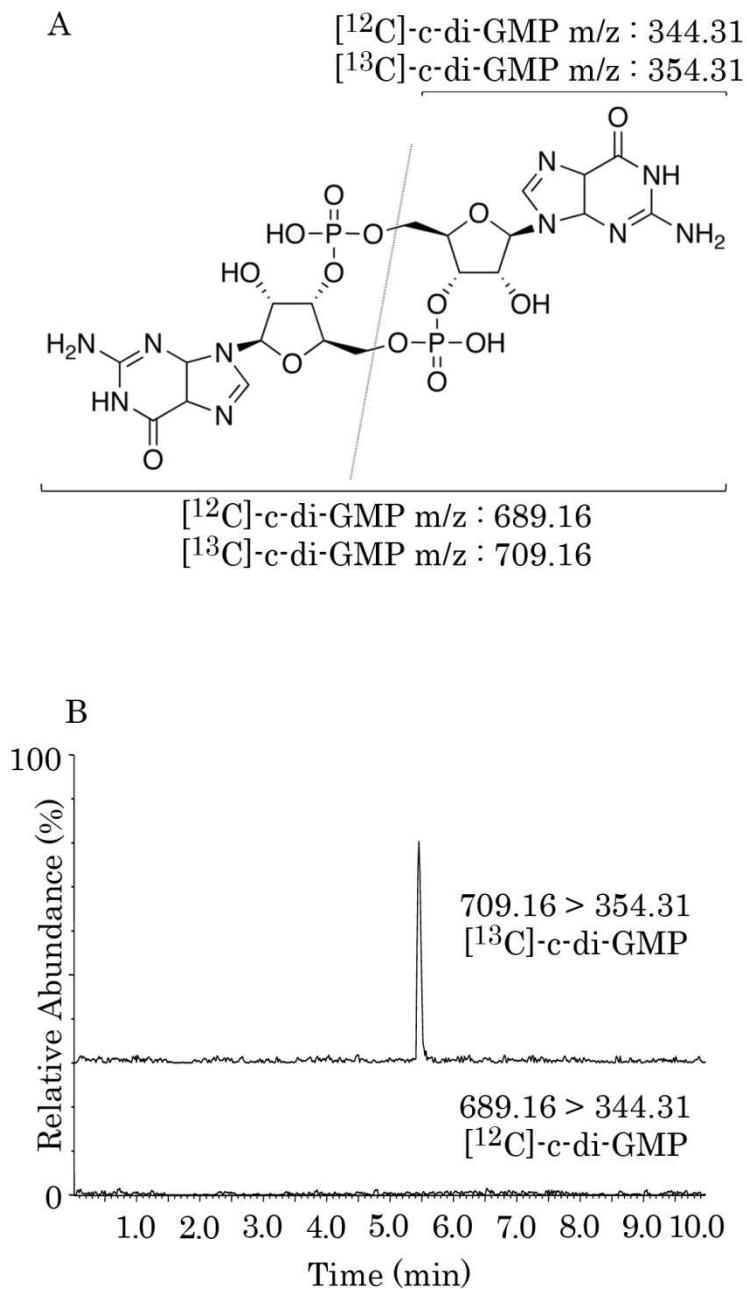


**Figure 1. LC-MS/MS differentiation of  $[^{12}\text{C}]\text{-c-di-GMP}$  and  $[^{13}\text{C}]\text{-c-di-GMP}$ .** (A) Molecular structure of c-di-GMP with the  $m/z$  used for detection and quantification. The top  $m/z$  describes the half of the molecule observed after fragmentation (as indicated by the line) while the bottom  $m/z$  represent the entire molecule. The values for both  $[^{12}\text{C}]\text{-}$  and  $[^{13}\text{C}]\text{-c-di-GMP}$  are indicated. (B) The spectrum of  $[^{13}\text{C}]\text{-c-di-GMP}$ . The top contains a peak at 5.4 minutes with a  $m/z$  of 709.16 > 354.31, indicating the presence of  $[^{13}\text{C}]\text{-c-di-GMP}$ . The bottom contains no peak at 5.4 minutes with a  $m/z$  of 689.16 > 344.31, indicating that no  $[^{12}\text{C}]\text{-c-di-GMP}$  is present.

A non-linear regression with a one-phase decay model (Graphpad Prism) was used to analyze the increase in [ $^{13}\text{C}$ ]-c-di-GMP concentrations over time. I constrained the maximum yield of the model to 0.5 mM [ $^{13}\text{C}$ ]-c-di-GMP as this is the maximum theoretical yield of the reaction. The lysate from *V. cholerae* expressing the DGC produced significantly more (two tailed Student's T-Test,  $p < 0.05$ ) [ $^{13}\text{C}$ ]-c-di-GMP over time, yielding 10.2 fold and 17.1 fold more c-di-GMP than the vector control and PDE lysates, respectively, after 120 minutes (Fig. 2). Furthermore, the rate constant for the DGC lysate, which represents the increase of c-di-GMP synthesis per unit time expressed as inverse minutes ( $6.9 \pm 1.1 \times 10^{-6} \text{ min}^{-1}$ ,  $R^2=0.76$ ) was significantly different (sum-of-squares F-test,  $p < 0.05$ ) than those of the vector control lysate ( $5.9 \pm 0.5 \times 10^{-7} \text{ min}^{-1}$ ,  $R^2=0.90$ ) and the PDE lysate ( $4.1 \pm 0.4 \times 10^{-7} \text{ min}^{-1}$ ,  $R^2=0.87$ ). This result indicates that TELCA is able to differentiate the cellular DGC activity of lysates containing a higher concentration of active DGCs. Furthermore, I found that lysates generated from *V. cholerae* expressing the PDE produced 1.7 fold less [ $^{13}\text{C}$ ]-c-di-GMP than the vector control lysate after 120 minutes and exhibited a lower rate constant, indicating that additional PDEs in the lysate can reduce the net c-di-GMP synthesis by hydrolyzing [ $^{13}\text{C}$ ]-c-di-GMP post synthesis.

Of note, [ $^{13}\text{C}$ ]-c-di-GMP accumulated in all three lysates including the PDE overexpression strain suggesting that given excess GTP, DGC activity supersedes PDE activity in these conditions over the time course examined. A subset of DGCs exhibit feedback inhibition by an allosteric RXXD inhibition site in close proximity to the DGC active site [10]. VCA0956 does not have a predicted inhibition site;

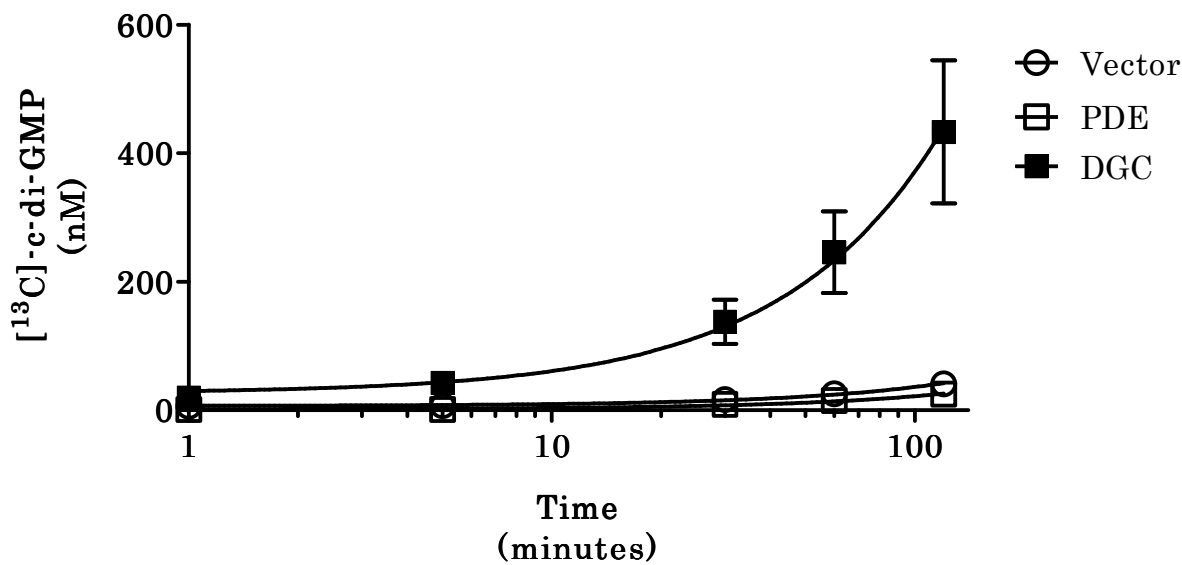


**Figure 2. TELCA of  $[^{13}\text{C}]$ -c-di-GMP synthesis of DGC and PDE ectopic expression strains.** TELCA was applied to lysates of *V. cholerae* strains ectopically expressing an active DGC (VCA956, solid squares), an active PDE (VC1086, empty squares), and an empty vector control (empty circles).  $[^{13}\text{C}]$ -GTP was added to each lysate and  $[^{13}\text{C}]$ -c-di-GMP synthesis was tracked over time using LC-MS/MS. A non-linear regression using a two-phase exponential decay model was applied to each lysate.

however, it is possible that the c-di-GMP synthesis of another DGC subject to feedback inhibition would have an altered synthesis profile. Additionally, it should be noted that I was not able to detect any hybrid c-di-GMP composed of one  $[^{12}\text{C}]$ -GTP and one  $[^{13}\text{C}]$ -c-di-GMP (detection  $m/z$  of  $709.16 > 344.31$ ), indicating that the native  $[^{12}\text{C}]$ -GTP is depleted upon addition of  $[^{13}\text{C}]$ -GTP. Furthermore, there was no  $[^{12}\text{C}]$ -c-di-GMP detected in the vector control lysate or the PDE lysate at any timepoint. However, in the DGC lysate, I did detect  $[^{12}\text{C}]$ -c-di-GMP in low abundance alongside synthesized  $[^{13}\text{C}]$ -c-di-GMP suggesting that if  $[^{12}\text{C}]$ -GTP is to

be used in lieu of [<sup>13</sup>C]-GTP, additional measures would be required to compensate for the existence of native c-di-GMP in certain strains.

*TELCA quantification of whole cell PDE activity*

I performed a similar experiment to determine if TELCA is effective at differentiating the PDE activity of different bacterial strains; however, instead of using [<sup>13</sup>C]-GTP as the initial substrate, [<sup>13</sup>C]-c-di-GMP was added. To generate [<sup>13</sup>C]-c-di-GMP, a c-di-GMP synthesis reaction was performed using [<sup>13</sup>C]-GTP and the DGC WspR that contained a mutation in the RXXD allosteric inhibition site (R242A, [87]). The remaining labeled GTP was removed by treating the reaction with Antarctic phosphatase, although quantification of enzymatically synthesized [<sup>13</sup>C]-c-di-GMP using LC-MS/MS indicated that the reaction went to completion, generating the expected hypothetical yield. I observed that the PDE lysate more rapidly degraded [<sup>13</sup>C]-c-di-GMP than both the vector control lysate and the DGC lysate (Fig. 3), as the PDE lysate retained an average of 20.5% [<sup>13</sup>C]-c-di-GMP after 120 minutes whereas the vector control lysate and the DGC lysate retained averages of 69.6% and 73.9% of the [<sup>13</sup>C]-c-di-GMP, respectively. The difference between the PDE lysate and both the vector control and DGC lysates were significantly different (two tailed Student's T-Test,  $p < 0.05$ ). Likewise, a non-linear regression with a one-phase decay model with a plateau constraint of zero was applied to the data, and I found that the rate constant of the PDE lysate ( $1.9 \pm 0.6 \times 10^{-2} \text{ min}^{-1}$ ,  $R^2=0.66$ ) was significantly higher (sum-of-squares F-test,  $p < 0.05$ ) than both the vector control lysate ( $2.5 \pm 1.0 \times 10^{-3} \text{ min}^{-1}$ ,  $R^2=0.35$ ) and the DGC

lysate ( $2.0 \pm 0.9 \times 10^{-3} \text{ min}^{-1}$ ,  $R^2=0.27$ ). As expected, there were no notable differences between the DGC-expressing lysate and the vector control lysate suggesting that a difference in DGC activity does not impact the PDE activity. From these data, I conclude that TELCA is sufficient to differentiate both the c-di-GMP synthesis and hydrolysis potential of whole-cell lysates.

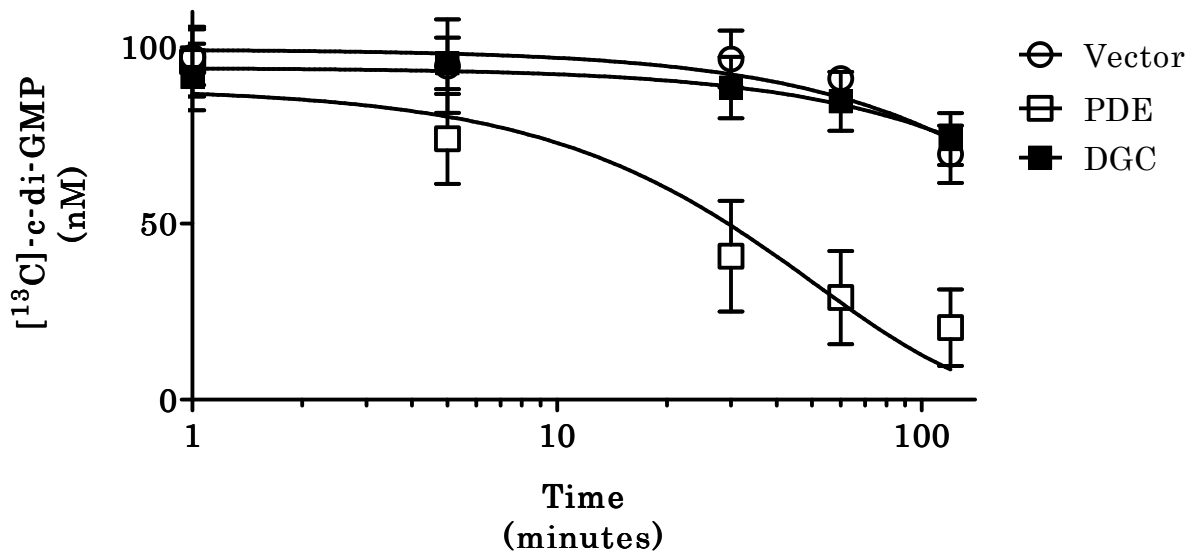


**Figure 3. TELCA of  $[^{13}\text{C}]$ -c-di-GMP hydrolysis of DGC and PDE ectopic expression strains.** TELCA was applied to lysates of *V. cholerae* strains ectopically expressing an active DGC (VCA956, solid squares), an active PDE (VC1086, empty squares), and an empty vector control (empty circles).  $[^{13}\text{C}]$ -c-di-GMP was added to each lysate and the hydrolysis was tracked over time using LC-MS/MS. A non-linear regression using a two-phase exponential decay model was applied to each lysate.

*The local environment alters the intracellular concentration of c-di-GMP in  
V. cholerae*

How the extracellular environment impacts the synthesis and degradation of intracellular c-di-GMP is poorly understood. It has been proposed that extracellular

stimuli, such as oxygen, light, amino acids, and AIs, regulate intracellular c-di-GMP by altering the activity of DGCs and PDEs [8, 19-24, 26, 27]. Also, many DGCs and PDEs have domains predicted to be involved in sensing extracellular ligands [93]. I hypothesized that *V. cholerae* growing in different environments would exhibit distinct concentrations of c-di-GMP due to alterations in the environmental inputs controlling DGC and PDE activity. To test this hypothesis, I quantified the intracellular c-di-GMP concentration of *V. cholerae* in six different growth media using LC-MS/MS. For the purposes of this study, I consider AKI [80], LB, and ASW complex, carbon rich media, while MOPS, AB [81] and M9 [82] are considered defined, carbon poor media. I sampled from each media during the latter half of steady-state growth, which I define as 1-2 doublings from stationary phase. This time point was determined by generating growth curves for *V. cholerae* in each different media (Fig. 4).

I found that *V. cholerae* demonstrated differences of up to 20-fold in the intracellular concentration of c-di-GMP when grown in these different media (Fig. 5). Consistent with prior studies, I measured the concentration of c-di-GMP in LB to be  $101.2 \pm 52.7$  nM [79]. The complex, carbon rich media AKI also produced relatively low intracellular c-di-GMP that was statistically indistinguishable from LB, measuring as  $113.9 \pm 43.3$  nM. In contrast, the carbon poor media AB and M9 exhibited significantly higher levels of intracellular c-di-GMP at  $529.4 \pm 307.2$  nM and  $2379.9 \pm 745.8$  nM, respectively, and M9 media had significantly higher intracellular c-di-GMP than AB media. Interestingly, the intracellular c-di-GMP of

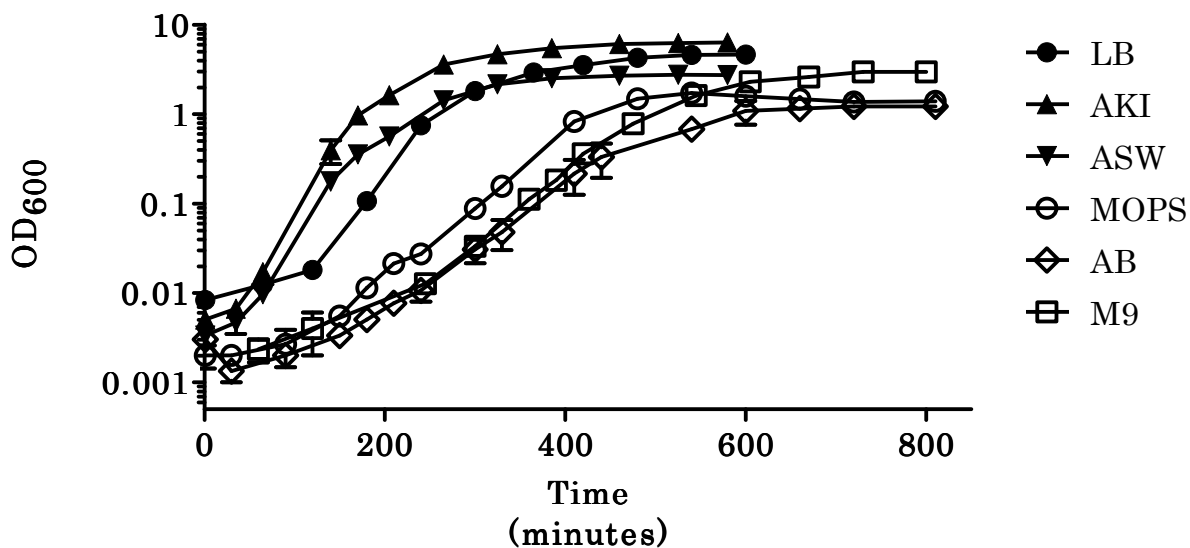


**Figure 4. Growth curves of *V. cholerae* grown in different media.** Cultures of *V. cholerae* were inoculated 1/1000 into 50 mL of the designated media, and OD<sub>600</sub> readings were taken at regular time intervals. Each point represents the mean of three replicates, and the error bars indicate standard error of the mean.

*V. cholerae* grown in MOPS more resembled LB and AKI, measuring at  $126.2 \pm 41.5$  nM; in contrast, intracellular c-di-GMP of *V. cholerae* grown in ASW was modestly higher, measuring at  $251.6 \pm 75.5$  nM. Thus, these results support the idea that c-di-GMP signaling systems primarily function as environmental sensors and modulate c-di-GMP accordingly. Moreover, the high concentration of c-di-GMP observed in M9 media suggests the range of physiologically relevant concentrations of c-di-GMP experienced by *V. cholerae* is greater than currently appreciated.

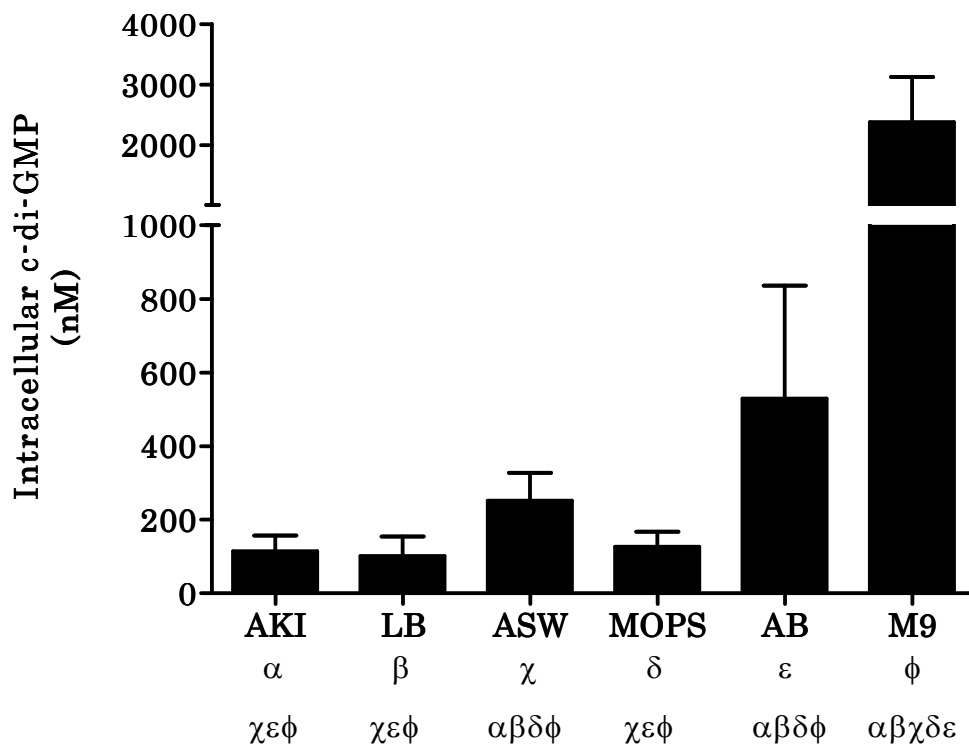


**Figure 5. Intracellular c-di-GMP concentrations of *V. cholerae* grown in different media.** *V. cholerae* was grown in 6 different media, and cells were harvested during late-exponential growth. The intracellular concentration was quantified using LC-MS/MS and calculated using cell counts, determined by OD<sub>600</sub> and plating, and cell size, determined by microscopy. Error bars represent standard deviation and corresponding symbols indicate statistical significance, which was determined using a two-tailed Student's T-Test ( $p < 0.05$ ).

*Growth environments modulate both c-di-GMP synthesis and hydrolysis*

While it is clear that the different growth environments alter intracellular c-di-GMP concentrations of *V. cholerae*, it is unclear if these changes are being driven by modulation of DGC and/or PDE activity. I addressed this question using TELCA on cultures that were grown in four of the six different growth media examined in Fig. 5. I hypothesized that [<sup>13</sup>C]-c-di-GMP synthesis would be greater when cells

were grown in both AB and M9 media, as the intracellular c-di-GMP of cells grown in these media is elevated. [<sup>13</sup>C]-GTP was added to lysates generated from *V. cholerae* grown in each environmental condition, and [<sup>13</sup>C]-c-di-GMP synthesis was quantified after 60 minutes using LC-MS/MS (Fig. 6A). Analogous to the intracellular c-di-GMP measurements, *V. cholerae* grown in AKI and LB exhibited similar c-di-GMP synthesis. Consistent with my hypothesis, growth of *V. cholerae* in AB media exhibited significantly elevated c-di-GMP synthesis, corresponding to its elevated intracellular c-di-GMP concentration. Interestingly, however, cells grown in M9 media showed a lower amount of c-di-GMP synthesis than those grown in AB, even though M9 produced the highest intracellular concentration of c-di-GMP that I observed.

Based on my analysis of DGC activity I hypothesized that cells grown in M9 must exhibit lower PDE activity relative to the other media to account for the high concentration of c-di-GMP. To test this hypothesis, TELCA was used to quantify [<sup>13</sup>C]-c-di-GMP hydrolysis of cell lysates (Fig. 6B). Consistent with the intracellular c-di-GMP measurements, cells grown in AKI and LB had similar PDE activity; cells grown in AB media also had similar c-di-GMP hydrolysis to AKI and AB. However, in support of my hypothesis, cells grown in M9 media had significantly lower PDE activity compared to cells grown in the other media conditions. TELCA analysis of *V. cholerae* grown in these four different media suggests that suppressed PDE activity increases intracellular c-di-GMP in M9 media, while elevated DGC activity increases intracellular c-di-GMP in AB media.

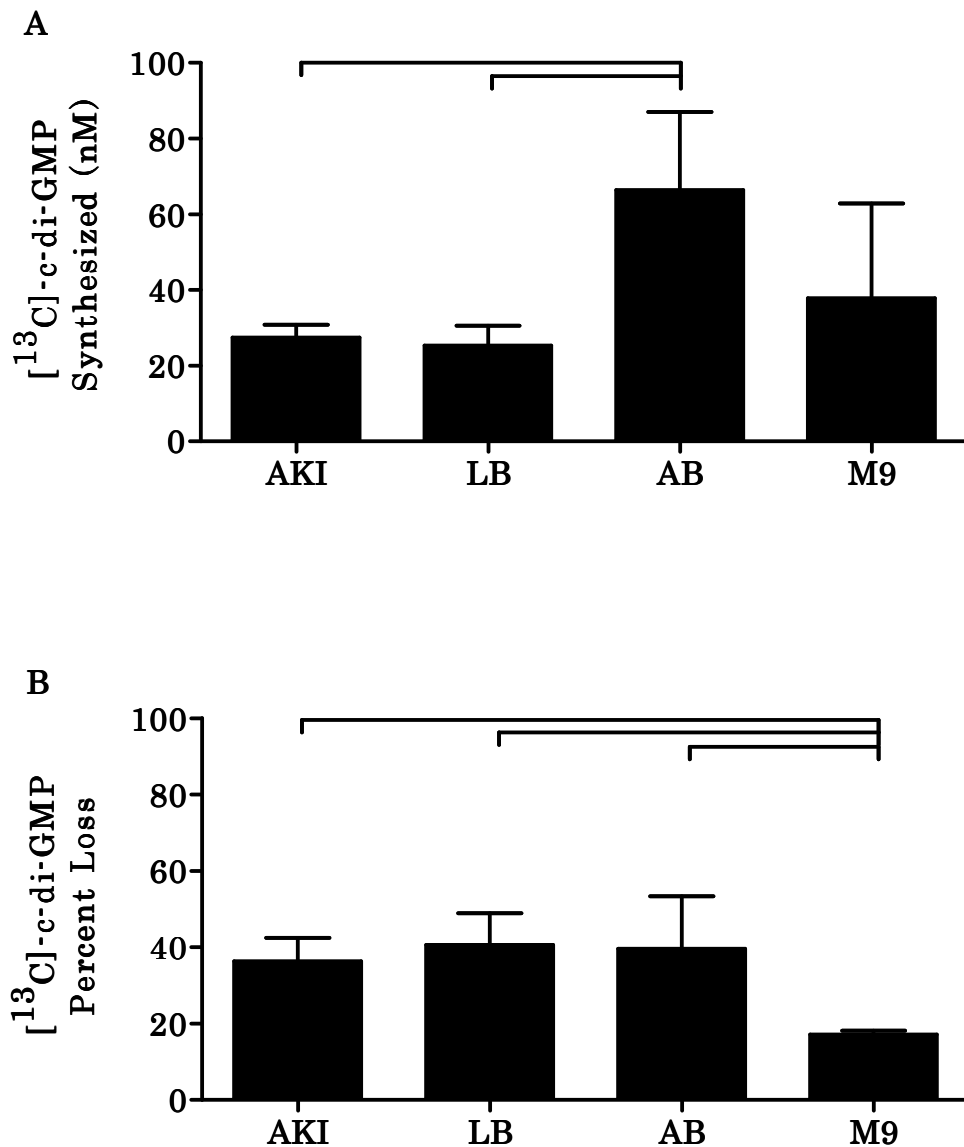


**Figure 6. TELCA of *V. cholerae* grown in different media.** (A) TELCA was applied to lysates of WT *V. cholerae* grown in different media. [<sup>13</sup>C]-GTP was added to each lysate and the amount of [<sup>13</sup>C]-c-di-GMP synthesis was quantified using LC-MS/MS. (B) TELCA was applied to lysates of WT and QS mutants of *V. cholerae*. [<sup>13</sup>C]-c-di-GMP was added to each lysate, and the amount of [<sup>13</sup>C]-c-di-GMP hydrolysis was quantified using LC-MS/MS. The percent loss was calculated by comparing each lysate to a no-protein control reaction. All cultures were grown in triplicate, and the error bars indicate the standard deviation from the mean. Brackets indicate statistical significance using a one-tailed Student's T-Test (p<0.05).

### *QS controls both total DGC and PDE activity in V. cholerae*

As mentioned above, QS modulates the intracellular concentration of c-di-GMP in *V. cholerae* to regulate biofilm formation, but the specific DGCs and PDEs involved in this regulation are not fully understood. This question is challenging to address as QS controls the transcription of 18 proteins that potentially alter c-di-GMP levels [66, 72]. Moreover, DGCs and PDEs could have differential enzymatic activities at low versus high cell density. To address this question, I used TELCA to determine if QS modulates the levels of c-di-GMP in *V. cholerae* by altering DGC and/or PDE activity. To analyze DGC and PDE activity of *V. cholerae* in different QS states, the WT,  $\Delta hapR$ , and  $\Delta luxO$  mutant strains were analyzed. The  $\Delta hapR$  strain is a QS mutant that is locked in low cell density as HapR is the master high cell density transcriptional regulator, whereas the  $\Delta luxO$  strain is a QS mutant locked in high cell density as the Qrr sRNAs are never expressed. Importantly, cultures were grown and harvested at an OD<sub>600</sub> of 0.2-0.3, corresponding to the low-cell-density state. Therefore, I expected the WT strain to be in low cell density and mimic the  $\Delta hapR$  mutant. Indeed, TELCA analysis indicated that the WT and the  $\Delta hapR$  lysates exhibited significantly elevated c-di-GMP synthesis compared to the  $\Delta luxO$  mutant (Fig. 7A), consistent with these strains having a higher concentration of c-di-GMP [66, 72]. Analysis of the DGC activity of WT cells grown to high cell density (compare Fig. 6A, LB to Fig. 7A, WT) indicates that the DGC activity decreases as cells reach a quorum. In fact, the DGC activity of the  $\Delta luxO$  mutant at

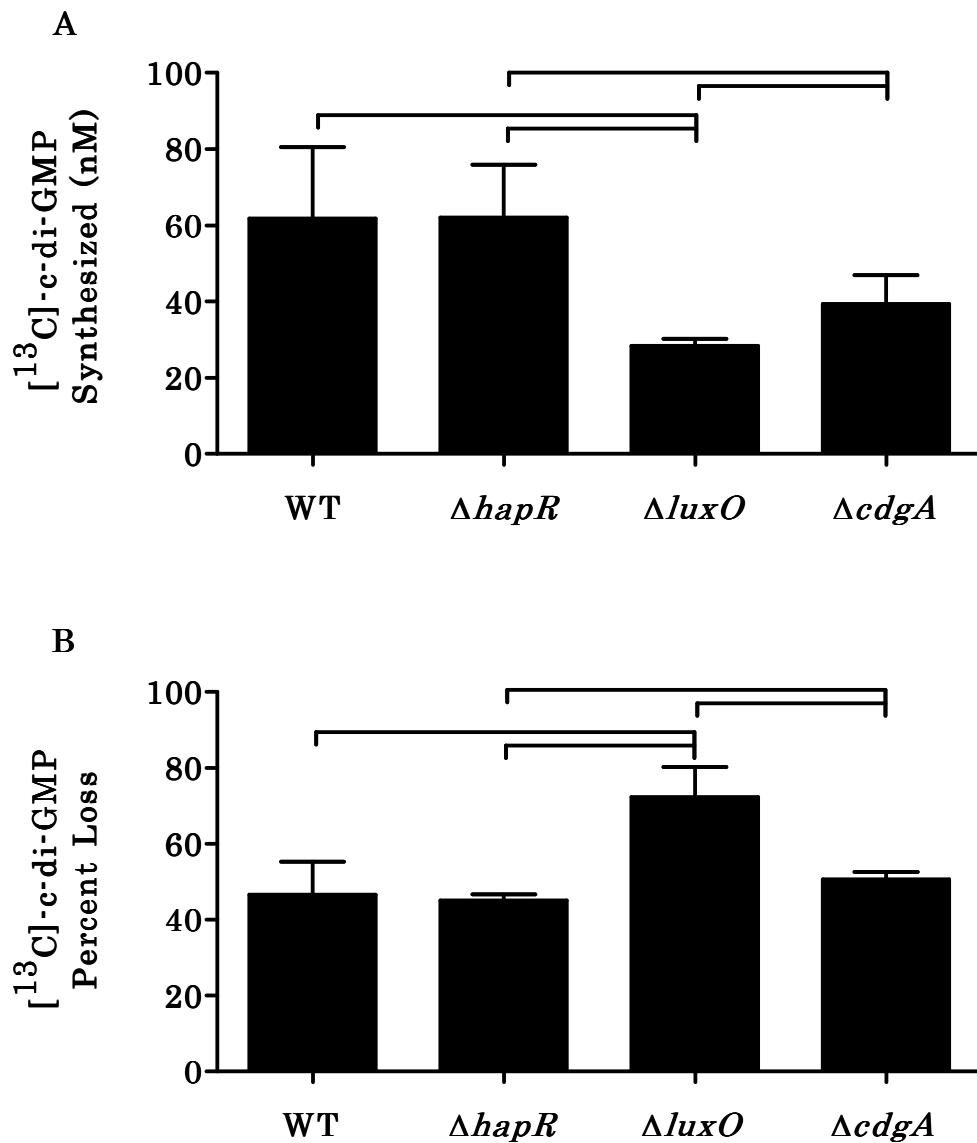


**Figure 7. TELCA of *V. cholerae* QS mutants.** (A) [<sup>13</sup>C]-GTP was added to each lysate and the amount of [<sup>13</sup>C]-c-di-GMP synthesis was quantified using LC-MS/MS. (B) [<sup>13</sup>C]-c-di-GMP was added to each lysate, and the amount of [<sup>13</sup>C]-c-di-GMP hydrolysis was quantified using LC-MS/MS. The percent loss was calculated by comparing each lysate to a no-protein control reaction. All cultures were grown in triplicate, and the error bars indicate the standard deviation from the mean. Brackets indicate statistical significance using a one-tailed Student's T-Test ( $p < 0.05$ ).

low cell density (Fig. 7A) is quite similar to that of WT *V. cholerae* grown to high cell density (Fig. 6A, LB).

I performed an analogous experiment to quantify the impact of QS on net PDE activity. The relative PDE activity was determined for each of the WT,  $\Delta hapR$ , and  $\Delta luxO$  lysates by measuring the percent loss of [ $^{13}C$ ]-c-di-GMP. I found that the percent loss of [ $^{13}C$ ]-c-di-GMP was significantly higher in the  $\Delta luxO$  strain compared to the  $\Delta hapR$  mutant and WT strain (Fig. 7B). The PDE activity of WT cells harvested at low cell density was indistinguishable from the  $\Delta hapR$  mutant. This result would suggest that PDE activity is increased as cells transition from low to high cell density. However, a comparison the WT strain grown to high cell density ( $40.6 \pm 8.3$  nM; Fig. 6B, LB) and the WT strain grown at low cell density ( $46.6 \pm 8.7$  nM; Fig. 7B) reveals a similar PDE activity. Indeed, the PDE activity of WT grown to high cell density ( $40.6 \pm 8.3$  nM; Fig. 6B, LB) was lower than the  $\Delta luxO$  mutant ( $72.2 \pm 8.0$  nM; Fig. 7B). This difference in PDE activity between the WT strain and  $\Delta luxO$  mutant was evident even if the WT strain was grown to stationary phase (data not shown). Thus, in regards to PDE activity the  $\Delta luxO$  strain has a more dramatic phenotype than WT *V. cholerae* growing in LB.

#### *CdgA contributes to the increased DGC activity at low cell density*

The above experiments suggest that increased DGC activity at low cell density contributes to the higher concentration of c-di-GMP. CdgA (VCA0074) is a well-studied DGC that is repressed in the high-cell-density state and is important

for biofilm formation [72, 75, 94-97]. Based on a large body of evidence that indicates CdgA plays an important role in bridging c-di-GMP signaling and QS (see discussion), I hypothesized that CdgA significantly contributed to the increased DGC activity I observed at low cell density. To test this hypothesis and determine if TELCA can detect the contribution of a single DGC to total cellular activity, lysates from the  $\Delta cdgA$  mutant grown to low cell density were analyzed. I observed a 36.4% decrease in DGC activity in the  $\Delta cdgA$  strain compared to the WT strain, although the differences did not quite reach statistical significance ( $p=0.06$ ) (Fig. 7A). As expected, there was no significant difference in the net PDE activity of the  $\Delta cdgA$  strain and the WT strain (Fig. 7B). These results confirm previous genetic studies that implicate CdgA as a major contributor to the increased DGC activity observed in the low-cell-density state in *V. cholerae*, and further illustrate the applicability of TELCA to analyze complex c-di-GMP signaling pathways.

### *Discussion*

The bacterial second messenger c-di-GMP is a central regulator of biofilm formation and motility in bacteria. Indeed, bioinformatic studies indicate that DGCs and PDEs are encoded by more than 80 percent of all sequenced bacteria [2]. C-di-GMP controls many important phenotypes in bacteria including biofilm formation, motility, production of virulence factors, and lifecycle progression, and this list continues to grow [11, 13, 16, 98-100].

Net changes in DGC or PDE activity leading to different intracellular c-di-GMP concentrations can be difficult to parse as bacteria often encode multiple DGCs and PDEs. Furthermore, it is often challenging to resolve differences in c-di-GMP signaling pathways in single DGC or PDE mutants due to this redundancy and the inherently low concentration of c-di-GMP in many bacterial species (for example, see [101]). To circumvent these challenges, I developed TELCA to quantify total cellular c-di-GMP synthesis and hydrolysis activities. The [<sup>13</sup>C]-labeled substrates TELCA utilizes are stable, safe to use, and can be distinguished from naturally occurring [<sup>12</sup>C]-c-di-GMP using mass spectrometry. To my knowledge, this is the first description of an *in vitro* assay to measure cellular DGC or PDE activity.

To test TELCA, I examined strains of *V. cholerae* ectopically expressing either a GGDEF or an EAL enzyme and observed enhanced DGC and PDE activity, respectively. These experiments validated the approach and demonstrated that I can differentiate lysates with increased synthesis and hydrolysis activities. As an *in vitro* assay, disruption of the cell might alter the activity of localized or membrane bound proteins in the lysate. However, it should be noted that CdgA is a predicted integral inner membrane protein yet I was able to quantify a loss in cellular DGC activity of a  $\Delta cdgA$  mutant using TELCA, showing that CdgA remained active during the assay.

Regulatory inputs of the c-di-GMP signaling network remain under-characterized. The consensus of the field is that c-di-GMP turnover enzymes bind and respond to environmental ligands, host derived metabolites, or are directly

modified by post-translational regulatory mechanisms to regulate c-di-GMP synthesis or hydrolysis, thus enabling the bacterium to fine tune intracellular c-di-GMP to its environment [6]. Indeed, I showed that when *V. cholerae* is cultured in different media, the intracellular c-di-GMP varies significantly (Fig. 5). Surprisingly, the changes in the c-di-GMP levels were dramatic with cells grown in M9 exhibiting 20 times more c-di-GMP than cells grown in LB. This result suggests that *V. cholerae*, and potentially other bacteria, experience a much wider range of c-di-GMP concentrations than previously appreciated. Moreover, cells grown in defined, carbon poor media demonstrated slower growth rates and higher levels of c-di-GMP compared with complex, carbon rich media.

The increased c-di-GMP observed in AB and M9 could be generated by three distinct processes: 1) increased DGC activity, 2) decreased PDE activity, or 3) modulation of both DGC and PDE activity. TELCA analysis revealed that c-di-GMP in AB media was driven by increased DGC activity while the c-di-GMP increase in M9 was driven by reduced PDE activity. This result highlights that bacteria can and do control intracellular c-di-GMP by regulating both c-di-GMP synthesis and hydrolysis. Moreover, one cannot distinguish the relative DGC and PDE inputs based solely on measuring the intracellular concentration of c-di-GMP.

I applied TELCA to further understand how QS controls intracellular c-di-GMP in *V. cholerae*. By analyzing mutants that lock the bacteria in the low- or high-cell-density state, I determined that DGC activity is increased at low cell density and decreases as the cells enter a quorum. Alternatively, I observed

increased PDE activity of the  $\Delta luxO$  high-cell-density mutant, compared to a locked low-cell-density mutant and the WT strain. However, I did not observe changes in PDE activity of the WT strain at different cell densities; thus, the  $\Delta luxO$  mutant exhibits a more pronounced modulation of PDE activity compared to the WT strain. A discrepancy in phenotypic expression of the WT and  $\Delta luxO$  mutant is not unprecedented. For example, the  $\Delta luxO$  mutant is deficient for colonization of the infant mouse whereas the WT is proficient [68]. Therefore, these strains should not be considered equivalent. The analysis of the  $\Delta luxO$  mutant does indicate that QS in *V. cholerae* has the potential to modulate cellular PDE activity. I speculate that in other conditions not examined here, in which the Qrr sRNAs are more fully repressed at high cell density, the WT strain would exhibit density dependent PDE activity. My results clearly show that in LB *V. cholerae* QS control of c-di-GMP occurs through modulation of c-di-GMP synthesis but not c-di-GMP degradation. These results experimentally validate previous transcriptional studies that have shown that the expression of both DGCs and PDEs are differentially regulated by QS [66, 72, 74].

One protein that has been implicated in QS-mediated control of c-di-GMP is the DGC CdgA. It has been previously shown that CdgA is capable of synthesizing c-di-GMP in *V. cholerae* [79]. The regulation of *cdgA* is controlled by QS, as *cdgA* is repressed at high cell density via direct binding of HapR to the promoter region [72, 74, 75]. Furthermore, CdgA actively regulates biofilm formation as a  $\Delta cdgA$  mutant strain demonstrates decreased colony rugosity [76] and ectopic expression of *cdgA*

leads to increased biofilm formation [79]. Also of note, a  $\Delta hapR\Delta cdgA$  double mutant strain has reduced biofilm formation compared to the  $\Delta hapR$  mutant, indicating that CdgA is involved in the HapR mediated increase in biofilm formation [102]. Taken together, this evidence suggested that repression of *cdgA* by HapR is one mechanism by which QS controls the intracellular concentration of c-di-GMP and biofilm formation. To confirm these previous genetic studies and quantify the contribution of CdgA to total DGC activity, I created a deletion mutant of *cdgA* and measured the relative c-di-GMP synthesis and hydrolysis potential using TELCA. My results are consistent with previous findings as the  $\Delta cdgA$  strain had reduced c-di-GMP synthesis compared to the  $\Delta hapR$  and WT strains while having similar c-di-GMP synthesis as the  $\Delta luxO$  mutant (Fig. 7). Importantly, this finding demonstrates that TELCA is able to distinguish the input of one DGC to total cellular DGC activity.

TELCA is a straightforward technique that can be utilized to quantify total DGC or PDE activity for any bacterium. This method allows a systems level analysis of total c-di-GMP synthesis or degradation activity and can serve as a complementary approach to the current methods of c-di-GMP detection to further unravel complex c-di-GMP signaling networks.

## CHAPTER 3 – Bile Acids and Bicarbonate Inversely Regulate Intracellular Cyclic di-GMP in *Vibrio cholerae*

### *Preface*

I hypothesized that bile is an environmental signal sensed by *V. cholerae* to recognize and adapt to growth in the human environment by modulating c-di-GMP signaling pathways. Based on current models postulating that *V. cholerae* reduces intracellular c-di-GMP in the human host, I predicted that bile acids would reduce global c-di-GMP concentrations. Surprisingly, I discovered that bile acids increase intracellular c-di-GMP. A screen of the activity of all 61 *V. cholerae* c-di-GMP turnover enzymes in the presence and absence of bile acids identified three DGCs that showed increased c-di-GMP synthesis in the presence of bile acids. Furthermore, a screen on the expression of all 61 *V. cholerae* c-di-GMP turnover enzymes revealed that bile acids inhibited the expression of one PDE. Deletion of these four enzymes abolished the induction of c-di-GMP by bile and negated the ability of *V. cholerae* to form biofilms in the presence of bile. Bicarbonate, a biological pH buffer secreted by intestinal epithelial cells in the small intestine, suppressed the bile-induced increases in intracellular c-di-GMP. I propose that bile and bicarbonate inversely control c-di-GMP levels in *V. cholerae*, allowing this bacterium to sense and adapt to local environmental niches within the small intestine.

### *Growth conditions and molecular methods*

All strains, plasmids, and primers used are listed in Tables A1-3. The *V. cholerae* El Tor biotype strain C6706str2 was used for all experiments [78] and *Escherichia coli* strains DH10B (Invitrogen) and S17- $\lambda$ pir [103] were used to harbor and conjugate plasmid DNA into *V. cholerae*. The construction of the  $\Delta vpsL$ ,  $\Delta luxO$ , and  $\Delta hapR$  strains has been described elsewhere [67, 68, 72]. For all experiments, unless otherwise specified, cultures were grown in LB media at 35°C with shaking at 220 rpm. When necessary, media was supplemented with kanamycin (Sigma) at 100  $\mu$ g/mL or chloramphenicol (Sigma) at 10  $\mu$ g/mL. The inducer isopropyl  $\beta$ -D-1-thiogalactopyranoside (IPTG) was added at 0.1 mM when required.

Synthetic human bile (SHB) is a mixture of six purified conjugated bile acids added to LB media at physiologically relevant concentrations to mimic the human small intestine [37, 38, 104, 105]. All bile acids were purchased from Sigma. The conjugated bile acids added were taurocholate (0.46 mM), glycocholate (0.93 mM), taurochenodeoxycholate (0.46 mM), glycochenodeoxycholate (0.93 mM), taurodeoxycholate (0.32 mM), and glycodeoxycholate (0.64 mM). Bovine bile (BV, Sigma) was supplemented at 0.4% w/v. 3-[(3-Cholamidopropyl)dimethylammonio]-1-propanesulfonate (CHAPS) was supplemented at 0.4% w/v, and sodium dodecyl sulfate (SDS) was supplemented at 0.01 % w/v due to its potent bactericidal activity. Taurine and glycine were each supplemented at 4 mM. Sodium bicarbonate (BiC) was supplemented when indicated at 0.3% w/v (49.2 mM), consistent with CT

inducing conditions [80], while 2-Amino-2-hydroxymethyl-propane-1,3-diol (Tris) was supplemented when indicated at 0.6% w/v (49.5 mM).

All of the protocols used in this study for DNA manipulation and plasmid construction were performed as previously described [106]. The DNA polymerase Phusion (Thermo Scientific) was used for all PCR reactions. The expression plasmids for the DGCs and PDEs were constructed as described elsewhere [79]. Briefly, these plasmids allow controlled expression of each DGC encoded by *V. cholerae* via induction of the Ptac promoter with IPTG. To construct the HD-GYP expression plasmids, each HD-GYP gene was amplified from the *V. cholerae* chromosome, then inserted into the pEVS143 vector using the EcoRI and BamHI insertion sites, as previously described [72]. The identification of the c-di-GMP reporter plasmid 6:C9-*lux* is described elsewhere [107]. The DGC mutant allele plasmids were generated using the Lightning Site-Directed Mutagenesis kit (Agilent) with the DGC expression plasmid as template using the primers listed in Table A3. The VC2497-*lux* reporter was constructed by amplifying the promoter of VC2497 from the *V. cholerae* chromosome by PCR, then inserting it into the pBBRlux vector using the SacI and BamHI insertion sites.

To generate the DGC and *toxR* deletion strains, natural transformation and homologous recombination were used. A PCR product was generated that contained a chloramphenicol resistance cassette (*cat*) bordered by FLP recombination target (FRT) sites from the plasmid pKD3 [84], flanked by 500 bp upstream and downstream of the targeted gene using the primers KO1/KO2 and KO3/KO4. The

PCR products generated with these promoters were fused to the *cat* gene using zipper PCR. Natural competence was induced by ectopically expressing *tfoX* (VC1153) [63] from the Ptac promoter using the plasmid pANDA2. pANDA2 was constructed by amplification of VC1153 with the primers CMW464 and CMW465 and insertion of this product into the EcoR1/BamH1 sites of the plasmid pEVS143. Homologous recombination events were selected by growing the culture on LB supplemented with chloramphenicol at 1 µg/mL. The *cat* gene was then removed by ectopically expressing a FLP recombinase on the vector pTL17 [86]. The *toxT* deletion mutant was constructed using allelic exchange as previously described via the plasmid pBK51, a derivative of the plasmid pKAS32 [108].

#### *Detection and quantification of intracellular c-di-GMP*

All c-di-GMP quantifications were analyzed using liquid chromatography coupled with tandem mass spectrometry (LC-MS/MS) as described in Chapter 2. Unless otherwise specified, cultures were grown to an OD<sub>600</sub> between 0.6 and 1, and a 1.5 mL aliquot of this culture was removed and centrifuged for 30 seconds at maximum speed. The supernatant was immediately removed and the pellet was resuspended in 100 µL of cold extraction buffer (40% acetonitrile/40% methanol/0.1 N formic acid) and incubated for 20 minutes at -20°C. The insoluble fraction was pelleted in a bench top centrifuge at 4°C for 5 minutes and the supernatant was collected and stored at -80°C. Prior to mass spectrometry, the extraction buffer was evaporated using a vacuum manifold. The pellet was then resuspended in 100 µL water.

### *Systematic screen of DGC and PDE activity*

To determine the *in vivo* activity of each *V. cholerae* DGC, each of the 40 DGC expression vectors was conjugated into a  $\Delta vpsL$  strain of *V. cholerae* harboring a separate reporter vector encoding a luciferase-transcriptional fusion of a c-di-GMP inducible promoter located within the open reading frame (ORF) of VC1673 (*6:C9-lux*, [107]). These strains were then grown in solid white 96-well clear-bottom plates (Costar 3903) in 150  $\mu$ L of LB or LB with SHB in the presence of IPTG inoculated as a 1/100 from an overnight culture. Luminescence and OD<sub>600</sub> values were recorded in a Spectramax M5 Platereader (Molecular Devices) after 8 hours of growth, and were reported as relative luminescence units (R.L.U.). The screen for PDE activity was performed in the same manner as the DGC assay with the addition of a third vector, pBRP02, which carry the allele of the DGC *qrgB* under pTac control. pBRP02 has the *Vibrio harveyi qrgB* allele cloned into the vector pMMB67eh [109], allowing it to coexist with the PDE expression vectors and the 6:C9-*lux* reporter plasmid.

### *Systematic screen of DGC and PDE expression*

DGC-*gfp* (GGDEF domain proteins) and PDE-*gfp* (GGDEF + EAL and EAL domain proteins) transcriptional fusion plasmids were constructed as previously described [72]. Strains containing the plasmids were grown in triplicate overnight and then inoculated 1/100 in 150  $\mu$ L LB or LB with SHB in a Costar black, clear-bottom 96 well plate (cat. # 3904). Cultures were grown for 8 hours, and then

fluorescence was quantified (excitation 475, emission 510) using a M5 Spectramax plate reader (Molecular Devices). Relative fluorescence was quantified by dividing the fluorescence by the OD<sub>600</sub> reading of the culture. PDE-*Iux* transcriptional fusion plasmids were constructed as previously described [66]. Strains containing the plasmids were grown in triplicate overnight and then inoculated 1/100 in 150  $\mu$ L LB or LB with SHB in a Costar white, clear-bottom 96 well plate (cat. # 3903). Cultures were grown for 6 hours, and then luminescence was quantified using an Envision plate reader (PerkinElmer). Relative luminescence was quantified by dividing the luminescence by the OD<sub>600</sub> reading of the culture.

### *Biofilm quantification*

Static biofilm formation was determined using a modified protocol from [47]. Overnight planktonic cultures of *V. cholerae* and *V. cholerae* DGC mutants were grown in LB media, and cultures were diluted 1:1000 into 1 mL LB or LB with BV as specified in 17 x 100 mm polystyrene test tubes (BD Falcon). These tubes were incubated at 35°C for 24 hours without shaking. The supernatant was then removed, an absorbance reading of the supernatant was taken (OD<sub>600</sub>), and the biofilm was gently washed with approximately 2 mL of phosphate buffer saline (PBS). The biofilm was then stained with 0.41% crystal violet (CV) in 12% ethanol for 3 minutes followed by three washes with PBS, elution of the CV in 10 mL 95% ethanol, and OD<sub>570</sub> measurement for each biofilm. Each OD<sub>570</sub> biofilm measurement was normalized to the OD<sub>600</sub> measurement of the planktonic culture to account for differences in growth.

*Bile increases the intracellular concentration of c-di-GMP in V. cholerae*

It has been proposed that *V. cholerae* has a high intracellular c-di-GMP concentration in environmental reservoirs where it predominantly exists as surface associated biofilm communities and reduces c-di-GMP upon entrance into the human host, leading to the activation of virulence factor expression [35]. As bile is a prevalent constituent of the human small intestine, I hypothesized that *V. cholerae* would reduce c-di-GMP levels in response to bile. To test this hypothesis, I grew wild type *V. cholerae* in the presence of a crude bovine bile extract (BV) or synthetic human bile (SHB) and quantified the intracellular c-di-GMP concentration using LC-MS/MS. BV was supplemented to the media at 0.4% w/v, a concentration which is physiologically relevant to that found in the small intestine [39, 110]. SHB is a mixture of six purified bile acids that replicate the physiological concentrations of bile acids found in the human small intestine [37, 38, 104, 105]. To my surprise, growth in both BV and SHB-containing media significantly increased the intracellular concentration of c-di-GMP 4.4 and 3.6-fold, respectively (Fig. 8).

To determine if the increase in intracellular c-di-GMP was due to the detergent activity of the bile acids, I grew *V. cholerae* in the presence of either the anionic detergent SDS (0.01% w/v) or the zwitterionic detergent CHAPS (0.4% w/v). I observed no significant difference in intracellular c-di-GMP upon addition of either detergent, suggesting that this increase in intracellular c-di-GMP is specific to bile acids. As the SHB mixture of bile acids contains bile acids conjugated to either taurine or a glycine, it was possible that these moieties were causing the increase in

intracellular c-di-GMP. However, there was no significant difference in the intracellular c-di-GMP concentration of *V. cholerae* grown with the addition of either taurine or glycine at equivalent concentrations (Fig. 8). Therefore, I conclude that bile acids increase the intracellular concentration of c-di-GMP in *V. cholerae*.

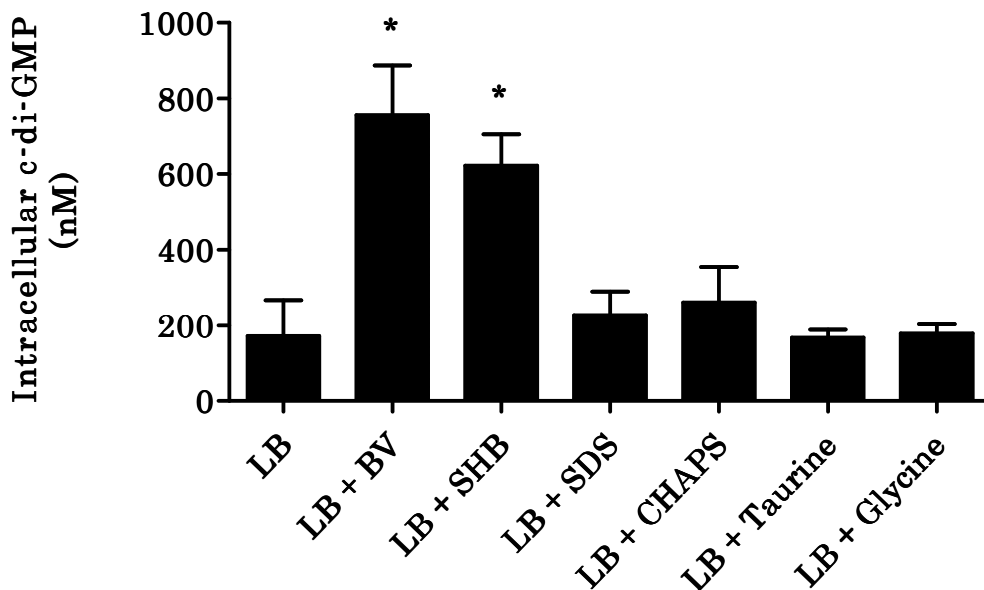


**Figure 8. Intracellular c-di-GMP concentrations of *V. cholerae* grown with different bile additives.** *V. cholerae* was grown in LB media and LB media with bovine bile (BV), synthetic human bile (SHB), the detergents SDS and CHAPS, and the amino acids taurine and glycine. Intracellular c-di-GMP was measured using LC-MS/MS. The reported values indicate the mean. Error bars indicate standard deviation, and \* indicates statistical significance compared to LB as determined by a Student's two-tailed T-Test (n=3, p < 0.05).

*The bile mediated increase of intracellular c-di-GMP is growth-phase dependent*

The experiments described thus far analyzed cultures grown to late exponential growth. I therefore examined the temporal dynamics of c-di-GMP induction by bile at various points during bacterial growth. When grown in

standard culture conditions with shaking, there is no significant difference in the doubling time of *V. cholerae* in the presence or absence of SHB (LB:  $22.3 \pm 0.3$  minutes, LB + SHB:  $21.6 \pm 0.6$  minutes). I measured intracellular c-di-GMP in three growth phases in the presence and absence of SHB: early exponential growth (OD<sub>600</sub> 0.2-0.3), late exponential growth (OD<sub>600</sub> 0.6-0.8), and stationary phase (OD<sub>600</sub> 1.0-1.2). When grown in LB alone, I observed elevated c-di-GMP in early exponential growth, and the concentrations of c-di-GMP decreased as the cell density increased. These observations are consistent with previous studies showing that c-di-GMP is elevated in the low-cell-density QS state [66, 72]. I observed significant increases of the intracellular c-di-GMP concentration in the presence of bile in early exponential and late exponential growth phases (Fig. 9). Alternatively, no significant induction of c-di-GMP was observed in stationary phase. These results indicate that bile induction of c-di-GMP is growth phase dependent. I speculated that QS might be responsible for density-dependent bile induction of c-di-GMP. However, bile induction of c-di-GMP was unchanged in *V. cholerae* mutants locked in either the low- or high-cell density QS state showing this process is independent of QS (data not shown).

### *Three DGCs are more active in the presence of bile*

As SHB increases intracellular c-di-GMP, I hypothesized that specific DGCs in *V. cholerae* would exhibit increased activity in the presence of SHB. To identify these DGCs, I developed a high-throughput screen where the *in vivo* activity of each of the 40 *V. cholerae* DGCs could be determined in the presence and absence of

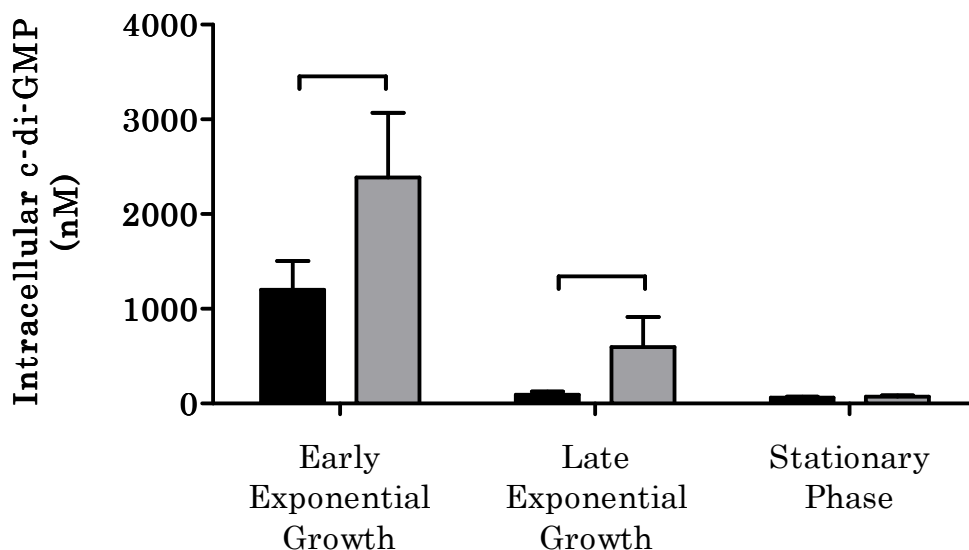


**Figure 9. Intracellular c-di-GMP concentrations of *V. cholerae* during the course of growth with bile.** All intracellular c-di-GMP concentrations were determined using LC-MS/MS. Black bars indicate strains grown in LB and grey bars indicate strains grown in LB + SHB. The reported values indicate the mean and the error bars indicate the standard deviation from the mean. Brackets indicate statistical significance as determined by a one-tailed Student's T-Test (n=3, p > 0.05).

SHB. This screen utilized a series of expression vectors carrying every *V. cholerae* DGC under the control of the IPTG-inducible Ptac promoter and a common ribosome binding site [79]. Therefore, I infer in this system that differences in activity are not due to changes in gene expression. In addition to the DGC expression vector, each strain contained a separate reporter plasmid that carried a transcriptional fusion of a c-di-GMP inducible promoter located within the ORF of VC1673 with the luciferase operon (named 6:C9-*lux*, [107]). These vectors were introduced into a  $\Delta vpsL$  strain of *V. cholerae* which abrogates biofilm formation and eliminates interference of aggregate formation on the analysis of reporter gene expression. In the absence of additional c-di-GMP generated by exogenous

expression of DGCs, the reporter plasmid does not produce significant luminescence in the presence or absence of SHB (Fig. 10, vector control). C-di-GMP production by active DGCs leads to increased luciferase production, as can be seen by induction of luminescence by expression of the constitutively active DGC *qrgB* from *V. harveyi* (Fig. 10, *qrgB*). Induction of this transcriptional reporter is dependent on c-di-GMP synthesis as expression of *qrgB\**, an allele of *qrgB* harboring a mutation in the active site of the protein, does not induce luminescence (Fig. 10, *qrgB\**).

6:C9-*lux* expression was determined upon induction of each DGC in the presence of LB and LB with SHB. Seven DGCs showed reduced luminescence expression in the presence of SHB, although the extent of this reduction was not large (< 3.5-fold). It is not currently known if this reduction of expression is related to bile inhibition of the DGC activity of these proteins, unrelated transcriptional regulation of 6:C9-*lux*, or a non-specific effect of SHB on luminescence. Due to the large number of DGCs that are negatively affected (7,  $p < 0.01$ ), the relatively low reduction, and that bile increases the total intracellular c-di-GMP concentration, I favor the latter two possibilities. Nevertheless, three DGCs demonstrated more than a five-fold fold increase luminescence in the presence of SHB ( $p < 0.01$ , Fig. 10); these DGCs are VC1067 (7.0 fold increase), VC1372 (47.6 fold increase), and VC1376 (6.7 fold increase).

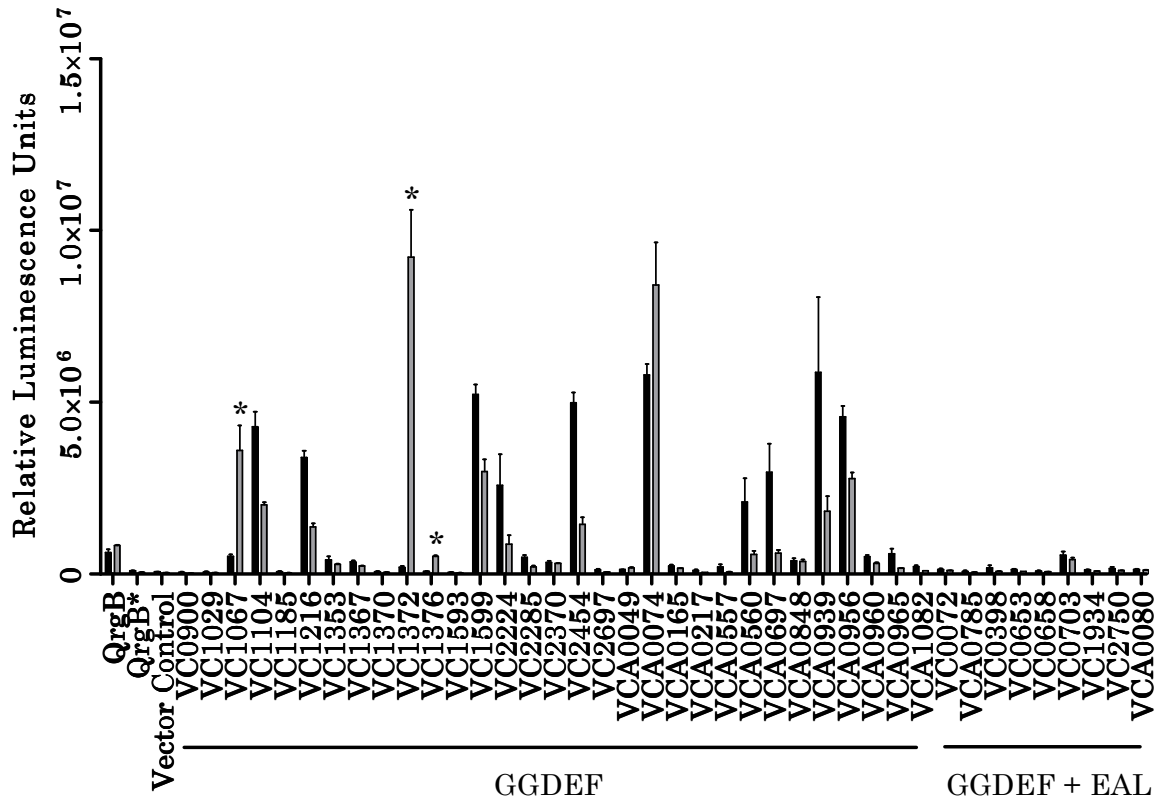


**Figure 10. High-throughput screen of the *in vivo* activity of each of the 40 *V. cholerae* DGCS with bile.** *V. cholerae* strains containing a DGC expression plasmid and the 6:C9-*lux* reporter plasmid were measured for luminescence in LB (black) and LB with SHB (grey). Expression plasmids encoding *qrgB* and its mutant allele counterpart *qrgB\** were included as positive and negative controls, respectively. The vector control indicates expression of 6:C9-*lux* in the absence of protein induction. The error bars indicate standard deviation. Statistical significance (\*) was determined for cultures exhibiting a positive fold change (LB + SHB / LB) greater than two as determined by a Student's one tailed T-Test (n=3, p < 0.01).

*The activity of PDEs in V. cholerae is not altered by bile*

The hydrolysis of c-di-GMP is driven by c-di-GMP-specific PDE enzymes, which contain either a C-terminal EAL or HD-GYP domain. Like DGC enzymes, these proteins are also modular and the variable N-terminal domain is thought to

respond to environmental stimuli. I hypothesized that an increase in intracellular c-di-GMP in response to bile acids could be caused by a repression of PDE activity. To examine this possibility, I developed a second high-throughput screen to analyze the enzymatic activity of the 29 predicted PDEs of *V. cholerae*. The sequence of one EAL protein, VC0515, was highly divergent from the sequenced N16961 strain upon amplification from the genome, and was thus excluded from analysis; this is consistent with other studies reporting sequence variance [72]. Similar to the screen above, each *V. cholerae* PDE is expressed from an inducible expression vector that has been introduced into a  $\Delta vpsL$  strain of *V. cholerae* containing the 6:C9-*lux* reporter vector. A third vector (pBRP02) was introduced containing the constitutively active DGC *qrgB*, effectively increasing the baseline c-di-GMP concentration and subsequently the baseline luminescence values. Robust reporter gene expression can be seen in a strain expressing *qrgB* with a vector control that has no exogenous PDE expression (Fig. 11, vector control).

Strains of *V. cholerae* expressing each PDE alongside the DGC *qrgB* were grown in LB and LB with SHB, and the expression of 6:C9-*lux* was quantified. 22 of the 29 PDEs showed appreciable decreases ( $> 2$ -fold,  $p < 0.01$ ) in luminescence when grown in LB compared to the vector control (Fig. 11), indicating that these PDEs are actively hydrolyzing c-di-GMP. However, none of the PDEs demonstrated any appreciable difference when grown in LB with SHB compared to LB alone (Fig. 11). Thus, I conclude that SHB does not affect the c-di-GMP hydrolysis of PDEs in the conditions I examined here.

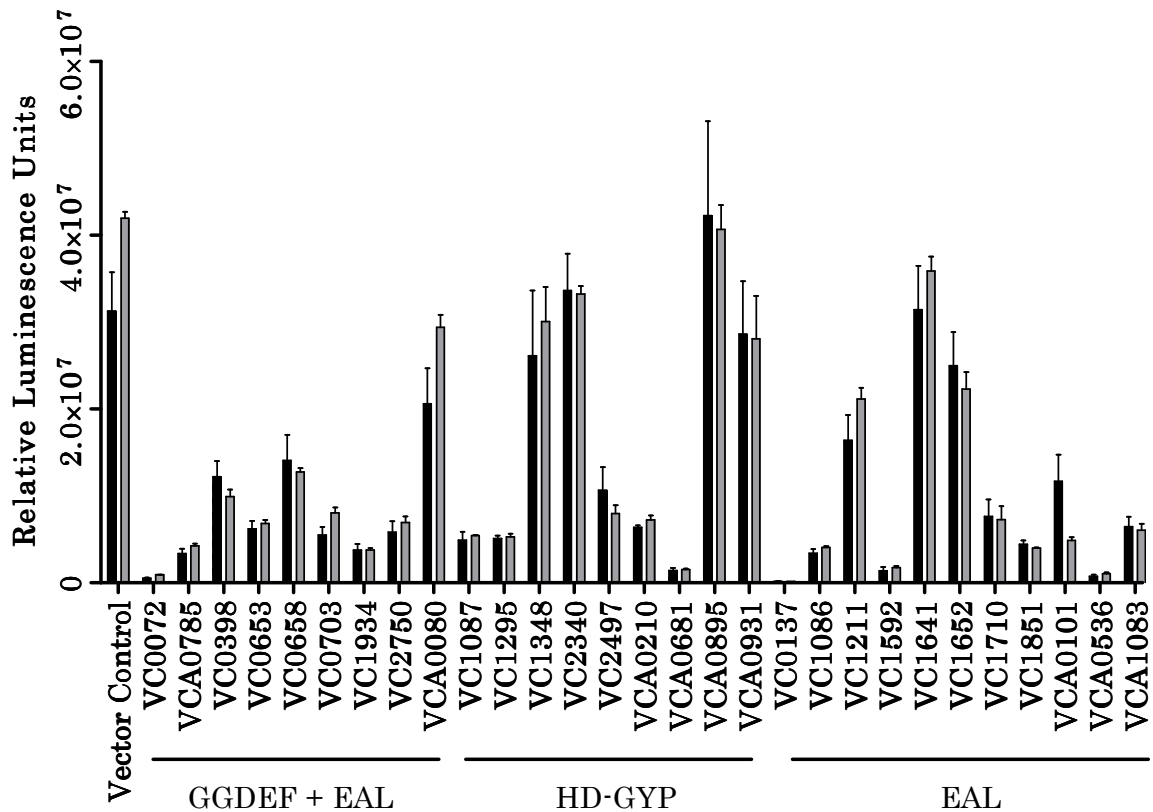


**Figure 11. High-throughput screen of the *in vivo* activity of each of the 40 *V. cholerae* PDEs with bile.** *V. cholerae* strains containing a PDE expression plasmid, the 6:C9-*lux* reporter plasmid, and the *qrgB* expression plasmid were measured for luminescence in LB (black bars) and LB with SHB (grey bars). The vector control indicates expression of 6:C9-*lux* with *qrgB* induction and without PDE expression. The error bars indicate standard deviation (n=3).

*The three bile-inducible DGCs are inner membrane proteins*

I analyzed the predicted domain structure and subcellular localization of the three bile inducible DGCs to search for commonalities. An analysis of the relative hydrophobicity of the amino acid sequence of these three DGCs using the program toppred predicts that all contain transmembrane spanning domains (Fig. 12, [111-113]). The DGC VC1067 (GI: 15641080), which has also been referred to as *cdgH*

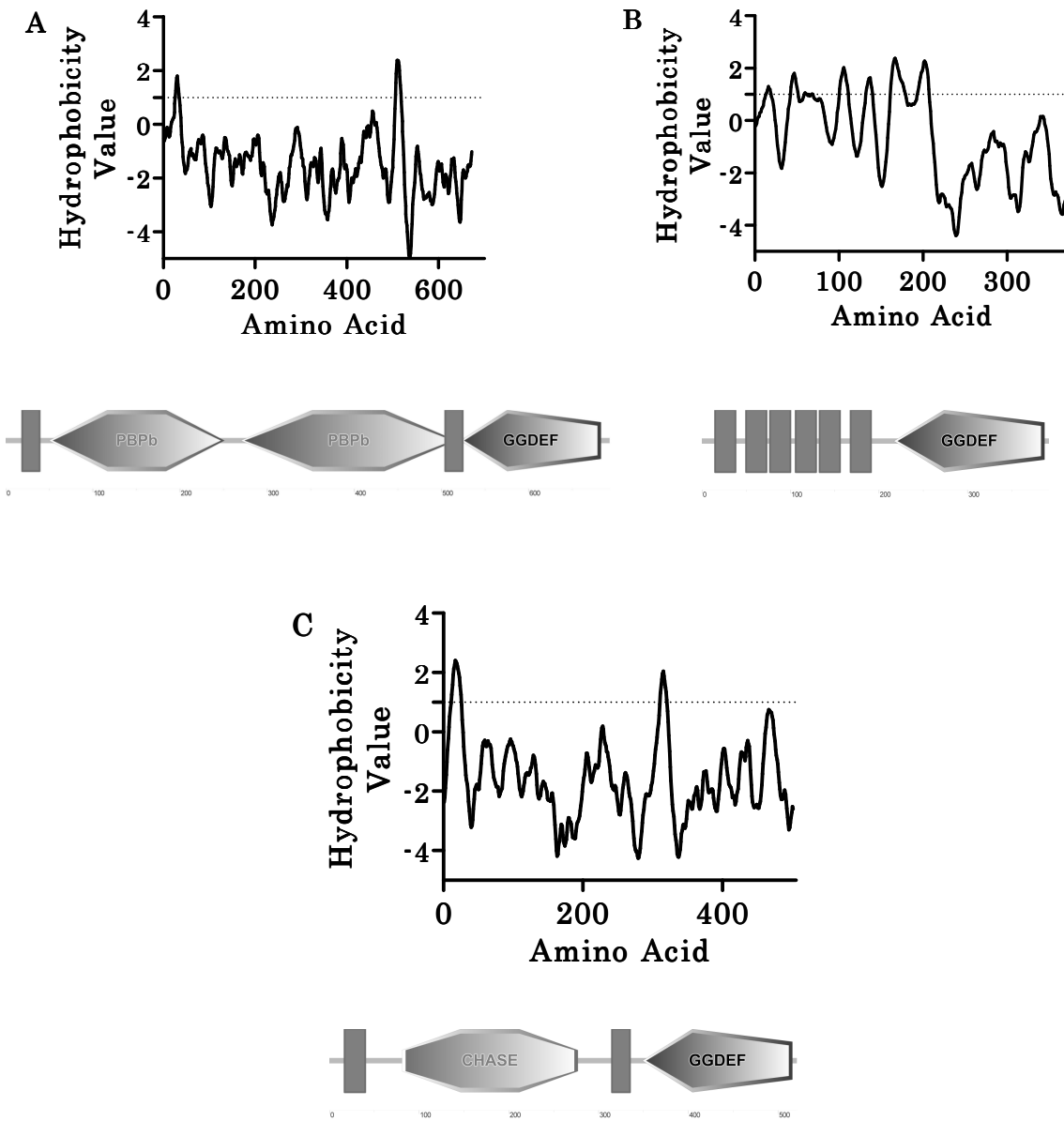


**Figure 12. The amino acid sequence hydrophobicity and predicted signaling domains of the bile-responsive DGCs.** The amino acid sequence of (A) VC1067, (B) VC1372, and (C) VC1376 was used to predict transmembrane domains using the toppred program. The dotted line indicates the cutoff value for a potential transmembrane domain. A depiction of the potential N-terminal signaling domains and transmembrane domains (grey rectangles) and the C-terminal GGDEF domain of each DGC are shown below each respective hydrophobicity plot. The images were adapted from the SMART database [113].

[94], is predicted to contain two sequential periplasmic substrate-binding domains (PBPb) in the N-terminus while VC1376 (GI: 15641388), which has also been referred to as *cdgM* [97], is predicted to contain a conserved CHASE domain. VC1372 (GI: 15641384) does not contain any conserved protein domains in the N-terminus; however, analysis of the relative hydrophobicity of the amino acid sequence using toppred predicts 6 sequential intra-membrane spanning domains.

*Three DGCs increase c-di-GMP synthesis in the presence of bile acids*

To directly examine if SHB increases the DGC activity of these three enzymes, I quantified the intracellular c-di-GMP concentration of strains ectopically expressing VC1067, VC1372, or VC1376 grown in the presence and absence of SHB. I similarly analyzed expression of active site mutant alleles of these genes (GG[D/E]EF -> AA[D/E]EF) that render them incapable of c-di-GMP synthesis. As addition of SHB increases the intracellular c-di-GMP concentration of *V. cholerae* (Fig. 8), I hypothesized that the strains expressing each AA[D/E]EF mutant would show increased intracellular c-di-GMP in the presence of bile similar to that of the WT strain. Moreover, induction of the bile-activated DGCs would lead to more c-di-GMP synthesis in the presence of bile versus LB alone.

When grown in LB media, there was no notable difference between strains expressing any of the AA[D/E]EF alleles and the vector control in LB media. As expected growth of the vector control or DGC mutants in bile showed similar increases in c-di-GMP. Induction of the DGCs VC1067 and VC1376 produced

significantly increased amounts of c-di-GMP in LB alone, leading to intracellular c-di-GMP concentrations of  $48.4 \pm 7.0 \mu\text{M}$  and  $19.3 \pm 10.0 \mu\text{M}$ , respectively (Fig. 13). Alternatively, the intracellular c-di-GMP of the VC1372 expression strain in the absence of bile ( $116.9 \pm 17.4 \text{ nM}$ ) was not significantly altered compared to the vector control ( $263.7 \pm 119.7 \text{ nM}$ ), indicating that this DGC does not produce c-di-GMP in LB media alone. Importantly, the intracellular concentration c-di-GMP was increased significantly upon ectopic expression of VC1067, VC1372, and VC1376 in the presence of LB with SHB versus LB alone resulting in intracellular concentrations of  $89.2 \pm 31.5 \mu\text{M}$ ,  $4.3 \pm 0.4 \mu\text{M}$ , and  $67.4 \pm 20.1 \mu\text{M}$  c-di-GMP, respectively (Fig. 13). These data together indicate that VC1067, VC1372, and VC1376 synthesize more c-di-GMP in the presence of bile acids.

*A toxR deletion mutant partially loses bile-mediated c-di-GMP increase*

One system that has been implicated in the bile response of *V. cholerae* is the ToxR virulence regulatory network. The transcriptional regulator ToxR controls the expression of the virulence regulator ToxT, as well as the expression of CT and TCP [114, 115]. Furthermore, ToxR mediates bile resistance in *V. cholerae* by altering the expression of *ompU* and *ompT* [43, 116]. It has also been shown that bile acids alter the protein activity of ToxR [117]. I hypothesized that bile acids act through ToxR or ToxT to alter the transcription of c-di-GMP turnover enzymes resulting in increased global c-di-GMP concentrations. To determine if bile mediated changes in ToxR or ToxT transcription regulation effect intracellular c-di-GMP, I generated  $\Delta\textit{toxR}$  and  $\Delta\textit{toxT}$  deletion strains and measured intracellular c-di-

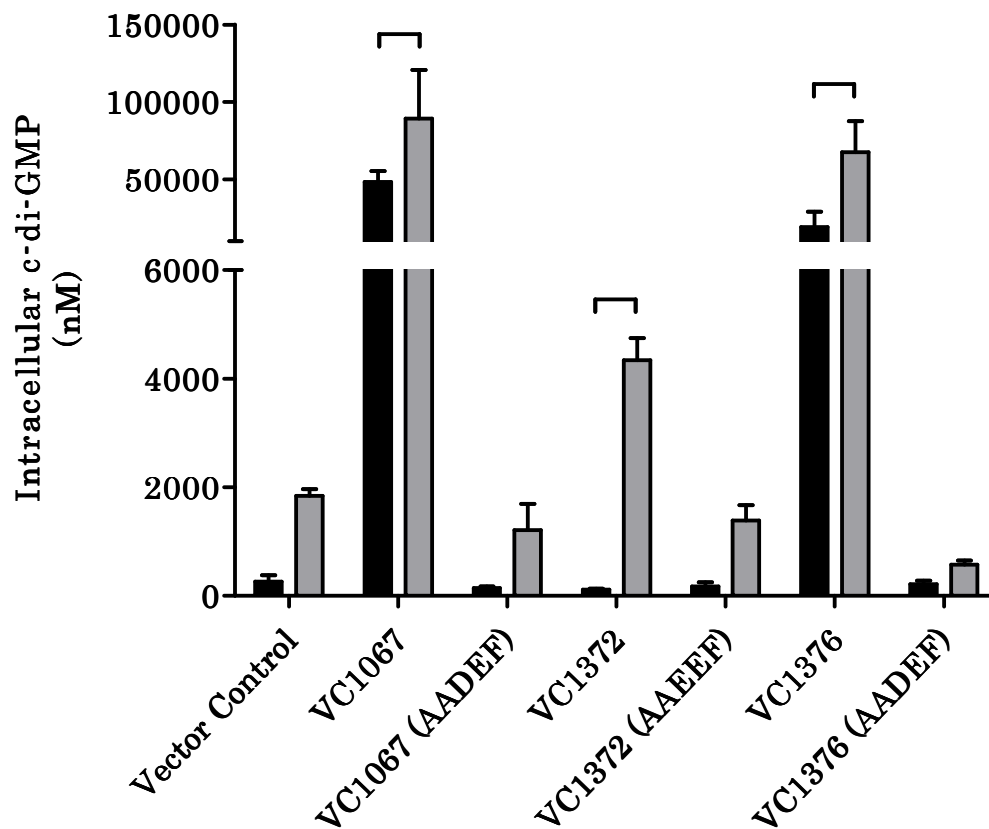


**Figure 13. Intracellular c-di-GMP concentrations of *V. cholerae* DGC expression strains in the presence and absence of SHB.** The c-di-GMP concentrations of the empty vector strain or the VC1067, VC1372, or VC1376 expression strains were quantified with LC-MS/MS. The intracellular c-di-GMP of strains expressing alleles containing mutations in the active site motif of each DGC were also quantified. The black bars indicate strains grown in LB, while the grey bars indicate strains grown in LB with SHB. Error bars indicate standard deviation. Brackets indicate statistical significance, which was determined using a Student's one tailed T-Test (n=3, p < 0.05).

GMP in the presence and absence of SHB. I found that while the  $\Delta toxR$  strain showed no significant difference to the WT strain in LB alone, intracellular c-di-GMP was 44.9% lower in the  $\Delta toxR$  strain compared to WT in LB with SHB (Fig. 14). Similar to the  $\Delta toxR$  strain, the intracellular c-di-GMP of the  $\Delta toxT$  strain is

not discernibly different in LB. In contrast, the intracellular c-di-GMP of the  $\Delta toxT$  strain is modestly reduced in LB with SHB compared to WT, however this difference is not statistically relevant. These results indicate that the transcriptional regulator ToxR plays a role in the bile-mediated increase in intracellular c-di-GMP.

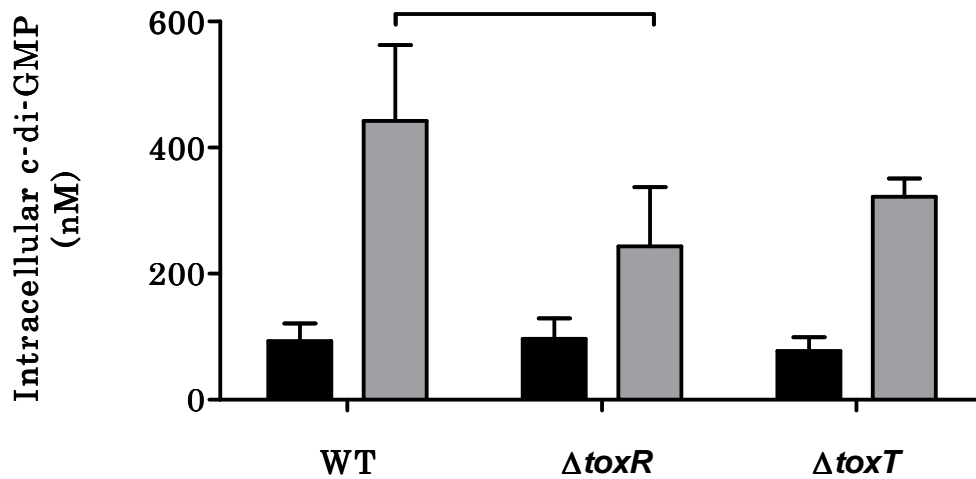


**Figure 14. Intracellular c-di-GMP concentrations of *V. cholerae*  $\Delta toxR$  and  $\Delta toxT$  deletion mutants in the presence of bile.** LC-MS/MS was used to quantify intracellular c-di-GMP. Black bars indicate strains grown in LB and grey bars indicate strains grown in LB with SHB. The reported values indicate the mean and the error bars indicate the standard deviation from the mean. Brackets indicate statistical significance as determined by a one-tailed Student's T-Test (n=6, WT and  $\Delta toxR$ , n=3,  $\Delta toxT$ , p > 0.05).

*Transcription of VC1295 is inhibited by bile acids*

I hypothesized that the presence of bile could also regulate the transcription of DGCs or PDEs to control intracellular c-di-GMP concentration. Specifically, bile could increase the expression of DGCs or decrease the expression of PDEs to

increase intracellular c-di-GMP. To examine this possibility, I measured the relative transcription of 51 GGDEF, GGDEF+EAL, and EAL proteins in LB and LB with SHB by growing strains of  $\Delta vpsL$  *V. cholerae* containing transcriptional fusions of approximately 500 bp DNA upstream of each gene to *gfp*. After 8 hours of growth, I found that there was less than a 2-fold difference in fluorescence between all GGDEF, GGDEF + EAL, and EAL strains grown in the presence and absence of bile (Fig. 15 A and B) suggesting that in the conditions examined here, regulation of GGDEF and EAL gene transcription by bile does not play a significant role in the bile mediated increase of intracellular c-di-GMP.

I also examined the relative transcription of the 8 HD-GYP proteins in LB and LB with SHB using transcriptional fusions of each promoter, defined as approximately 500 bp upstream of each HD-GYP gene, to the *lux* operon. The HD-GYP gene VC1087 is encoded in a putative operon with the EAL gene VC1086, and thus the expression is presumed to be synonymous with VC1086 (Fig. 15 B). The luminescence of each reporter strain was determined after 6 hours of growth in either LB or LB with SHB. The expression of six of the genes encoding HD-GYP proteins was not significantly changed in LB with SHB compared to LB (> 2-fold), whereas the expression of VC2497 was modestly increased in the presence of SHB (2.2-fold,  $p < 0.05$ ). Importantly, the expression of VC1295 (GI: 15641308) was decreased 2.8 fold when grown in the presence of SHB (Fig. 15C,  $p < 0.05$ ). VC1295 appears to be an active PDE when ectopically expressed in *V. cholerae* (Fig. 11).

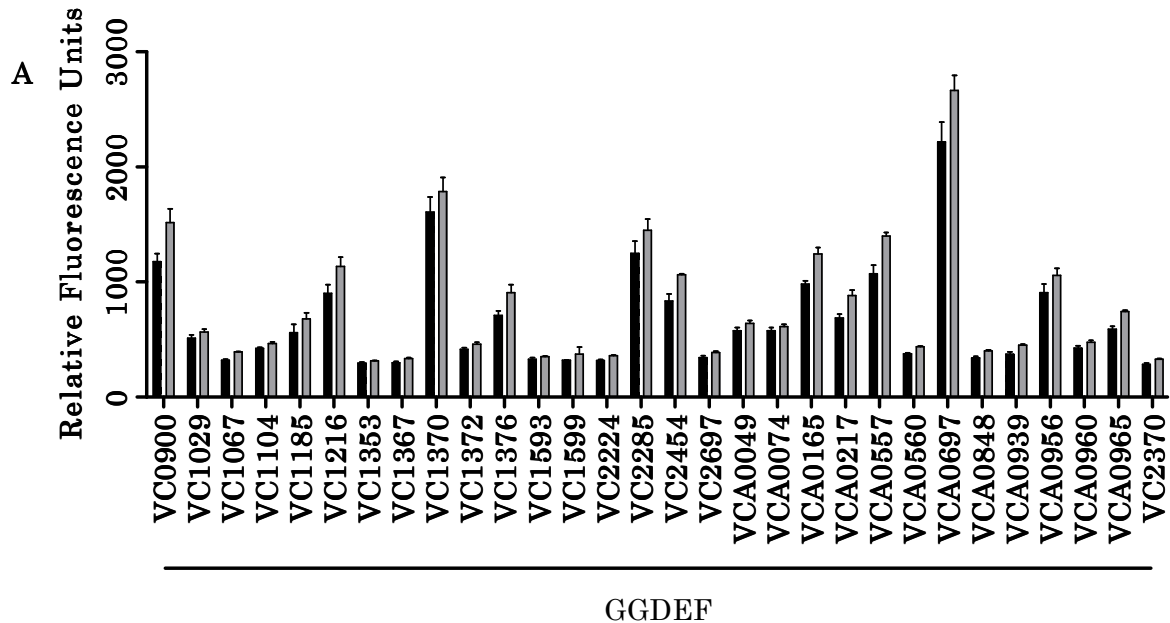


**Figure 15. Relative transcription of DGCs and PDEs in the presence and absence of bile.** (A) *V. cholerae* strains containing a transcriptional fusion of each GGDEF protein promoter to *gfp* was grown in LB (black) or LB with SHB (grey). The fluorescence in each environmental condition was quantified after 8 hours of growth (n=3). (B) *V. cholerae* strains containing a transcriptional fusion of each GGDEF + EAL or EAL protein promoter to *gfp* was grown in LB (black) or LB with SHB (grey). The fluorescence in each environmental condition was quantified after 8 hours of growth (n=3). (C) *V. cholerae* strains containing a transcriptional fusion of each promoter driving expression of an HD-GYP to luciferase were grown in LB (black) or LB with SHB (grey). Luminescence was quantified after 6 hours of growth (n=4) in each environmental condition. All cultures were normalized to an OD<sub>600</sub> reading. Error bars indicate standard deviation. \* indicates statistical significance from the LB condition, determined by a one-tailed Students T-Test ( $p < 0.05$ ).



This result indicates that bile acids decrease the expression of VC1295, possibly resulting in decreased c-di-GMP hydrolysis contributing to increased intracellular c-di-GMP.

*Three DGCs and one HD-GYP account for bile-mediated c-di-GMP induction*

To determine if the DGCs VC1067, VC1372, and VC1376 contribute to the bile-mediated increase of intracellular c-di-GMP in *V. cholerae*, I constructed unmarked *V. cholerae* DGC deletion mutants and examined SHB mediated induction of c-di-GMP (Fig. 16). Similar to my previous findings, the intracellular c-di-GMP concentration of *V. cholerae* increased 4.1 fold in the presence of SHB in the WT strain. Both the  $\Delta$ VC1067 and  $\Delta$ VC1376 single mutants showed a modest but significant reduction of c-di-GMP when grown in bile compared to the WT strain, having 29.6% and 24.9% less c-di-GMP, respectively. The  $\Delta$ VC1372 single mutant and  $\Delta$ VC1372 $\Delta$ 1376 double mutant were not statistically different from the WT strain. Importantly, the  $\Delta$ VC1067 $\Delta$ VC1372 $\Delta$ VC1376 triple mutant strain exhibited the greatest reduction of intracellular c-di-GMP in the presence of bile, losing 46.8% of the intracellular c-di-GMP compared to the WT strain in LB with SHB ( $p < 0.05$ ). These results suggest that VC1067, VC1372, and VC1376 function redundantly in the bile-mediated c-di-GMP induction.

As the expression of the HD-GYP VC1295 was inhibited by bile acids, I constructed an unmarked *V. cholerae* VC1295 deletion mutant and quantified intracellular c-di-GMP in the presence and absence of SHB. In LB alone, the

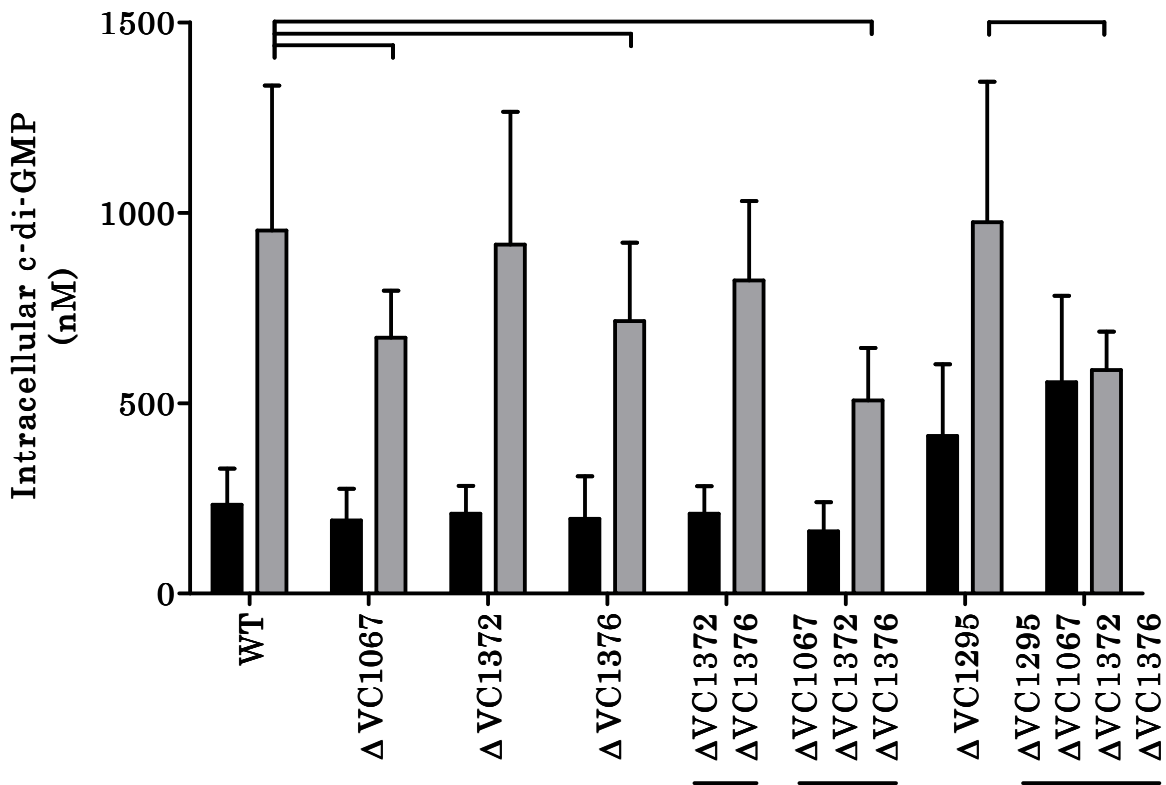


**Figure 16. Intracellular c-di-GMP concentrations of *V. cholerae* DGC and PDE mutant strains in the presence and absence of bile.** LC-MS/MS was used to quantify c-di-GMP after growth in LB (black) or LB with SHB (grey). The reported values indicate the mean and the error bars indicate standard deviation. Brackets indicate statistical significance as determined by a one-tailed Students T-Test (n=9-10, p < 0.05).

intracellular c-di-GMP was modestly increased 1.8 fold in the ΔVC1295 mutant compared to WT (Fig. 16, p < 0.05). This result is expected as deletion of an active PDE will increase intracellular c-di-GMP. However, the intracellular c-di-GMP concentrations of the ΔVC1295 strain grown in the presence of SHB were indistinguishable from WT. I hypothesized that both activation of DGC activity and transcriptional regulation of VC1295 contribute to bile induction of c-di-GMP. To test this, I created a quadruple ΔVC1295ΔVC1067ΔVC1372ΔVC1376 mutant and

measured intracellular c-di-GMP in the presence and absence of SHB. Similar to the  $\Delta VC1295$  single mutant, when grown in LB alone the quadruple mutant had elevated intracellular c-di-GMP compared to the WT strain (2.4 fold,  $p < 0.05$ ). Importantly, this strain showed no change in intracellular c-di-GMP in the presence of SHB. This indicates that these four proteins are responsible for the bile-mediated changes in intracellular c-di-GMP.

*Deletion of the bile-responsive DGCs and PDE reduces bile induction of V. cholerae biofilm formation*

It has been previously reported that BV (i.e., bovine bile) increases biofilm formation of *V. cholerae*, and this induction is dependent on the transcriptional regulator *vpsR* [47]. VpsR binds c-di-GMP to regulate the transcription of biofilm genes [107]. I wondered if the levels of c-di-GMP measured in the various DGC and PDE mutants strains with and without bile would correlate with biofilm formation. To test this, I performed a static biofilm assay where the wild type,  $\Delta vpsL$  mutant, and the DGC and PDE *V. cholerae* mutant strains were grown in polystyrene test tubes containing LB or LB with BV without shaking followed by crystal violet (CV) staining of the resulting attached biofilm. The  $\Delta vpsL$  mutant cannot produce exopolysaccharide and thus does not form biofilms. BV was used to induce biofilm formation to remain consistent with prior studies [47, 117] and because it induced more robust biofilm formation in this assay than SHB (data not shown).

I observed that all cultures of *V. cholerae* grew to a significantly lower optical density, as measured by OD<sub>600</sub>, after static growth in the presence of BV. To account for these growth differences, the biofilm formation of each culture was normalized to the OD<sub>600</sub> of the planktonic culture. Consistent with previous reports [47], BV increased biofilm formation in the WT strain 2.7-fold, and this response was eliminated in the  $\Delta vpsL$  strain (Fig. 17). While the  $\Delta VC1067$ ,  $\Delta VC1376$ , and  $\Delta VC1372\Delta 1376$  mutants all showed modest to no loss of bile induced c-di-GMP (Fig. 16), these mutants no longer exhibited significant bile-induced biofilm formation. Only the  $\Delta VC1372$  mutant induced biofilm formation in response to bile, indicating that this DGC contributes less to biofilm formation. As expected, the triple DGC mutant showed the lowest level of biofilm formation and was not responsive to bile addition. Although the  $\Delta VC1295$  strain had modestly elevated c-di-GMP in LB, deletion of VC1295 had no noticeable impact on biofilm formation. Like the triple mutant, the DGC/PDE quadruple mutant exhibited low biofilm formation that was unresponsive to bile addition. These results demonstrate that the bile responsive DGCs are required for c-di-GMP dependent biofilm formation in response to bile acids. However, the HD-GYP VC1295 did not contribute to biofilm formation in this assay.

*Bicarbonate decreases the bile-mediated increase of c-di-GMP in V. cholerae*

As c-di-GMP has been shown to repress virulence gene expression in *V. cholerae*, it remained puzzling as to why bile would increase c-di-GMP [35]. I hypothesized that additional signals in the small intestine could override this

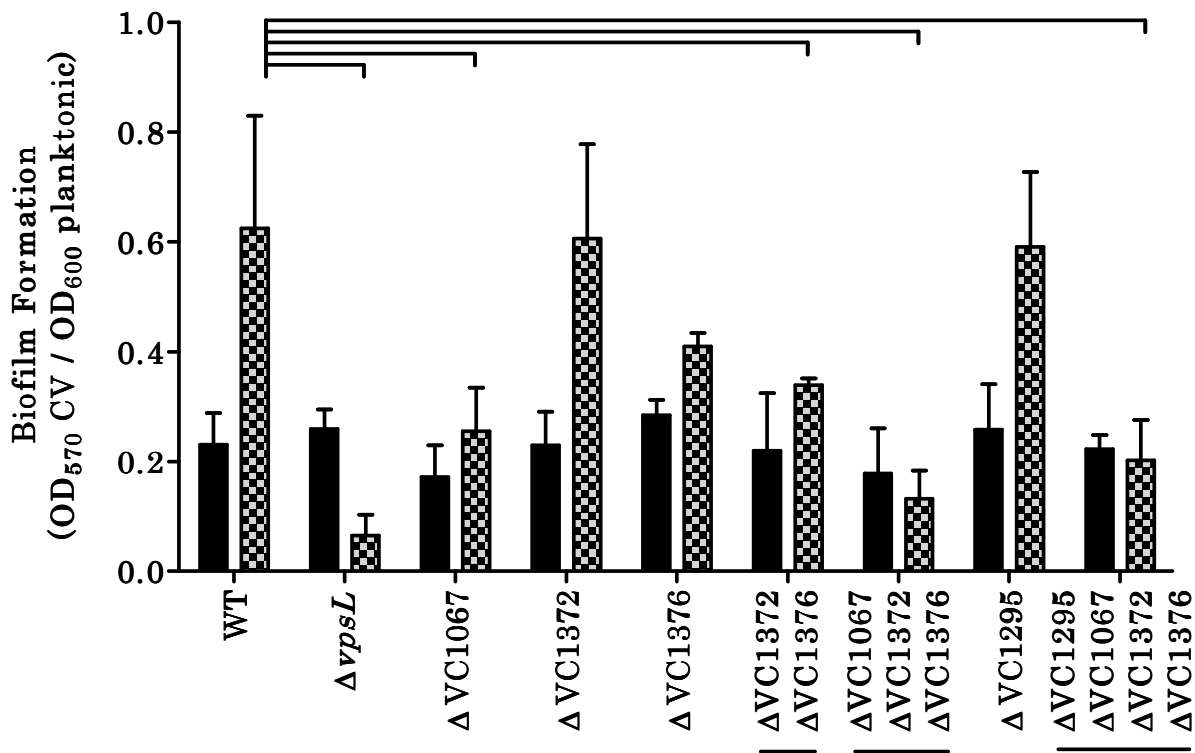


**Figure 17. Biofilm formation of *V. cholerae* DGC and PDE mutants in the presence of BV.** Biofilm formation was quantified in test tubes using CV. A strain containing a mutation in the *vpsL* gene was included as a negative control. The CV value was normalized by the OD<sub>600</sub> value of the planktonic culture to account for differences in growth. The reported values indicate the mean, and error bars indicate standard deviation from the mean. Brackets indicate statistical significance as determined by a Student's one tailed T-Test (n=3, p < 0.05).

induction. Another major component of the human small intestine is bicarbonate, which is secreted by the pancreas as well as the small intestinal epithelial cells. Bicarbonate acts as a pH buffer to neutralize acids secreted by the stomach [118, 119]. Bicarbonate has also been implicated in virulence gene regulation in *V. cholerae* [120]. As bicarbonate is abundant in the small intestine, I hypothesized that it may contribute to the regulation of intracellular c-di-GMP in *V. cholerae*. To examine if bicarbonate impacted bile induction of c-di-GMP, I measured

intracellular c-di-GMP of *V. cholerae* when grown in the presence and absence of SHB and bicarbonate. I observed no significant difference in intracellular c-di-GMP of *V. cholerae* in the presence of bicarbonate alone (Fig. 18). However, growth of *V. cholerae* in the presence of both SHB and bicarbonate completely abolished bile induction of c-di-GMP (Fig. 18).

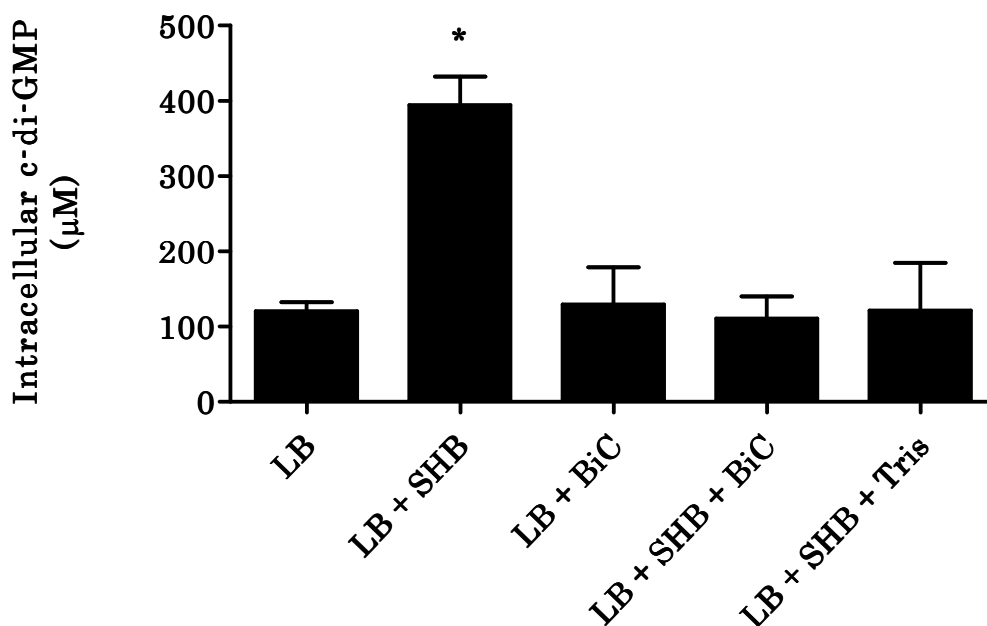


**Figure 18. Intracellular c-di-GMP concentrations of *V. cholerae* grown in the presence of bile and bicarbonate.** LC-MS/MS was used to quantify c-di-GMP of *V. cholerae* grown in LB, LB with bicarbonate (BiC), or LB with SHB and different supplements. The reported values indicate the mean and the error bars indicate the standard deviation. \* indicates statistical significance compared to LB as determined by a one-tailed Student's T-Test (n=3, p > 0.05).

As bicarbonate acts as a buffer in the small intestine, I hypothesized that bicarbonate suppression of the bile induction of c-di-GMP was due to pH changes. I tested this idea by growing *V. cholerae* in the presence of SHB with the pH buffer

Tris. The pH of LB media and LB with SHB media was approximately the same and did not change significantly over the course of growth (pH LB, pre growth: 7.3, post growth: 7.0; pH LB with SHB, pre growth: 7.3, post growth: 7.1). Upon addition of bicarbonate, the pH increased substantially (pH LB with SHB and BiC, pre growth: 8.1, post growth: 8.7). The addition of Tris caused a similar increase in pH (pH LB with SHB and Tris, pre growth: 8.7, post growth: 8.6). Analogous to bicarbonate, the addition of Tris to LB with SHB media inhibited the normal induction of c-di-GMP by bile (Fig. 18), indicating that this inhibition of bile induced c-di-GMP is pH dependent.

### *Discussion*

Bile is an abundant component of the human small intestine, and thus a probable physiological cue for *V. cholerae* to recognize upon entry into this environment. A number of lines of evidence suggest that bile is an important signal in the transition of *V. cholerae* between environmental and infectious lifestyles. Bile acids increase the expression of *ompU* in a *toxR*-dependent manner to increase bile resistance, indicating that the classical biotype of *V. cholerae* is capable of sensing the presence of bile [116]. There are conflicting reports regarding bile control of virulence factor expression. Bile acids were reported to negatively regulate the expression of the TCP and CT in a *toxT*-dependent manner in a classical biotype, demonstrating that there is a link between bile and virulence [121]. Contrary to this finding, bile acids were reported to induce CT and TCP in a *toxR*-dependent manner in a classical *V. cholerae* biotype and a *tcpP*-dependent manner in the El Tor

biotype used in this study [117, 122]. From these studies, it is clear that *V. cholerae* responds to bile to induce a number of physiological changes. In this work, I explore the connections between bile and c-di-GMP.

Based on the prevailing *V. cholerae* disease model hypothesizing that c-di-GMP levels are decreased upon infection, I predicted that bile acids would decrease intracellular c-di-GMP concentrations. Contrary to this prediction, I found that bile acids increase the intracellular c-di-GMP concentration of *V. cholerae* (Fig. 8). This finding suggests that the dynamics of the c-di-GMP signaling system in the human host are more complex than previously appreciated. Furthermore, I have found the difference in the bile mediated change of c-di-GMP is largest during exponential growth and that at stationary phase this difference was negated. Consistent with these findings, it has been shown that intracellular c-di-GMP is depleted at high cell density, and that these changes are due in part to quorum sensing [66, 72, 77]. My results indicate that this regulation is dominant over the increase in intracellular c-di-GMP caused by bile.

To begin to understand how *V. cholerae* modulates its intracellular c-di-GMP in response to bile, I determined if the activity of any DGCs or PDEs were affected by bile using a novel high-throughput *in vivo* assay. This assay is easily adaptable to examine the response of DGCs and PDEs to any environmental cue, and it can be modified to explore other bacteria if a suitable *in vivo* reporter of c-di-GMP levels is available. Three DGCs (VC1067, VC1372, and VC1376) exhibited increased c-di-GMP synthesis activity in the presence of SHB (Fig. 10, 13). The DGC activity of

VC1372 appeared to be absolutely dependent on bile whereas bile modulated the basal activities of VC1067 and VC1376. All of these DGCs are important for the bile-induced increase of intracellular c-di-GMP and biofilm formation of *V. cholerae* (Fig. 16, 17).

The mechanisms by which these three DGCs respond to bile acids are currently unknown. All three DGCs are predicted to be associated with the inner membrane. VC1067 has been implicated in biofilm formation as it induces rugosity associated phenotypes in *V. cholerae* [94]. Furthermore, it has been shown that both VC1067 and VC1376 actively produce c-di-GMP and stimulate biofilm formation [79, 94], and a VC1376 mutant strain also demonstrates lower *vpsL* expression [97]. VC1376 has also been implicated in the indole-induced increase in biofilm formation [96]. Furthermore, all three DGCs also have been shown to repress motility when ectopically expressed in *V. cholerae*; this is particularly interesting as the levels of motility repression of the VC1372 and VC1376 expression strains do not seem to correlate with the intracellular c-di-GMP levels reported here (Fig. 13) [123]. Analysis by BLAST revealed that homologous sequences to VC1372 are only found in a few *Vibrio* species dominated by strains of *V. cholerae*. A previous study has also noted that VC1372 is unique to *V. cholerae* amongst the genus *Vibrio* [124].

The phylogenetic link of VC1372 with an enteric human pathogen, the domain structure of VC1372, and my observation that the activity of VC1372 is absolutely dependent on the presence of bile suggest the physiological cue which controls VC1372 is bile. Bile acids are known to interact with the cell membrane

due to their detergent activity [41]. Moreover, I observed bile-mediated activation of VC1372 in *E. coli* (data not shown), an orthologous system with no clear homolog to VC1372. Alternatively, as both VC1067 and VC1376 maintain robust activity upon exogenous expression even in the absence of bile, I postulate these DGCs might be controlled indirectly by bile through sensing perturbations in the membrane.

Additionally, the expression of the PDE VC1295 was inhibited by bile acids (Fig. 15C). This HD-GYP actively hydrolyzes c-di-GMP in both LB and LB with SHB, but bile acids do not affect this activity (Fig. 11). VC1295 is predicted to be composed of 492 amino acids and contains 6 predicted N-terminal transmembrane domains preceding a HAMP domain linked to the HD-GYP domain [111-113]. The mechanism governing this transcriptional regulation of VC1295 by bile remains unknown. Analysis of the VC1295 promoter region reveals motifs resembling the ToxR binding site (-127 bp, TCAAA-N<sub>11</sub>-TTAAA [114]). While this gene is not listed amongst the known genes regulated by ToxR [33] there is evidence that the activity of ToxR is altered by bile [117], suggesting that the ToxR regulon could be altered when bile acids are present. As a  $\Delta$ *toxR* strain of *V. cholerae* partially loses the bile-induced increase in c-di-GMP (Fig. 14), I hypothesize that in the presence of bile, ToxR inhibits the expression of VC1295. Although VC1295 contributed to bile-induced c-di-GMP, I did not observe any effect of VC1295 on biofilm formation. I speculate that this result is due to the distinct experimental differences in which c-di-GMP and biofilm formation were measured.

Another important host derived cue is bicarbonate, a biological pH buffer that is highly abundant in the human small intestine [119]. Bicarbonate has been shown to be important for virulence, as bicarbonate is critical for *in vitro* production of CT [80]. Bicarbonate is capable of activating *V. cholerae* virulence gene expression via the transcriptional regulator *toxT* [120]. I have shown that bicarbonate is able to suppress the bile-mediated induction of c-di-GMP in *V. cholerae*. Furthermore, this regulation is driven by changes in pH, as the bile-mediated induction is similarly repressed by Tris (Fig. 18). It is possible that the change in pH alters the structure of bile so that it no longer triggers the c-di-GMP synthesis activity of the DGCs. Alternatively, the bicarbonate could directly interact with DGCs or PDEs to competitively alter intracellular c-di-GMP.

As bile has strong antimicrobial properties [125], it may be physiologically advantageous for *V. cholerae* to increase c-di-GMP to grant elevated tolerance to bile acids and other stresses associated with the intestinal environment. Other studies have indicated that biofilm formation is important for increased acid shock tolerance and protection from bile acids [47, 75], and biofilms increase infectivity and intestinal colonization in a mouse infection model [126]. Indeed, I confirmed that BV induces biofilm formation in *V. cholera* and showed that all three bile-responsive DGCs were required for bile-induction of biofilm formation.

I propose that bile stimulates a high intracellular c-di-GMP concentration in the intestinal lumen (Fig. 19). Upon penetration of the mucosal layer where the bicarbonate concentration and thus the pH is elevated [127], the response to bile is

abrogated leading to a corresponding decrease in intracellular c-di-GMP. The physiological consequences of spatial alteration of c-di-GMP within the small intestine remain to be determined although I speculate c-di-GMP could be modulating biofilm formation, motility, and virulence gene expression. My model predicting high c-di-GMP concentrations in the lumen and decreased c-di-GMP proximal to the intestinal epithelial cells is consistent with previously described virulence gene regulatory models for *V. cholerae* and *S. enterica* [120, 128, 129].

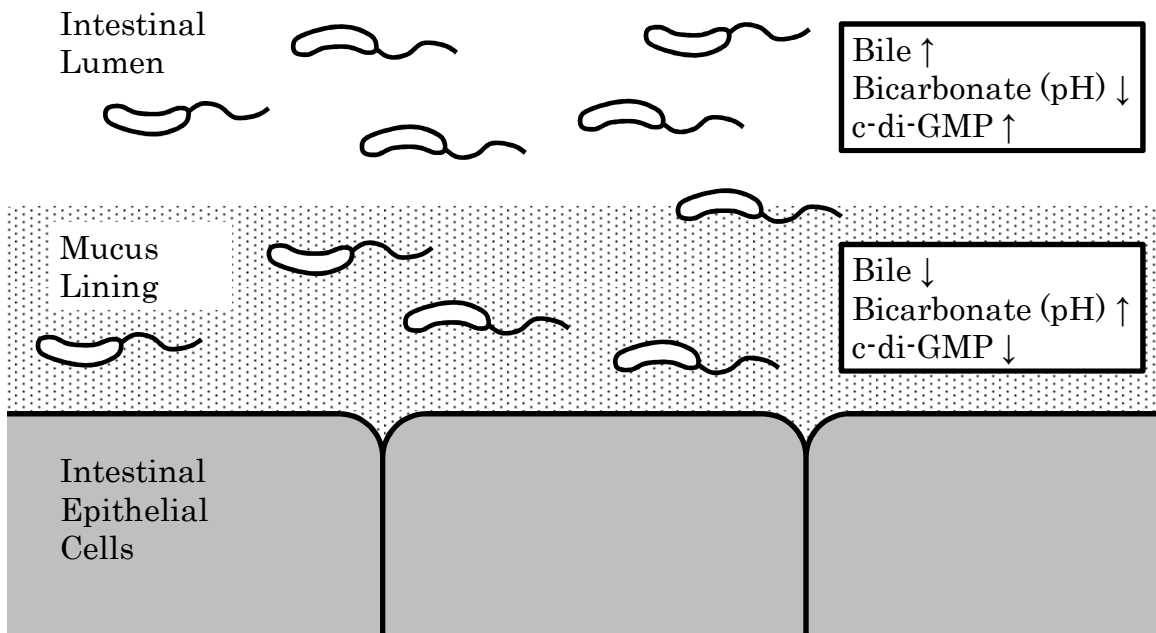


**Figure 19. Proposed model of *V. cholerae* c-di-GMP regulation in the human small intestine.** C-di-GMP is elevated in the lumen, where the concentration of bile is elevated and the concentration of bicarbonate is low. Upon entry into the mucosal layer where bile is low and the bicarbonate concentration is elevated, c-di-GMP is repressed.

My findings indicate that both bile and bicarbonate are environmental cues that modulate c-di-GMP signaling in *V. cholerae* and facilitate the transition from aquatic environments to the human host. They suggest that modulation of c-di-GMP levels by *V. cholerae* upon entry into the human host is more complex than previously appreciated, and that both bile and bicarbonate act together to inversely regulate the intracellular concentration of c-di-GMP to presumably enable the bacteria to adapt and thrive in the diverse intestinal environment.

### *Future directions*

In the search to identify specific environmental signals that affect c-di-GMP levels, I found that bile acids increase intracellular c-di-GMP in *V. cholerae*. Furthermore, I showed that bile acids increase the c-di-GMP synthesis of three DGCs. However, the mechanisms that govern the behavior of these three enzymes are unknown. One common attribute that these proteins share is that they all have predicted trans-membrane domains. It is possible that changes in the cell membrane caused by bile acids could serve as a signal to alter DGC activity. In support of this, it has been shown that temperature mediated changes in membrane properties can alter protein behavior and initiate phenotypic changes [130, 131]. I hypothesize that bile acids are acting through DGC transmembrane domains to influence c-di-GMP synthesis by altering the physical properties of the lipid membrane. To test this hypothesis, I propose to examine the effect of temperature on the bile-induced increase c-di-GMP. *V. cholerae* cultures can be grown at either 35 °C or 20 °C in the presence and absence of bile acids. Membrane fluidity can be

assessed using fluorescence anisotropy as previously described [132] and intracellular c-di-GMP can be measured using LC-MS/MS. In addition, the VC1067, VC1372, and VC1376 ectopic expression strains and their mutant allele counterparts also should be examined at the two temperatures in the presence and absence of bile. If membrane fluidity is affecting the c-di-GMP synthesis of these proteins, I expect reduced c-di-GMP synthesis in the presence of bile at the lower temperatures.

Alternatively, it is possible that bile induces composition changes of the lipid membrane of *V. cholerae*, which then alters the c-di-GMP synthesis of the three bile-responsive DGCs. This phenomenon has been observed in *Lactobacillus reuteri*, where bile acids alter the lipid membrane profile [133]. To test the effect of membrane composition on c-di-GMP synthesis, I propose ectopically express fatty acid biosynthesis enzymes to artificially modify the fatty acid composition of the cell membrane. Increased expression of the fatty acid biosynthesis gene *fabF* in *B. subtilis* promotes the proportion of long-chain fatty acids leading to decreased membrane fluidity, while expression of the gene *fabH* promotes branched-chain fatty acids and increases membrane fluidity [132, 134]. Either the *fabF* gene homolog (VC2019) or the *fabH* gene homologs (VC2023, VCA0751) can be ectopically expressed alongside each of the three bile-responsive DGCs, and intracellular c-di-GMP can be measured using LC-MS/MS. Fluorescence anisotropy can confirm changes in membrane fluidity. I hypothesize that the DGCs expressed alongside *fabF* (reduced membrane fluidity) will have reduced c-di-GMP synthesis, whereas

DGCs expressed alongside *fabH* (increased membrane fluidity) will have increased c-di-GMP synthesis.

In addition to the three DGCs that increased c-di-GMP synthesis in the presence of bile, I demonstrated that bile acids decrease the expression of one PDE, VC1295. However, the regulators driving bile-mediated expression changes of VC1295 are undefined. As I have identified putative ToxR binding sites in the promoter region of VC1295, and I have demonstrated that a  $\Delta$ *toxR* mutant reduces induction of c-di-GMP in the presence of bile acids, I hypothesize that ToxR binds to the promoter region in the presence of bile acids to inhibit VC1295 expression. In support of this, it has been shown that the transcriptional regulation activity of ToxR is altered in the presence of bile acids, and that this regulation is dependent on the transmembrane domain of ToxR [117]. To test the hypothesis that bile and ToxR drive VC1295 expression, I propose introducing the VC1295-*lux* vector in the  $\Delta$ *toxR* mutant strain and examining the expression of VC1295 in the presence and absence of bile. I expect that the luminescence will be unchanged in the presence of bile acids in the  $\Delta$ *toxR* mutant strain. Electromobility gel-shift assays (EMSA) can be performed as previously described [107] using purified ToxR protein and DNA from the promoter region of VC1295 in the presence of increasing amounts of purified bile acids [135]. If ToxR is interacting with the VC1295 promoter in the presence of bile, I expect to see increased binding of DNA in the presence of bile acids. Finally, I propose creating mutations in the predicted ToxR binding sites on the VC1295-*lux* promoter vector, and examining luminescence in the WT strain in

the presence and absence of bile acids. These experiments will elucidate the role ToxR plays in altering the expression of VC1295 and increasing intracellular c-di-GMP concentrations in the presence of bile acids.

While bile acts to increase intracellular c-di-GMP in *V. cholerae*, I have shown that bicarbonate can quench this response; however, it remains unclear how this occurs. To explore this question, I propose to comprehensively examine the expression of genes in *V. cholerae* cultures grown in LB, LB with bicarbonate, LB with SHB, and LB with SHB and bicarbonate. To do this, RNA can be extracted from each culture and whole transcriptome shotgun sequencing (RNAseq) can be used to quantify gene expression. I expect that differences in gene expression will be observed in cultures grown in the presence of SHB versus SHB with bicarbonate. After genes have been identified that are differentially regulated in the presence of bicarbonate, genomic knockout mutant strains can be made of these target genes and the intracellular c-di-GMP of these strains can be determined when grown in the presence of SHB and SHB with bicarbonate.

I demonstrated that the deletion of the enzymes responsible for the bile-mediated c-di-GMP induction reduces bile-induced biofilm formation. However, the full physiological implications of increased c-di-GMP in the presence of bile and subsequent consequences on the pathogenesis of *V. cholerae* have yet to be determined. To ascertain if increased c-di-GMP is beneficial for bile tolerance, I propose competing the WT *V. cholerae* strain and the *V. cholerae* quadruple DGC/PDE mutant strain in the presence and absence of bile and measuring relative

fitness. Neutral markers can be inserted into the genomes of each strain, such as antibiotic resistance genes or fluorescent proteins, to differentiate the strains. I hypothesize that the quadruple mutant will have lower competitive fitness in the presence of bile acids compared to the WT strain. As controls, the  $\Delta vpsL$  strain should be competed against the WT strain to determine the role of biofilm formation plays in competitive fitness. Likewise, as positive controls,  $\Delta toxR$  and  $\Delta ompU$  mutants should be competed against WT in the presence and absence of bile, as these genes are important for bile resistance and fitness [43, 116, 136]. To determine the role bile-induced c-di-GMP plays *in vivo*, I propose determining the competitive index of the quadruple DGC/PDE mutant to the WT strain of *V. cholerae* in an infant mouse model as previously described [35, 116]. While the bile composition of a mouse is different from that of a human [137], the infant mouse model has been used to study the effects of proteins related to bile resistance in pathogenesis [45, 46, 116]; thus I expect that this model will be sufficient to examine the role of c-di-GMP in bile-related fitness. I expect that the quadruple mutant has significantly reduced competitive index in a mouse model. These experiments will clarify the role c-di-GMP plays *in vivo* during *V. cholerae* pathogenesis.

## CHAPTER 4 – Intracellular c-di-GMP Negatively Correlates with the Growth Rate and Ribosomal RNA of *V. cholerae*

### *Preface*

It has been observed that ectopic DGC expression can cause a growth deficiency in both *V. cholerae* and *E. coli* [4, 79]. It remains unknown as to why ectopic DGC expression would affect growth rate. Many factors influence bacterial growth rate; the growth rate of bacteria is positively correlated with the ribosomal RNA (rRNA) gene copy number, and this phenotype is associated with how bacteria respond to resource availability [138]. Furthermore, ribosome abundance in the cell correlates with growth rate, although it remains unclear if ribosome depletion inhibits growth rate or if growth rate inhibition causes ribosome depletion [139-146]. In support of the former, it has been shown that (p)ppGpp accumulates in the cell upon nutrient deprivation, altering GTP homeostasis and inhibiting RNA synthesis in the cell resulting in reduced growth rate [143, 147-151].

There are numerous phenotypes controlled by c-di-GMP including motility, biofilm formation, and virulence [11, 13, 16, 98]. Here, I examine the hypothesis that c-di-GMP negatively regulates the growth rate of *V. cholerae*. I have shown that there is a correlation between intracellular c-di-GMP and growth rate of *V. cholerae* grown in different media. Furthermore, I have shown that ectopic DGC expression represses the growth rate in *V. cholerae* in a dose-dependent manner, and that the efficiency of this repression varies between different DGCs. Finally, I

have shown that ectopic expression of the DGC VC1067 reduces rRNA in the cell. Together, I propose that c-di-GMP is negatively regulating growth rate in *V. cholerae* by reducing intracellular ribosomes via an unidentified molecular mechanism.

### *Measuring growth rate of V. cholerae*

Growth curves were determined by taking OD<sub>600</sub> readings of liquid cultures at regular intervals. For cultures grown in 150 µL volumes in clear 96-well plates (Greiner), OD<sub>600</sub> readings were taken with a SpectraMax M5 plate reader (Molecular devices) every 10 minutes for a period of 15 hours. For cultures grown in 2 mL volumes in 14 mL round-bottom polystyrene tubes (Falcon), OD<sub>600</sub> readings were taken with a DU 700 series spectrophotometer (Beckman Coulter) approximately every 30 minutes for a period of 6 hours. All cultures were grown at 35 °C, with shaking at 220 rpm, and DGC expression strains were supplemented with kanamycin at 100 µg/mL. Relative growth rates were determined by plotting each curve in Graphpad Prism and calculating area under the curve. The area under the curve values for each strain at each inducer concentration were normalized to the area under the curve of a no-inducer control. For calculating specific growth rates, growth curves were analyzed with the grofit package in R [152, 153]. C-di-GMP was quantified using LC-MS/MS as described in Chapter 2.

### *RNA extractions and quantification*

For RNA quantification, 5mL of LB media supplemented with 100 µg/mL kanamycin and 0.1 mM IPTG in 25 mL Erlenmeyer flasks were inoculated with 5 µL overnight *V. cholerae* cultures and grown to an OD<sub>600</sub> of approximately 0.6-0.8 (late exponential growth). Cultures were then diluted to an OD<sub>600</sub> of 0.5, and RNA extractions were performed using Trizol reagent (Ambion, Life Technologies) as per the manufacturer's instructions. Total RNA was quantified using a NanoDrop 1000 (Thermo Scientific). rRNA was then quantified in each sample using a 2100 Bioanalyzer (Agilent).

### *Intracellular c-di-GMP and growth rate of *V. cholerae* are correlated*

In Chapter 2, I showed that intracellular c-di-GMP concentrations of *V. cholerae* vary when the bacteria are grown in different growth media (Fig. 5) and I observed that these concentrations tended to be higher in minimal media, where the growth rate was slower (Fig. 4). I hypothesized that intracellular c-di-GMP may be negatively correlated with bacterial growth rate. To examine this hypothesis that c-di-GMP and growth rate are connected, I determined the doubling times (in minutes) during exponential growth of *V. cholerae* grown in different media (Fig. 4) by selecting two timepoints during exponential growth in each environment and log-transforming the fold-change of OD<sub>600</sub><sup>-2</sup> and then multiplying this value by the time elapsed. The doubling time of *V. cholerae* grown in LB determined here is consistent with previous studies [154]. Growth rate (divisions per hour) was determined by

dividing 1 hour by the doubling time; these growth rates were then regressed on intracellular c-di-GMP concentrations (Fig. 20). I found that there was a negative trend of intracellular c-di-GMP and growth rate, although the slope bordered outside of statistical significance from zero ( $p=0.056$ ). Furthermore, the goodness of fit ( $R^2=0.163$ ) indicates that only a modest portion of this relationship can be attributed to intracellular c-di-GMP. This analysis provides preliminary evidence that there is a relationship between intracellular c-di-GMP and growth rate.

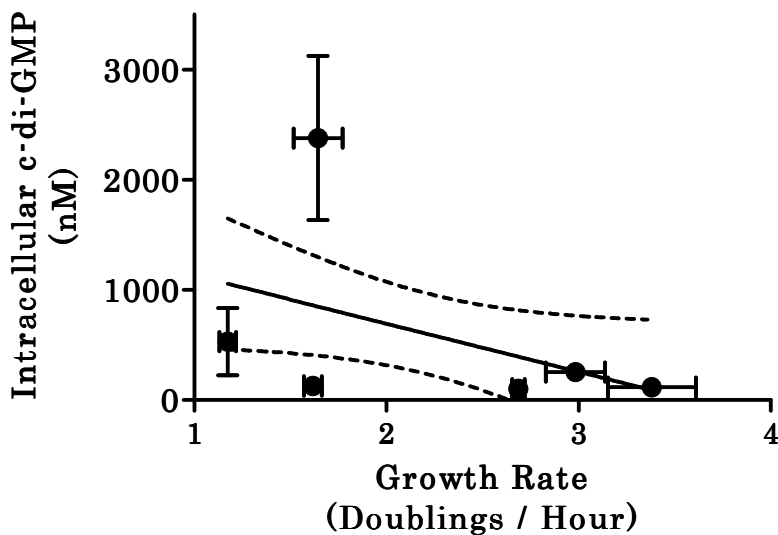


**Figure 20. Linear regression of intracellular c-di-GMP concentrations on growth rates of *V. cholerae* grown in different media.** Dotted lines indicate 95% confidence intervals. Goodness of fit ( $R^2$ ) was 0.163, and non-zero significance ( $p$ ) was 0.056.

*Growth rate inhibition caused by ectopic DGC expression is dose-dependent*

Previous studies have indicated that ectopic expression of a DGC can inhibit bacterial growth [4, 79], corroborating my hypothesis that c-di-GMP negatively affects growth rate. I wanted to further explore the dynamics of the relationship

between growth rate repression and ectopic DGC expression; specifically, I sought to confirm these previous observations and determine if this inhibition of growth is DGC dose-dependent. I utilized two DGC inducible expression vectors encoding VC1067 and VC2285 to alter the intracellular concentration of c-di-GMP. These two DGCs have been shown to synthesize high levels of intracellular c-di-GMP upon IPTG induction (Chapter 3, [79]). I measured the growth of *V. cholerae* strains harboring these DGC expression vectors at IPTG concentrations ranging from 0.002 mM to 0.1 mM by growing the strains in a 96-well plate and taking OD<sub>600</sub> readings every 10 minutes for 15 hours. The growth rate of each strain at each IPTG concentration was determined by fitting each growth curve to an exponential growth model using the program *grofit* [152, 153], and determining the maximum slope of each curve (Fig. 21). In an empty vector negative control, I observed no change in growth rate across the inducer gradient. In contrast, both the VC1067 and VC2285 expression strains showed a dose-dependent reduction in growth rate. The VC2285 strain showed a greater reduction in growth at all timepoints compared to the VC1067 strain. This is consistent with observations that the VC2285 strain produces more c-di-GMP than the VC1067 strain [79]. I conclude from these data that ectopic DGC expression inhibits growth rate in a dose-dependent manner.

I next sought to determine what concentrations of c-di-GMP lead to growth inhibition in *V. cholerae*. I selected nine DGC expression strains and grew them in 8 different IPTG concentrations ranging from 0.0005 mM to 1.0 mM. The relative

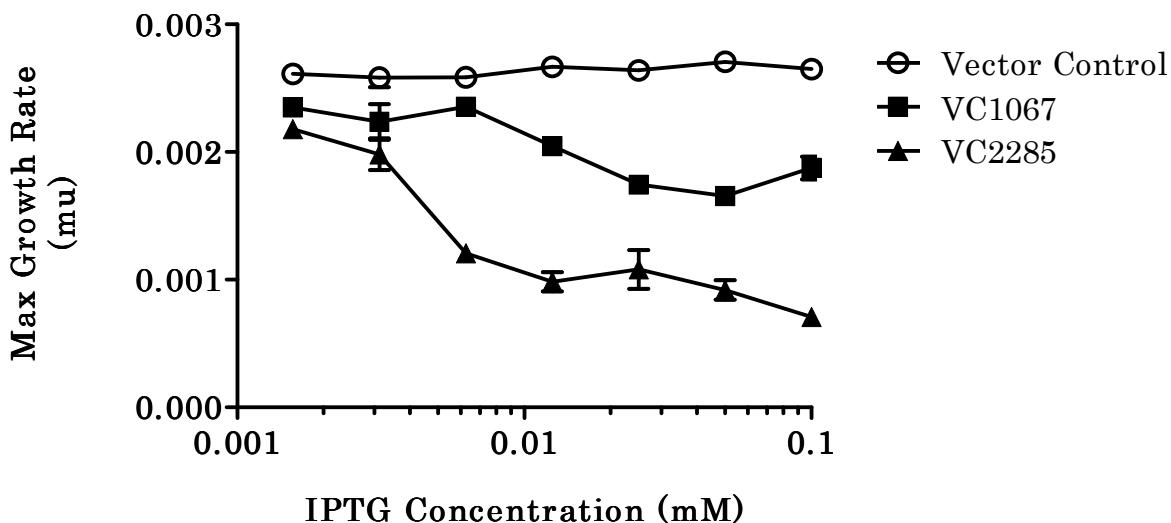


**Figure 21. Growth rates of *V. cholerae* DGC expression strains.** *V. cholerae* DGC expression cultures were grown in a 96-well plate and growth rate was determined at a range of IPTG concentrations. The max growth rate ( $\mu$ ) indicates the maximum slope during log-phase growth of  $OD_{600}$  curves fit to exponential growth models. Each point represents the mean of three replicates, and error bars indicate standard deviation.

growth rate of each strain was determined by measuring  $OD_{600}$  at regular intervals, then determining the area under each curve. Intracellular c-di-GMP of each strain was determined at each inducer condition during late-stationary growth using LC-MS/MS as previously described [79]. Then, the growth rate of each strain at each inducer concentration was regressed on the intracellular c-di-GMP concentrations. I found that 4 of the 9 regressed strains had slopes significantly different from zero, indicating that these DGCs are capable of inhibiting growth of *V. cholerae* upon ectopic expression (Table 1).

Expression strain	Max intracellular c-di-GMP (nM)	Min Area under the curve	Slope	Nonzero significance (p < 0.01)	r <sup>2</sup>
VC1067	98111.4	0.11 ± 0.03	-1.0e-5 ± 8.1e-7	*	0.88
VC1104	3476.9	0.64 ± 0.05	-8.5e-5 ± 1.3e5	*	0.65
VC1216	5840.2	0.86 ± 0.08	-2.8e-5 ± 2.0e-5		0.12
VC1353	1596.2	0.94 ± 0.07	-7.6e-5 ± 4.1e-5		0.14
VC1599	888.7	0.91 ± 0.04	1.5e-4 ± 1.1e-4		0.07
VC2224	22249.3	0.5 ± 0.05	-2.4e-5 ± 2.3e-6	*	0.83
VC2454	809.5	0.82 ± 0.03	-1.3e-4 ± 1.5e-4		0.03
VCA0074	3515.7	0.51 ± 0.09	-1.1e-4 ± 2.0e-5	*	0.59
VCA0165	541.0	0.88 ± 0.07	-2.6e-4 ± 1.1e-4		0.20

**Table 1. Description of DGC expression strain intracellular c-di-GMP levels and growth inhibition.** Max intracellular c-di-GMP indicates the highest level of intracellular c-di-GMP over the IPTG gradient. Min area under the curve indicates the lowest area under the curve value of each strain grown in the corresponding IPTG concentration. Linear regression analysis of c-di-GMP and growth rate was performed, and the resulting slopes are displayed here. The nonzero statistical significance and the r<sup>2</sup> values are also shown.

To compare the concentrations of c-di-GMP required to inhibit growth rate across different DGCs, the maximum c-di-GMP produced by each DGC expression strain capable of inhibiting growth was regressed on the minimum growth rate observed for each strain. I separately analyzed the DGC expression strains that were unable to significantly alter growth rate (Fig. 22A). I found that strains expressing DGCs capable of inhibiting growth rate did so in a c-di-GMP dose-

dependent manner, where the slope demonstrated a significant negative deviation ( $p < 0.05$ ). Interestingly, two DGCs (VC1104 and VCA0074) inhibited growth rate at c-di-GMP concentrations less than that of the DGC VC1216, which did not show any significant growth rate inhibition.

I went on to analyze the dynamics of growth inhibition of the four DGCs that inhibited growth rate of *V. cholerae*. Two of the DGC expression strains, VC1104 and VCA0074, produced similar levels of c-di-GMP upon expression resulting in similar levels of growth rate inhibition (Fig. 22B). In contrast, the VC1067 and VC2224 strains required significantly more intracellular c-di-GMP to achieve the same level of growth rate inhibition as either the VC1104 or VCA0074 strains. From this, I conclude that certain DGCs are able to inhibit growth rate at lower concentrations of c-di-GMP than other DGCs, suggesting there is signaling specificity within this pathway.

*Intracellular c-di-GMP concentration required for growth inhibition varies for different DGCs*

The growth rate inhibition of ectopic DGC expression has been attributed to c-di-GMP toxicity [4]. However, my data indicate that DGCs inhibit growth rate at different concentrations of c-di-GMP, suggesting that this inhibition is occurring independent of generalized c-di-GMP toxicity. I hypothesize that c-di-GMP is regulating growth rate in *V. cholerae* through a specific, unknown mechanism. I selected two DGCs that inhibit growth rate at different c-di-GMP concentrations;

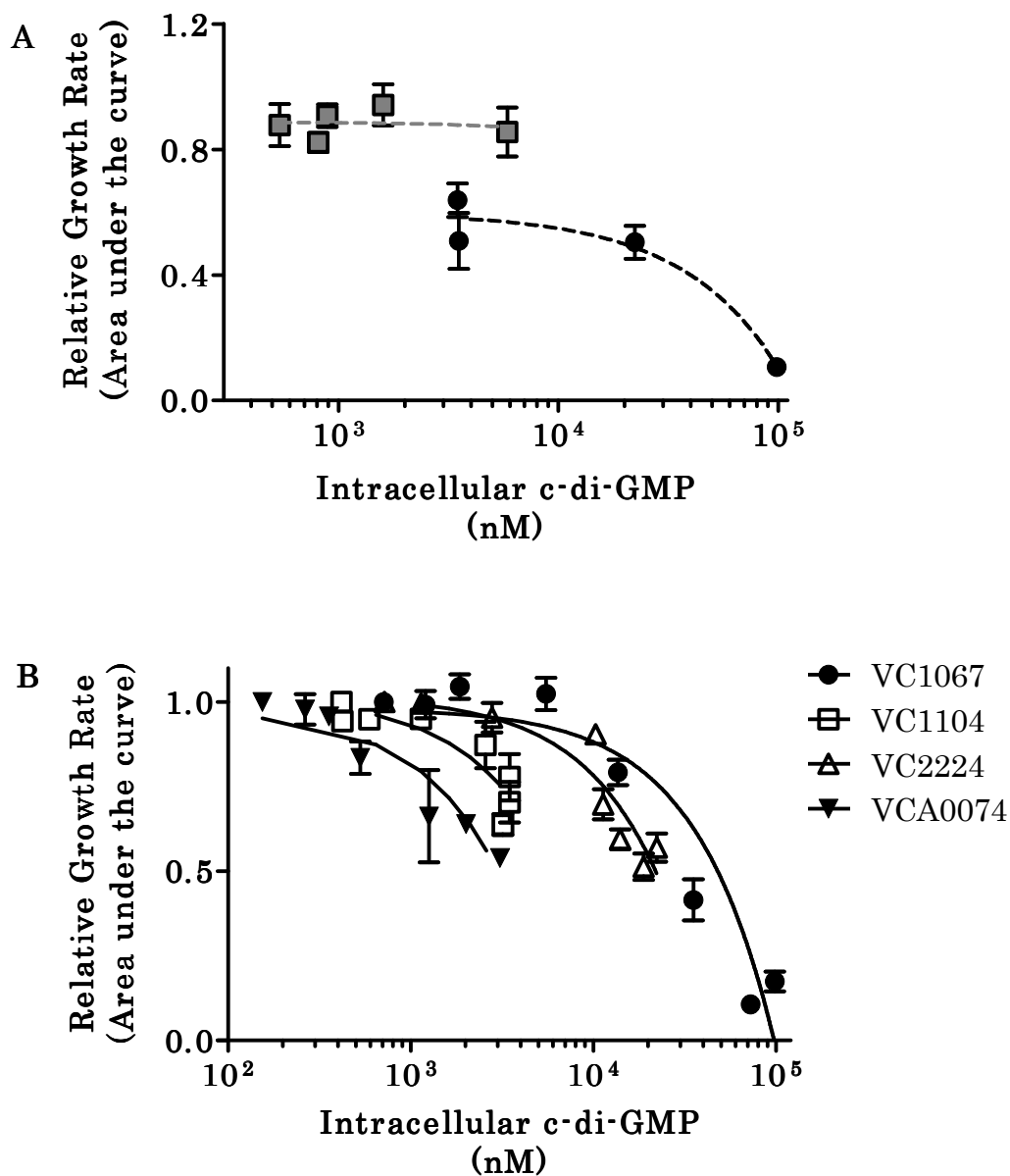


**Figure 22. Linear regression of intracellular c-di-GMP concentrations on growth rates of *V. cholerae* DGC expression strains.** (A) Regression analysis of maximum intracellular c-di-GMP and maximum growth rate of different DGCs of *V. cholerae*. Dotted lines indicate linear regression of DGCs that significantly inhibit growth (black circles) or DGCs that do not significantly inhibit growth (grey squares). (B) The intracellular c-di-GMP concentrations of individual DGCs was regressed on relative growth rates over a range of IPTG concentrations. Each point represents the mean of three replicates. Error bars indicate standard deviation.

these DGCs are VC1067 and VCA0074. Intracellular c-di-GMP was measured using LC-MS/MS at an inducer concentration that was predicted to produce equal levels of growth rate inhibition at different c-di-GMP concentrations, which was 0.1 mM IPTG (Fig. 22B). I found that VC1067 produced 4.0-fold more intracellular c-di-GMP at this inducer concentration than VCA0074 ( $p < 0.05$ , Fig. 23). In contrast, intracellular c-di-GMP concentrations of strains containing mutant alleles (GG[D/E]EF  $\rightarrow$  AA[D/E]EF) of either VC1067 or VCA0074 were indistinguishable from those of the vector control.

I then measured growth of the VC1067 and VCA0074 strains grown at an IPTG concentration of 0.1 mM to confirm that ectopic expression of each of these DGCs inhibits growth rate at equivalent levels (Fig. 24A). These curves were used to calculate the doubling time of each strain by fitting each curve to an exponential growth equation using grofit [152, 153] and deriving the maximum slope. The doubling time was determined from the slope by dividing  $\log_{10}(2)$  by each slope value. I found that the doubling time of both the VC1067 and VCA0074 expression strains was significantly increased over the vector control and their respective active site mutant alleles (Fig. 24B). To account for growth rate deficiency caused by the burden of ectopically expressing each DGC, the doubling time of the VC1067 and VCA0074 expression strains was divided by the doubling time of their respective mutant allele counterpart expression strains. The VC1067 strain demonstrated a 1.47-fold increase in doubling time over its mutant allele, whereas the VCA0074 strain demonstrated a 1.45-fold increase in doubling time. I thus

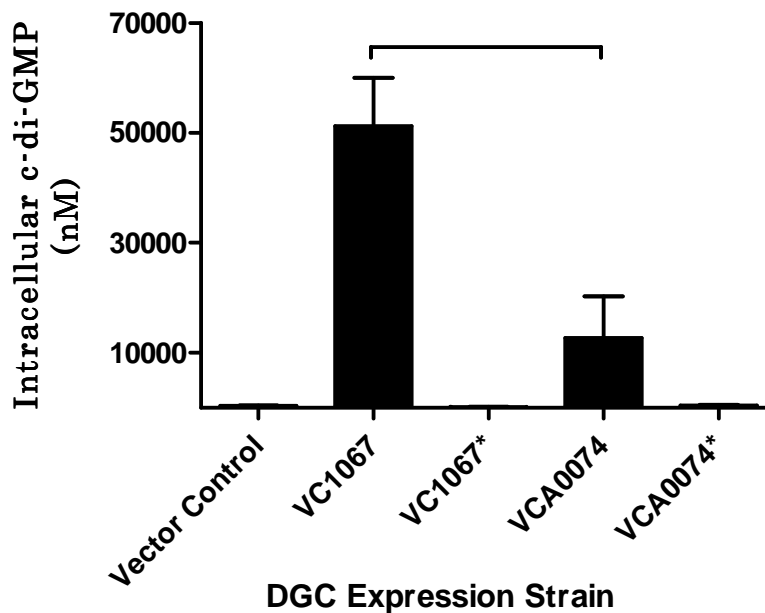


**Figure 23. Intracellular c-di-GMP concentrations of *V. cholerae* DGC expression strains.** Cultures were grown in the presence of 0.1 mM IPTG. Bars indicate the mean of three replicates, and error bars indicate standard deviation. Brackets indicate statistical significance, which was determined using a two-tailed Students T-test ( $p < 0.05$ ).

conclude that while the VC1067 strain synthesizes significantly more c-di-GMP at this inducer concentration compared to the VCA0074 strain, the growth rate is virtually indistinguishable.

*Increased intracellular c-di-GMP reduces the expression of rRNA*

As my evidence indicates that intracellular c-di-GMP is negatively impacting growth rate, I sought the mechanism governing this phenomenon. Numerous studies have demonstrated that growth rate and ribosome abundance are inextricably linked [139-151]. I hypothesized that c-di-GMP negatively affects the transcription of rRNA in *V. cholerae*. This would lead to decreased ribosomes in the

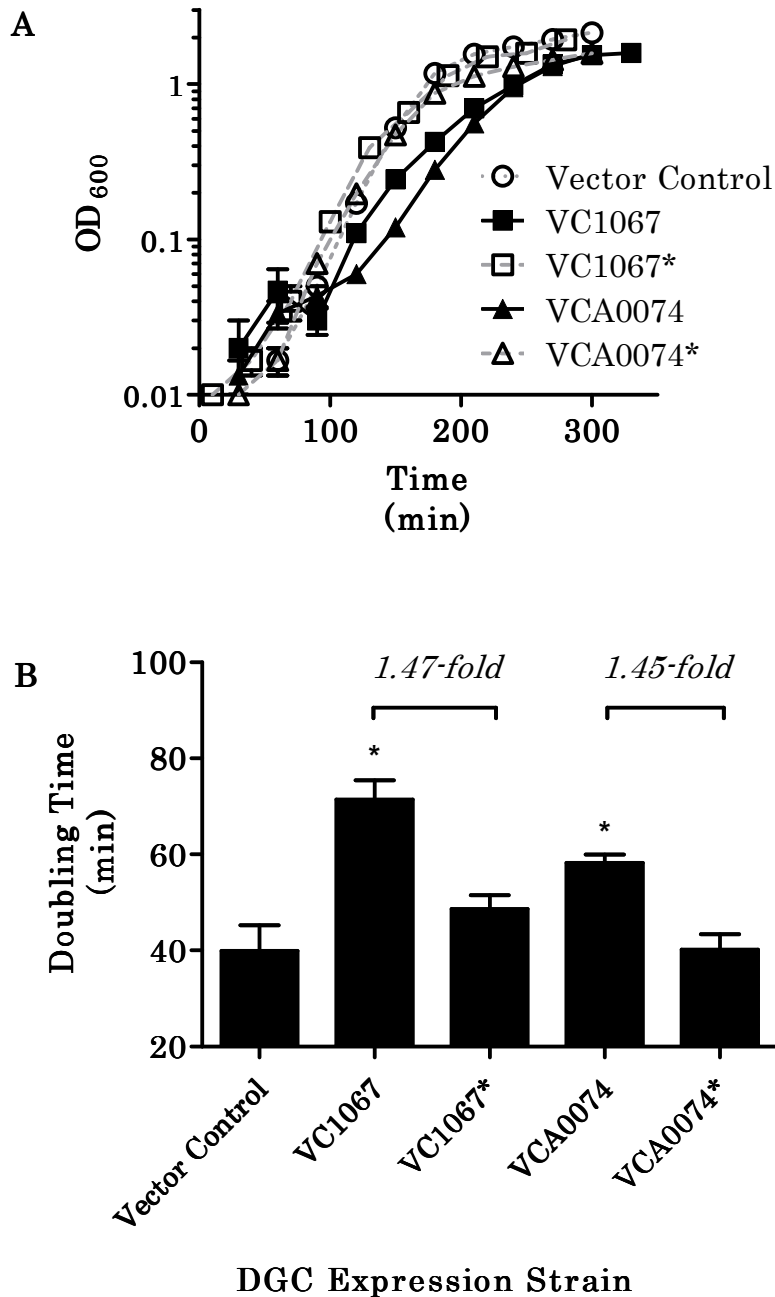


**Figure 24. Growth rates of *V. cholerae* DGC expression strains.** (A) Growth curves of DGC expression strains grown in the presence of 0.1 mM IPTG. OD<sub>600</sub> readings were taken at regular intervals (B) Doubling times were determined from growth curves. Each bar represents the mean of three replicates, and error bars indicate standard deviation. \* indicates statistical significance from their respective mutant alleles, as determined by a Student's two-tailed T-test ( $p < 0.05$ ).

cell, resulting in slower protein synthesis and subsequently slower cell division. To examine this hypothesis, RNA extractions were performed on the VC1067 expression strain and its mutant allele on cultures normalized to equal cell density. 16S and 23S rRNA was quantified using a 2100 Bioanalyzer (Agilent). Relative RNA abundance was determined by normalizing the respective RNA abundance by the initial RNA concentration of each sample. I found that strains ectopically expressing VC1067 strain had 39.6% and 32.2% less 16S and 23S rRNA, respectively, compared to the VC1067\* mutant allele ( $p < 0.05$ , Fig. 25). These data support the hypothesis that c-di-GMP regulates growth rate by altering ribosome abundance in the cell.

### *Discussion*

The regulation of bacterial growth rate has been the subject of study for over 50 years [146]. Indeed, the rate at which bacteria are able to reproduce has large implications for pathogenesis and epidemiology of disease, and involves core biological functions that are widely conserved amongst bacteria. The concept of a second messenger controlling bacterial growth rate is not novel. It has been shown that the small nucleotide signal (p)ppGpp regulates growth in response to metabolic stresses [143, 147-151]. Here, I explore the connection between growth rate regulation and c-di-GMP. I have shown that there is a correlation between intracellular c-di-GMP and growth rate in *V. cholerae* grown in different media, as well as *V. cholerae* ectopically expressing different DGCs (Fig. 20, 21, 22). It has

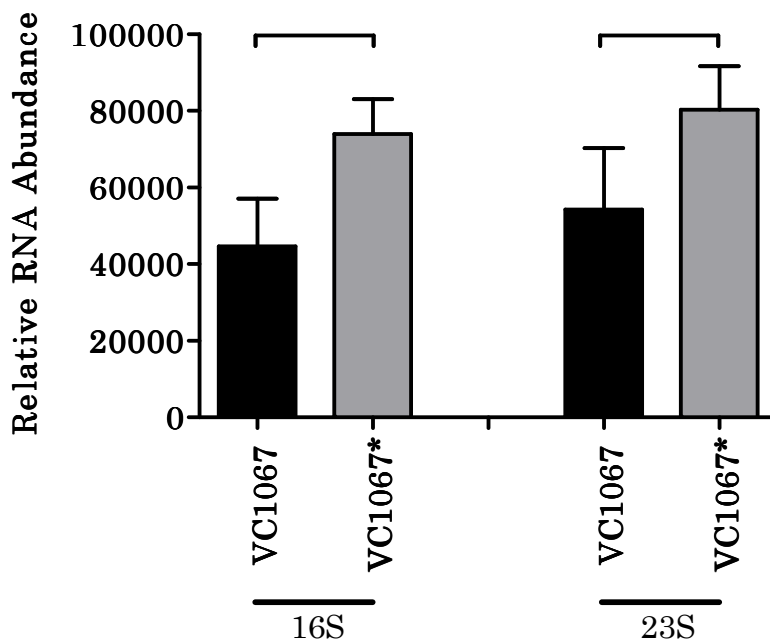


**Figure 25. Relative rRNA abundance of *V. cholerae* DGC expression strains.** The rRNA of RNA extractions from *V. cholerae* strains ectopically expressing VC1067 (black) or the active-site mutant allele VC1067\* (grey) were quantified using a 2100 Bioanalyzer. Each bar represents the mean of five replicates, and error bars indicate standard deviation. Brackets indicate statistical significance, as determined using a Students two-tailed T-test ( $p < 0.05$ ).

been noted in previous studies that ectopic DGC expression leads to growth rate inhibition in *E. coli* and *V. cholerae* [4, 79].

I have shown that growth rate inhibition is dependent on the c-di-GMP synthesis of DGCs, as expression of DGC mutant alleles had no significant impact on growth rate (Fig. 24). This inhibition has been previously attributed to a c-di-GMP toxicity associated with unnaturally high intracellular c-di-GMP concentrations in the cell. However, my data indicate that this is not necessarily the case, as growth rate inhibition was observed upon the expression of VC1104, while

expression of VC1216 and VC1353 produced equal or greater concentrations of c-di-GMP while failing to inhibit growth (Fig. 22). Furthermore, I also observed that the DGCs VC1067 and VCA0074 produce different levels of intracellular c-di-GMP yet produce the same growth rate inhibition. These findings suggest that growth rate inhibition is subject to DGC signaling specificity, a phenomenon where c-di-GMP produced by certain DGCs effects downstream phenotypes at concentrations different from other DGCs. Other studies have validated the concept of high specificity c-di-GMP signaling for phenotypes such as biofilm formation [79, 91, 98, 155, 156].

Although the mechanisms by which c-di-GMP inhibits growth have not yet been fully characterized, I have shown that ectopic expression of a DGC can lead to decreased 16S and 23S rRNA in the cell (Fig. 25). This change in intracellular ribosomes could account for the decreased growth rate observed in cells containing elevated c-di-GMP (Fig. 24). Growth rate has been correlated with rRNA gene copy number in bacteria, and it is well established that ribosome abundance in the cell is correlated with growth rate [139-151]. Furthermore, it has been shown that disrupting the rRNA copy number in *E. coli* has negative implications for fitness [157]. Transcriptional regulation of rRNA has been associated with nutrient abundance; specifically, during periods of starvation, the stringent response is activated, resulting in increased (p)ppGpp and simultaneous repression of rRNA transcription [143, 147-151]. Thus it makes sense that c-di-GMP, a second

messenger affected by environmental factors, would regulate growth rate by altering ribosome abundance.

From these studies, I postulate two hypotheses to explain the phenomenon of c-di-GMP-dependent growth rate inhibition I observe. The first hypothesis is that c-di-GMP is inhibiting rRNA transcription through some yet unidentified effector protein. I propose that a subset of DGCs, such as VC1104 and VCA0074, specifically regulate growth rate through this unknown factor. It is possible c-di-GMP acts through a similar mechanism as (p)ppGpp, which binds RNA polymerase to regulate transcription [158]. The second hypothesis is that DGC expression is leading to a depletion of GTP, which subsequently alters growth rate. Previous studies have shown that GTP depletion can lead to growth rate inhibition in *B. subtilis* [159]. Furthermore, the growth rate regulator (p)ppGpp has also been shown to be a critical regulator of GTP homeostasis [151]. I propose that DGCs that produce very high amounts of c-di-GMP, such as VC1067, inhibit growth by disrupting GTP homeostasis. These hypotheses have not yet been tested.

### *Future directions*

C-di-GMP has been shown to regulate numerous bacterial phenotypes, and more have yet to be identified [73]. I have shown that growth rate and c-di-GMP are correlated and that ectopic expression of select DGCs results in c-di-GMP dependent growth rate inhibition. This is significant, as the growth rate has important implications in bacterial ecology and pathogenesis [138, 143, 157, 160]. The

mechanism governing the c-di-GMP mediated inhibition of growth rate is unknown. I have shown that the DGCs VC1067 and VCA0074 produce significantly different levels of c-di-GMP in the cell yet result in the same level of growth rate inhibition. In order to explore this relationship and determine how this growth rate inhibition is occurring, I propose extracting RNA from both the VC1067 and VCA0074 expression strains. RNAseq can then be performed on extracts from both cultures to identify differentially regulated transcripts. As controls, the vector control and the active site mutant allele strains should be included. Since these two DGCs inhibit growth at different concentrations of c-di-GMP, they may be acting through two distinct pathways. I propose focusing on differentially regulated genes targeting known growth rate factors, metabolic enzymes, and genes of unknown function. *V. cholerae* deletion mutants of promising targets will be made, and subsequently analyzed for growth in the presence and absence of elevated intracellular c-di-GMP.

An alternative method for determining the mechanism of c-di-GMP mediated growth rate inhibition is to utilize experimental evolution to generate *V. cholerae* strains that do not exhibit growth rate inhibition at high c-di-GMP concentrations. To do this, I propose creating a c-di-GMP strain with a neutral-site chromosomal insertion of the VC2285 gene under the control of the pTac promoter. VC2285 will be used due to its ability to synthesize very high levels of c-di-GMP and its robust inhibition of growth rate (Fig. 21, [79]). As I have shown that expression of VC2285 inhibits growth, I postulate that if VC2285 is grown and subsequently passaged repeatedly, spontaneous suppressor mutants will arise in the population that will

be able to grow faster in the presence of high levels of c-di-GMP. These mutants will be able to out-compete their ancestors and overtake the population over the course of the experiment. This strain can be passaged in the presence of the inducer IPTG once a day; when cultures arise that exhibit faster growth rates than their ancestors, members of the culture population will be isolated and whole-genome sequencing will be used to identify where on the chromosomes the mutations occurred.

Alternatively, it is possible that while c-di-GMP and growth rate are correlated, c-di-GMP is not directly regulating growth rate. An alternative hypothesis is that growth rate is regulating intracellular c-di-GMP. This could be occurring through protein dilution [161], where protein synthesis cannot keep up with cell division during rapid growth, resulting in different DGC and PDE abundance in the cell and subsequently altering intracellular c-di-GMP concentrations. To examine this hypothesis, I propose artificially altering the growth rate of *V. cholerae* using a continuous culture chemostat, and measuring intracellular c-di-GMP at different growth rates. I hypothesize that c-di-GMP would be lower at faster dilution rates where the culture is growing faster, and higher c-di-GMP in the slower dilution rates where growth rate is lower.

Another mechanism by which DGC expression could be altering growth rate is by interacting with the (p)ppGpp signaling network. It has been shown that (p)ppGpp negatively regulates growth rate in response to nutrient deprivation [143, 147-151]. I postulate that c-di-GMP regulates (p)ppGpp synthetases and hydrolases

to alter intracellular (p)ppGpp concentrations and subsequently regulates growth rate. To examine this hypothesis, I propose to use LC-MS/MS to quantify (p)ppGpp of the VC1067 DGC expression strain and its mutant allele counterpart over a range of inducer concentrations. I expect that the VC1067 strain would have elevated (p)ppGpp concentrations compared to the VC1067\* mutant strain, and that this relationship would be dose dependent. One important regulatory target of (p)ppGpp is GTP homeostasis [151]; this is particularly relevant, as c-di-GMP is synthesized from GTP. To determine if there is any link between intracellular c-di-GMP, (p)ppGpp, and GTP, I propose to also measure the intracellular concentration of GTP and GTP precursors of cells expressing either VC1067 or the VC1067\* mutant allele. Concentrations of GTP are approximately 5 mM in *E. coli* [88]; in contrast, intracellular c-di-GMP of the VC1067 expression strain in the presence of 0.1 mM IPTG (where growth rate is inhibited) is approximately 50  $\mu$ M. Thus, as one c-di-GMP molecule is synthesized from two GTP molecules and assuming *V. cholerae* has similar intracellular GTP homeostasis, I would expect that ectopic expression of VC1067 could detract approximately 2% of the normal intracellular GTP pool. Whether the extent of these changes on intracellular GTP or fluxes of GTP precursors would be enough to effect growth rate is yet to be determined.

## CHAPTER 5 - A novel Adenovirus Adjuvant Stimulates Innate Immunity by *in vivo* cyclic di-GMP Synthesis

### *Preface*

Thus far, I have described the interaction between environmental factors and intracellular c-di-GMP, and its impact on the physiology of *V. cholerae*. As a byproduct of this research, I have determined which of the *V. cholerae* DGCs actively produce c-di-GMP (Fig. 2, 10, 13, 22, 23). I sought to use this information to develop a clinical application. Other studies have demonstrated that c-di-GMP has potent immunostimulatory properties [49-57]. I postulated that a DGC from *V. cholerae* could be introduced into a eukaryotic cytoplasm to synthesize c-di-GMP *in vivo* and subsequently activate the innate arm of the immune system.

One vehicle that has been used for antigen and adjuvant delivery is replication deficient adenovirus based vectors [162]. Adenovirus vectors transduce large fragments of DNA into a wide range of cells in order to synthesize proteins *in vivo*, and gene expression can be modulated and even localized to specific cell types. Unlike other types of viral delivery systems, DNA delivered by adenovirus vectors does not integrate into the genome and thus circumvents the danger of insertional mutagenesis [163]. Additionally, adenovirus vectors can be produced cost-efficiently in high abundance. Importantly, adenovirus vectors are currently being used in human clinical trials world-wide [164].

Here I have investigated whether an adenovirus vector could be used to deliver DGC DNA into eukaryotic cells to synthesize c-di-GMP *in vivo*, manipulating a host-pathogen interaction to activate the innate arm of the immune system and improve the immune response against co-administered antigen. I have constructed an adenovirus containing an allele encoding the *V. cholerae* DGC VCA0956. I have shown that this DGC is capable of synthesizing c-di-GMP when virally transduced into cell culture lines. Furthermore, I have demonstrated that use of the VCA0956 adenovirus construct in a murine system results in c-di-GMP synthesis and subsequent upregulation of genes associated with innate immunity as well as increased secretion of numerous cytokines and chemokines. Finally, I have shown that c-di-GMP produced by VCA0956 *in vivo* functions as an adjuvant by reducing the effective dose of a *C. difficile* toxin A antigen necessary to generate a potent immune response. I propose that this novel adenovirus c-di-GMP delivery system offers a more efficient and cost-effective method for use of c-di-GMP as an adjuvant to stimulate innate immunity.

#### *DNA manipulation and virus construction*

All strains, plasmids, and primers used are listed in Tables A1-3. All of the DNA manipulation and plasmid construction was performed as previously described [82]. The DGC alleles were amplified from *V. cholerae* El tor strain C6706 or the plasmids pCMW75 and pCMW98 using the DNA polymerase Phusion (New England Biolabs) and the oligonucleotides listed in Table A3 (IDT). This product was then inserted into the plasmid pShuttle-CMV [165] by digesting with Kpn1 and

XhoI (Fermentas), and then ligated with a T4 DNA ligase (Invitrogen). *E. coli* strain DH10B (Invitrogen) was used for harboring plasmid DNA, and sequence fidelity was confirmed by sequencing (Genewiz). The active site mutant alleles were generated using the QuickChange Lightning site-directed mutagenesis kit (Agilent).

A first-generation, human Adenovirus type 5-derived (Ad5) replication deficient vector (deleted for the E1 and E3 genes) was used in this study [166]. Recombination, viral propagation of the Ad5 vectors, and subsequent virus characterization was performed as previously described [166, 167]. Viral particle number and infectious units titer (TCID/ml) was determined by optical density measurement at 260 nm and validated as previously described [168]. Construction of the Ad5-Null and Ad5-TA is described elsewhere [169, 170]. All virus constructs were confirmed to be RCA negative using RCA PCR and direct sequencing methods [166] and the bacterial endotoxin content was found to be < 0.15 EU per mL [166]. All procedures with recombinant adenovirus constructs were performed under BSL-2 conditions.

#### *HeLa cell transformation*

All transfections of plasmid DNA into HeLa cells was performed with the TransIT-HeLaMONSTER transfection kit (Mirus) in 6-well plates with 2.5 µg plasmid DNA. For HeLa cell infections with adenovirus vectors, cells were infected with  $2.0 \times 10^9$  viral particles (multiplicity of infection, M.O.I. of 500). Cell cultures were all checked for confluence and morphology before and after transfection and

infection using microscopy. After 24 hours of growth at 37 °C in 5% CO<sub>2</sub>, the cells were dissociated using 300 µL 0.25% trypsin, and then cells were resuspended in 4 mL PBS and then pelleted by centrifugation at 1600 RPM at 4 °C. Afterwards the cells were resuspended in 100 µL extraction buffer (40% acetonitrile, 40% methanol, and 0.1 N formic acid). The cell lysate was incubated at -20 °C for 30 minutes, and then centrifuged at max speed for 10 minutes. The extraction buffer was removed from the pelleted debris and stored at -80 °C until analysis. Immediately prior to analysis, the extraction buffer was evaporated using a vacuum manifold, and the samples were rehydrated in 100 µL water. C-di-GMP was quantified as described in Chapter 2.

### *Animal protocols*

Adult BALB/c WT male mice (6-8 weeks old) were used for all animal experiments (Jackson Laboratory). For c-di-GMP quantification and innate studies, mice were anesthetized using isofluorane, and  $2 \times 10^{11}$  adenovirus viral particles (vp) per mouse (200 µL total volume, suspended in PBS) were administered intravenously (IV) via retro-orbital injection. After administration, mice were monitored every 6 hours by lab personnel for mortality and other health parameters in accordance with Michigan State EHS and IACUC. After 24 hours the mice were sacrificed, and the spleen and liver were isolated from each animal. Each tissue was placed in 500 µL PBS, and then the tissue suspension was homogenized using an Omni Tissue Homogenizer (Omni International). 300 µL of homogenate was added to an equal volume of equilibrated Phenol Solution (Sigma). The homogenate-phenol

solution was then vortexed and then centrifuged at 15,000 rpm for 10 minutes. The aqueous phase was removed and added to 500  $\mu$ L chloroform. The mixture was vortexed and then centrifuged at 15,000 rpm for 10 minutes. The aqueous phase was then removed and stored at -80 °C until analysis.

### *Quantitative PCR*

Quantitative PCR was used to determine adenovirus abundance from DNA extracted from liver tissue as previously described [171]. Ad5 genome copy numbers were quantified using an ABI 7900HT Fast Real-Time PCR system and the SYBR Green PCR Mastermix (Applied Biosystems) in a 15  $\mu$ L reaction using a primer set for the Ad5 Hexon gene that has been previously described [172]. All PCRs were subjected to the following procedure: 95.0 °C for 10 minutes, followed by 40 cycles of 95.0 °C for 15 seconds and 60.0 °C for 1 minute. Standard curves to determine the number of viral genomes per liver cell were run in duplicate and consisted of 6 half-log dilutions using DNA extracted from purified Ad5 virus [166]. As an internal control, liver DNA was quantified using primers spanning the GAPDH gene [171] and standard curves were generated from total genomic DNA. Melting curve analysis was performed to confirm the quality and specificity of the PCR (data not shown).

To determine relative abundance of specific liver-derived RNA transcript, reverse transcription was performed on RNA derived from the liver tissue using SuperScript III (Invitrogen) and random hexamers (Applied Biosystems) as per the

manufacturer's instruction. RT reactions were diluted to a total volume of 60  $\mu$ L, and 2  $\mu$ L from each sample was used as template for subsequent PCR. Quantitative PCR was subsequently performed as described above using an ABI 7900HT Fast Real-Time PCR system and SYBR Green PCR Mastermix (Applied Biosystems) using primer sets that have been previously described [166]. The comparative Ct method was used to determine relative gene expression using GAPDH to standardize expression levels across all samples. Relative expression changes were calculated by comparing experimental levels of liver transcript to levels of liver transcript derived from mock-treated animals.

#### *Cytokine and chemokine quantification*

Cytokine and chemokine concentrations were quantified from plasma samples using a Bio-Plex multiplex bead array system (Bio-Rad). At 6 and 24 hours, blood samples were taken from mice using heparinized capillary tubes and EDTA-coated microvettes (Sarstedt). The samples were centrifuged at 3,400 rpm for 10 minutes to isolate plasma. Samples were assayed for 23 independent cytokines and chemokines (IL-1 $\alpha$ , IL-1 $\beta$ , IL-2, IL-3, IL-4, IL-5, IL-6, IL-9, IL-10, IL12-p40, IL-13, IL-17, IFN- $\gamma$ , G-CSF, GM-CSF, Eotaxin, KC, MCP-1, MIP-1 $\alpha$ , MIP-1 $\beta$ , RANTES, and TNF- $\alpha$ ) as per the manufacturer's instructions (Bio-Rad) via Luminex 100 technology (Luminex).

### *ELISPOT analysis*

For adaptive immunity studies, mice were administered adenovirus ranging from  $1 \times 10^6$  to  $5 \times 10^9$  vp per mouse suspended in 25  $\mu$ L PBS via IM injection into the tibialis anterior of the right hindlimb. To measure antigen specific recall responses, mice were sacrificed and the spleen was harvested after 14 days. Splenocytes were isolated and *ex vivo* stimulated with immunogenic peptides from *C. difficile* TA library as previously described [170]. ELISpot analysis for was performed as previously described [170] using 96-well multiscreen high-protein binding Immobilon-P membrane plates (Millipore) and the Ready-Set Go IFN- $\gamma$  mouse ELISpot kit (eBioscience). Spots were photographed and counted using an automated ELISpot reader system (Cellular Technology).

### *C. difficile challenge*

*C. difficile* mouse challenges were performed as previously described [173, 174]. Mice were administered Ad5 vectors; after 10 weeks, mice were administered cefoperazone in their drinking water at 0.5 mg / mL for 10 days, followed by 2 days with untreated drinking water. Immediately prior to the challenge, weights of each mouse were recorded. Mice were then administered 100  $\mu$ L *C. difficile* CD2015 spores by oral gavage. Mice were monitored twice a day, and the endpoint was determined when mice lost  $\geq 20\%$  of their initial body weight.

All animal procedures were reviewed and approved by the Michigan State University EHS and IACUC. Care for the mice was provided in accordance with

PHS and AAALAC standards. Plasma and tissue samples were collected and handled in accordance with the Michigan State University Institutional Animal Care and Use Committee.

### *Generating an adenovirus harboring a V. cholerae DGC*

There is an abundance of literature demonstrating that c-di-GMP is able to act as a vaccine adjuvant by stimulating the innate immune system [59]. However, these studies utilized chemically synthesized c-di-GMP delivered intramuscularly or intravenously, which is cost prohibitive and inefficient in delivery. Because c-di-GMP is synthesized from GTP and GTP is abundant in the cytoplasm of eukaryotic organisms, I postulated that a DGC expressed under the control of a strong eukaryotic promoter/enhancer element would lead to c-di-GMP synthesis within the eukaryotic cell and subsequent enhancement of downstream innate immune responses. To identify a DGC that would produce c-di-GMP in the cytoplasm of a eukaryotic cell, I examined the two DGCs VCA0848 and VCA0956 from *V. cholerae*, as *V. cholerae* is a well-studied model system for c-di-GMP signaling and many *V. cholerae* DGCs have been shown to synthesize c-di-GMP in high concentrations [79]. Additionally I examined the DGC *qrgB* from *V. harveyi*, which has been shown to synthesize c-di-GMP in *V. cholerae* [72]. I selected these three DGCs since they had no predicted N-terminal regulatory or trans-membrane domains and canonical GGDEF domains and active site motifs. Ectopic expression of VCA0956 has been shown to increase biofilm formation in both *V. cholerae* and *Vibrio vulnificus* [79,

175], repress motility in *V. cholerae* [123], and increase intracellular c-di-GMP in *V. cholerae* and *Shewanella oneidensis* [35, 77, 176].

To determine if any of these DGCs are able to synthesize c-di-GMP in a eukaryotic cytoplasm, I constructed plasmids containing each DGC under the control of the constitutive CMV promoter/enhancer in the plasmid pShuttleCMV. I also constructed corresponding vectors containing the same DGC alleles with a mutation in the active site of the GGDEF domain (GG[D/E]EF -> AA[D/E]EF). These plasmids were transfected into HeLa cells, and c-di-GMP levels were measured in cell lysates after 24 hours using LC-MS/MS. I found that eukaryotic cells transfected with both the VCA0848 and VCA0956 alleles produced detectable levels of c-di-GMP; in contrast, no detectable c-di-GMP was observed in cells transfected with the *qrgB* allele, or the active site mutant alleles and mock treatment controls (Fig. 26A). The VCA0848 vector produced 31.6-fold more c-di-GMP than the VCA0956 vector. Cell cultures were checked by microscopy and I observed no discernible morphological differences between expression of VCA0848, VCA0956, and the controls. Furthermore, trypan blue staining indicated that treatment with VCA0848 or VCA0956 did not appear to impact overall cell viability. Additionally, HeLa cells transfected with the VCA0956 plasmid and measured 48 hours after had less intracellular c-di-GMP, suggesting that c-di-GMP synthesized intracellularly is transient (data not shown). These results indicate that VCA0848 and VCA0956 are capable of synthesizing c-di-GMP in the cytoplasm of a eukaryotic cell.

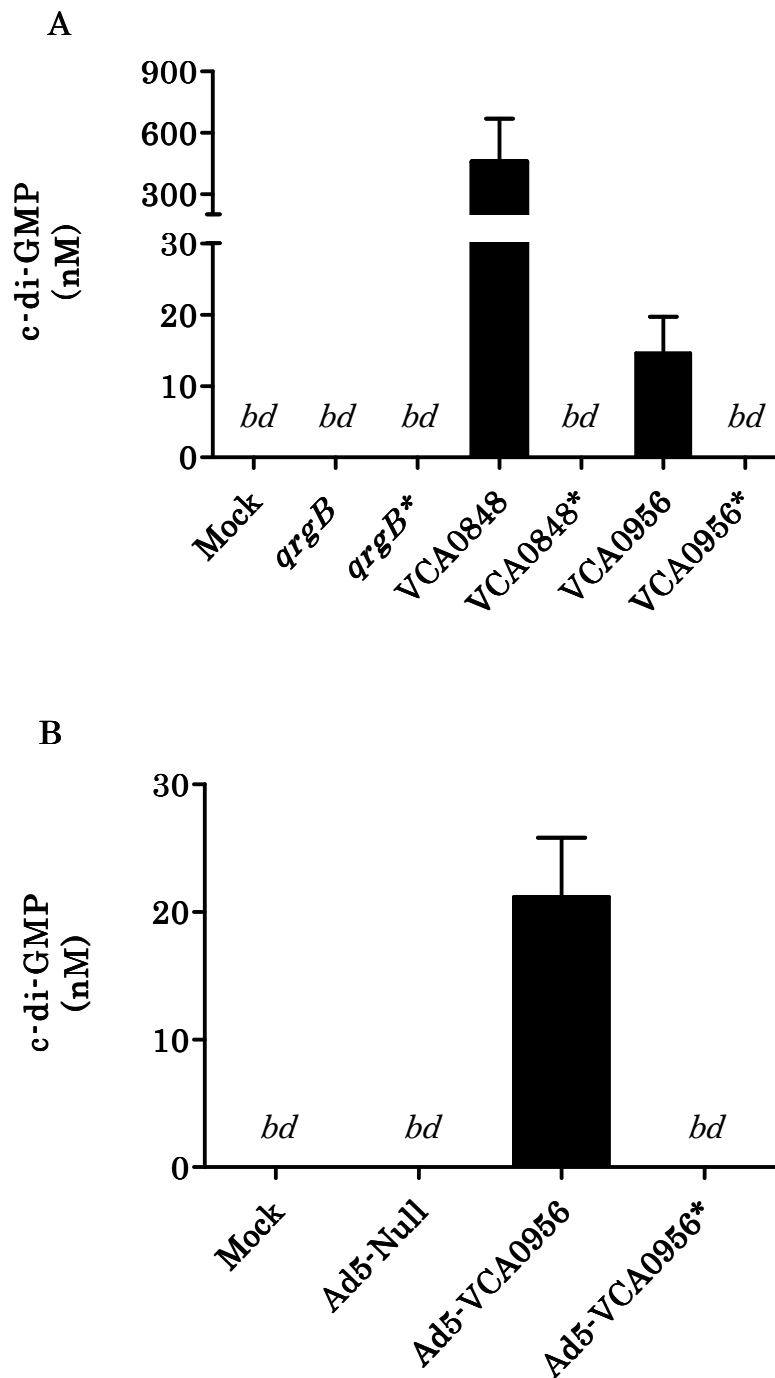


**Figure 26. C-di-GMP synthesized *in vivo* by VCA0956 in HeLa cells.** LC-MS/MS was used to quantify c-di-GMP in HeLa cells. (A) HeLa cells were transfected with plasmid vectors containing the VCA0956 allele or the active site mutant allele, VCA0956\*. (B) HeLa cells were infected with Ad5 vectors. Bars represent the mean of 3 replicates; error bars indicate standard deviation. *bd* indicates below detection.

I selected VCA0956 for further analysis, as this DGC has been the most extensively characterized. The pShuttleCMV-VCA0956 plasmid and its mutant allele counterpart were used to construct and purify to high concentration the respective recombinant Ad5-based vectors. To confirm that the VCA0956 Ad5 construct, herein referred to as Ad5-VCA0956, was able to produce c-di-GMP in a eukaryotic cytoplasm, I infected HeLa cells (500 M.O.I.) with the Ad5-VCA0956 and Ad5-VCA0956 mutant allele (Ad5-VCA0956\*) adenovirus vectors and measured c-di-GMP using LC-MS/MS after 24 hours. The Ad5-Null vector, an adenovirus construct carrying no transgene, was also included as a negative control. I found that cells infected with the Ad5-VCA0956 produced high concentrations of c-di-GMP, whereas cells infected with the Ad5-VCA0956\* or the Ad5-Null produced no detectable c-di-GMP (Fig. 26B). Importantly, similar to VCA0956 plasmid transfections, infection with Ad5-VCA0956 had no noticeable impact on cell morphology or viability. These results demonstrate that an adenovirus vector can be used to deliver a *V. cholerae* DGC into a eukaryotic cell to synthesize c-di-GMP.

#### *Synthesis of c-di-GMP in a murine system*

As the Ad5-VCA0956 vector is capable of producing c-di-GMP in HeLa cells *in vitro*, I next determined if my vector produces c-di-GMP *in vivo* in a murine model system. Therefore, BALB/c mice (n=3) were IV injected with the Ad5-Null, Ad5-VCA0956, or the Ad5-VCA0956\* vectors and quantitative PCR was utilized to measure adenovirus genomes in the spleen and liver of injected mice at 24 hours post injection (h.p.i.). I observed comparable Ad5 genome counts for each treatment

in both the liver and spleen (Fig. 27A). Consistent with previous reports that the predominant tropism of adenovirus is in the liver [172, 177, 178], there were significantly more Ad5 genomes in the liver cells than in the spleen cells. I then measured c-di-GMP in both the liver and spleen using LC-MS/MS, and found that the Ad5-VCA0956 vector produced detectable c-di-GMP in both tissues, whereas the Ad5-Null and Ad5-VCA0956\* vectors produced no detectable c-di-GMP (Fig. 27B). The concentration of c-di-GMP was consistent with the abundance of Ad5-VCA0956 genomes per cell, as the amount of c-di-GMP was significantly higher in the liver tissue than the spleen. These data indicate that the Ad5-VCA0956 vector is capable of initiating c-di-GMP synthesis in a murine model system.

*C-di-GMP synthesized in vivo stimulates innate immunity in a mouse model*

It has been previously shown that adenovirus vectors stimulate several pro-inflammatory innate immune response genes [162, 166, 171]. To examine if the Ad5-VCA0956 alters the profile of innate immune gene expression compared to the Ad5 vector alone, Balb/c mice (n=3) were IV injected with Ad5-Null, Ad5-VCA0956, and Ad5-VCA0956\* and qRT-PCR was utilized to quantify the expression levels of several liver gene transcripts at 24 h.p.i. Infection with Ad5-VCA0956 had no observable effect on the health of the mice. I found that the Ad5-Null treatment was able to stimulate 6 of the 12 markers examined (> 2-fold; ADAR, MCP-1, TLR2, IP10, Oas1a, RIG1) (Fig. 28). These results are consistent with previous studies demonstrating that the adenovirus vector alone is capable of altering gene expression in the liver [165, 166]. The expression of four genes was significantly

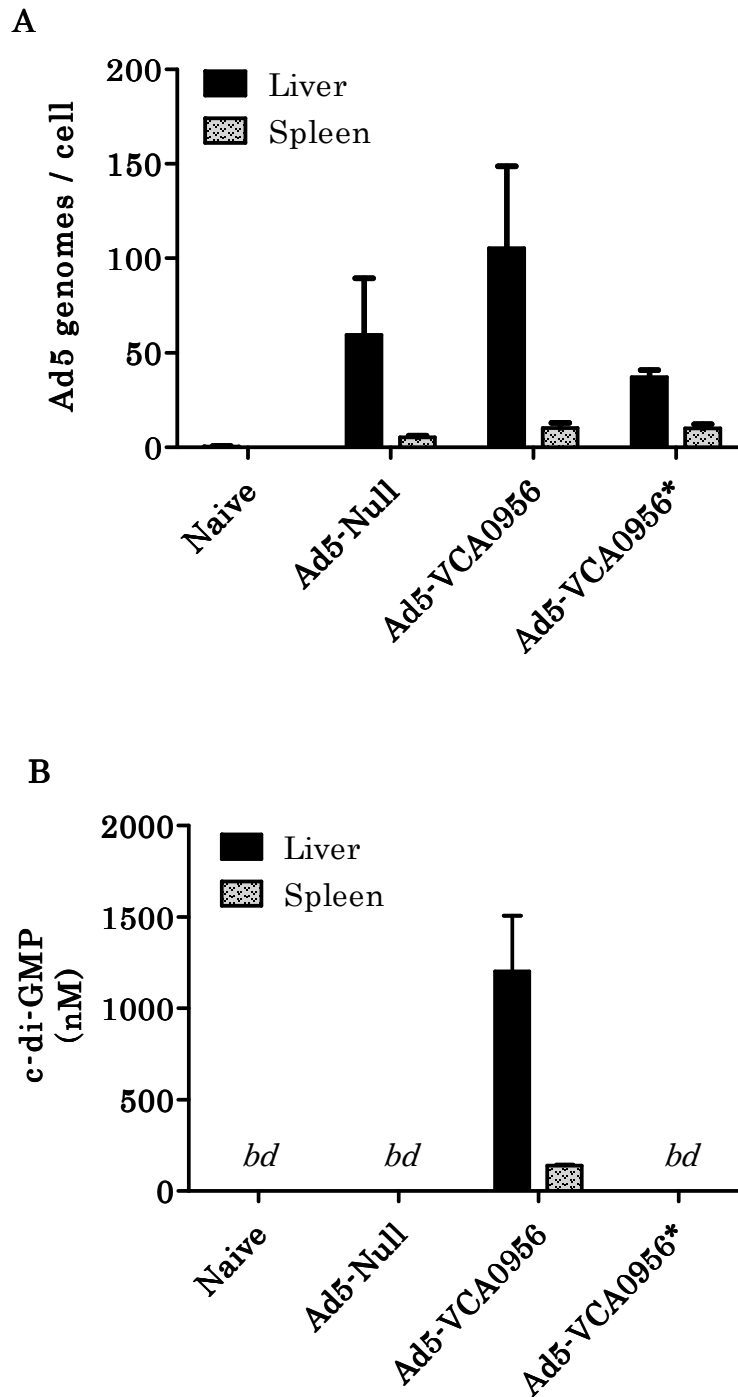


**Figure 27. Infection of Ad5-VCA0956 in a murine model system.** Mice were infected with Ad5 vectors intravenously. (A) After 24 hours qPCR was used to quantify Ad5 genomes in liver cells (black) or spleen cells (hashed). Data were normalized to internal GAPDH control. (B) LC-MS/MS was used to quantify c-di-GMP extracted from the liver (black) or spleen (checked). Bars represent the mean of 3 replicates; error bars indicate standard deviation. *bd* indicates below detection.

( $p < 0.05$ ) higher in the Ad5-VCA0956 treatment compared to the Ad5-VCA0956\* treatment (Fig. 28A); these include the IFN-responsive gene ADAR, the monocyte and basophil chemotractant MCP-1, the toll-like receptor (TLR) signaling pathway gene MyD88, and the pattern recognition receptor TLR2. It is worth noting that c-di-GMP sensing in the cytoplasm is thought to be independent of TLRs [53].

Additionally, the expression of three genes was significantly ( $p < 0.05$ ) repressed in the Ad5-VCA0956 treatment compared to the Ad5-VCA0956\* treatment (Fig. 28B): the pro-inflammatory interleukin genes IL18 and IL1 $\beta$ , and the interferon transcription factor IRF3. Interestingly, IRF3 has been shown to interact with STING to initiate a c-di-GMP-mediated host type I interferon response [48, 179, 180].

In the cytoplasm, c-di-GMP interacts with STING to activate IRF3, NF- $\kappa$ B, and the p38/JNK/ERK MAP kinase signaling pathways, resulting in increased production of numerous cytokines and chemokines characteristic of an innate immune response [48]. To determine if the Ad5-VCA0956 vector is capable of increasing cytokine and chemokine secretion, I directly quantified the abundance of cytokines and chemokines in the plasma of mice treated with Ad5-VCA0956 using a multiplexed assay system at 6 (Table 2) and 24 (Table 3) h.p.i. Consistent with prior studies showing that the adenovirus vector stimulates the secretion of pro-inflammatory cytokines and chemokines [166, 167], I observed 9 cytokines and

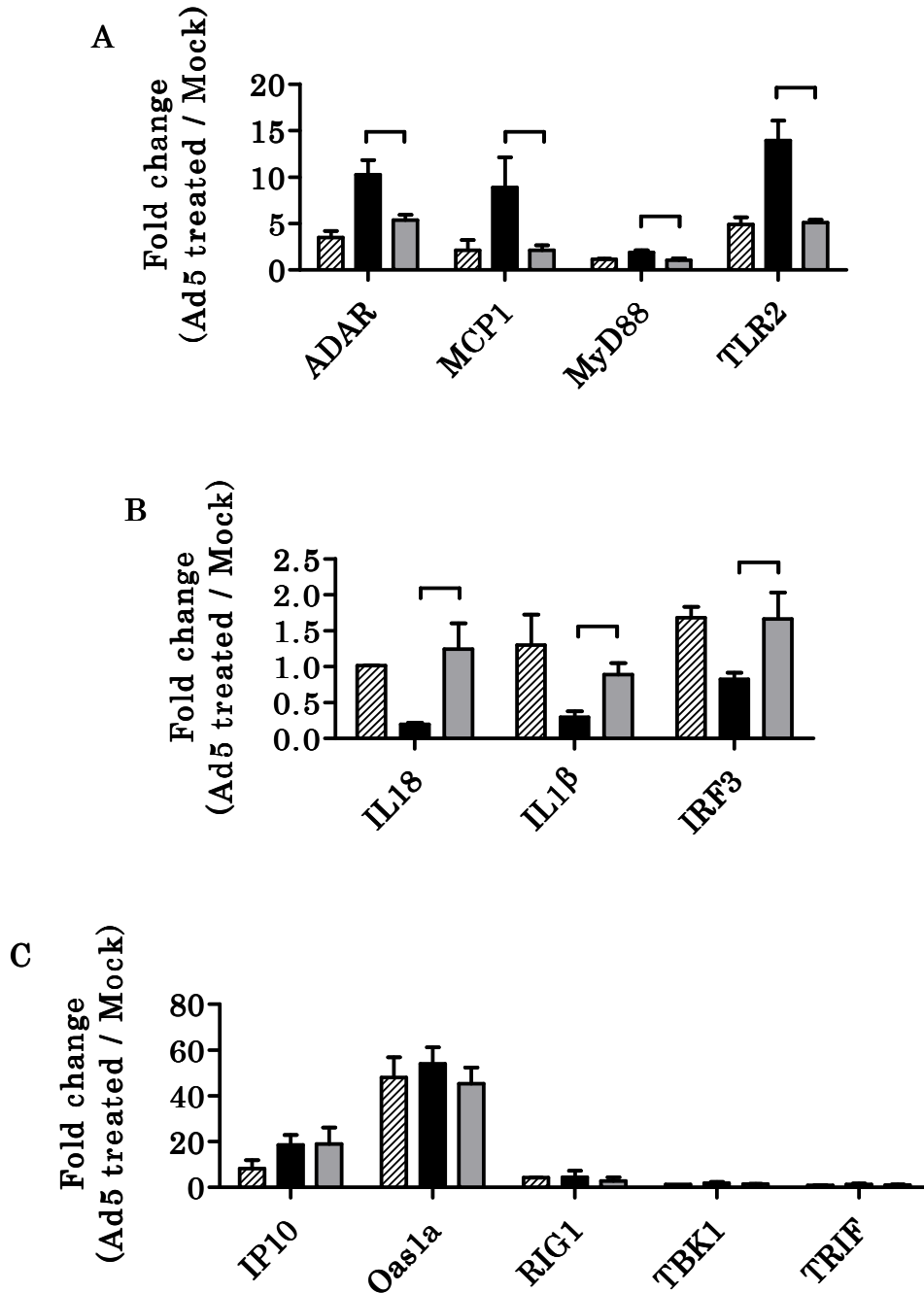


**Figure 28. qRT-PCR of mouse liver gene transcripts 24 hours after infection with Ad5 vectors.** Ad5-Null (striped), Ad5-VCA0956 (black), or Ad5-VCA0956\* (grey) were normalized to internal GAPDH control. Fold change indicates each value normalized to values measured from mock treated mice. Results are separated into liver gene expression increased by Ad5-VCA0956 (A), decreased by Ad5-VCA0956 (B), or unaffected by Ad5-VCA0956 (C). Bars represent the mean of 3 replicates; error bars indicate standard deviation. Brackets indicate statistical significance,

which was determined using a two-tailed Student's t-test ( $P < 0.05$ ). chemokines that were modestly induced in the Ad5-Null treated mice compared to the naïve mice (IFN- $\gamma$ , MCP-1, G-CSF, MIP-1 $\alpha$ , IL-6, MIP-1 $\beta$ , IL-12p40, KC, RANTES; > 3-fold), and these differences were greatest at the 6-hour time point. I found that 15 cytokines and chemokines were significantly increased in the plasma of the Ad5-VCA0956 treated mice compared to the control Ad5-VCA0956\* treated mice at one or both of the two timepoints. Furthermore, for the majority of cytokines and chemokines examined, the largest differences observed were at the 24 hour time point, indicating that the effect of Ad5-VCA0956 is both more potent and longer lasting than that of the adenovirus vector alone. The induction of most of these cytokines and chemokines are consistent with other studies examining the immunostimulatory effects of c-di-GMP [50, 52-56]. Interestingly, I observed increases in IL-1 $\alpha$ , G-CSF, and Eotaxin levels in the Ad5-VCA0956 injected mice, which have not been previously reported to be induced by c-di-GMP. These data together indicate that the Ad5-VCA0956 vector is capable of inducing a robust innate response beyond that of the adenovirus vector alone in a murine model system.

*C-di-GMP synthesized in vivo lowers the effective antigen dose of Ad5-TA*

The purpose of an adjuvant is to enhance the efficacy of a paired antigen by increasing the longevity, potency, or reducing the effective dose. To determine how well the Ad5-VCA0956 construct functions as a vaccine adjuvant, I tested if Ad5-VCA0956 could enhance the adaptive response to a *C. difficile* antigen. *C. difficile*, a

	6 h.p.i			
	Mock	Ad5-Null	Ad5-VCA0956	Ad5-VCA0956*
IL-1 $\alpha$	26.93 $\pm$ 5.33	33.96 $\pm$ 3.90	39.19 $\pm$ 11.51	35.67 $\pm$ 18.20
IL-1 $\beta$	1266.47 $\pm$ 976.22	597.54 $\pm$ 54.53	601.11 $\pm$ 135.01	792.85 $\pm$ 177.15
IL-4	2.70 $\pm$ 0.39	4.26 $\pm$ 0.47	4.11 $\pm$ 0.33	3.51 $\pm$ 0.33
<b>IL-6</b>	27.89 $\pm$ 31.57	137.62 $\pm$ 25.88	2836.67 $\pm$ 313.53**	135.95 $\pm$ 72.95
IL-10	<i>bd</i>	26.65 $\pm$ 11.62	45.46 $\pm$ 3.5	32.71 $\pm$ 9.65
IL-12(p40)	511.64 $\pm$ 210.70	3351.06 $\pm$ 368.94	3847.84 $\pm$ 733.63	4165.28 $\pm$ 601.5
IL-13	164.30 $\pm$ 205.70	171.12 $\pm$ 85.67	231.81 $\pm$ 44.87	156.88 $\pm$ 13.23
Eotaxin	1033.46 $\pm$ 286.53	1578.95 $\pm$ 204.69	2582.84 $\pm$ 189.22	2181.27 $\pm$ 413.21
<b>G-CSF</b>	93.43 $\pm$ 100.88	1265.03 $\pm$ 771.43	3722.93 $\pm$ 577.59**	1173.55 $\pm$ 235.67
GM-CSF	<i>bd</i>	84.27 $\pm$ 6.55	142.15 $\pm$ 14.05	85.35 $\pm$ 41.35
<b>IFN-<math>\gamma</math></b>	3.66 $\pm$ 4.81	28.14 $\pm$ 4.64	452.73 $\pm$ 90.62*	37.45 $\pm$ 4.85
KC	5.16 $\pm$ 5.48	257.61 $\pm$ 96.01	346.74 $\pm$ 39.01	174.94 $\pm$ 136.14
<b>MCP-1</b>	<i>bd</i>	4309.67 $\pm$ 213.69	7146.20 $\pm$ 1166.34**	4816.93 $\pm$ 2357.41
MIP-1 $\alpha$	7.98 $\pm$ 5.56	47.50 $\pm$ 10.61	61.10 $\pm$ 5.88	48.89 $\pm$ 20.07
MIP-1 $\beta$	73.61 $\pm$ 92.93	582.11 $\pm$ 108.91	1022.01 $\pm$ 105.93	754.20 $\pm$ 354.18
RANTES	22.10 $\pm$ 11.30	71.37 $\pm$ 4.45	109.03 $\pm$ 10.51	67.26 $\pm$ 16.77
<b>IL-12(p70)</b>	15.17 $\pm$ 2.33	345.81 $\pm$ 81.94	1091.77 $\pm$ 331.08**	463.09 $\pm$ 106.69

**Table 2. Cytokine and chemokine secretion of mice infected with Ad5 vectors after 6 hours.** Mice were infected IV with either Ad5-Null (n=2), Ad5-VCA0956 (n=3), or Ad5-VCA0956 (n=3). Values indicate the mean pg / mL  $\pm$  standard deviation. Asterisks (\*) indicate a statistically significant difference between Ad5-VCA0956 and Ad5-VCA0956\*, which was determined using a two-way ANOVA test combined with a Bonferroni posttest (\* p <0.05; \*\* p < 0.01).

	24 h.p.i.			
	Mock	Ad5-Null	Ad5-VCA0956	Ad5-VCA0956*
<b>IL-1<math>\alpha</math></b>	9.99 ± 2.16	15.96 ± 4.12	115.58 ± 30.86**	18.78 ± 5.57
IL-1 $\beta$	1056.48 ± 950.52	441.68 ± 6.21	723.60 ± 63.81	642.02 ± 259.42
<b>IL-4</b>	2.88 ± 0.13	2.79 ± 0.25	6.08 ± 0.87**	3.25 ± 0.47
IL-6	4.18	<i>bd</i>	640.05 ± 291.76	27.03
<b>IL-10</b>	<i>bd</i>	6.22 ± 4.09	212.84 ± 145.12*	11.91 ± 5.82
<b>IL-12(p40)</b>	309.78 ± 63.47	989.84 ± 20.73	11602.17 ± 3585.45**	1069.21 ± 335.21
<b>IL-13</b>	55.80 ± 68.56	19.00 ± 16.51	287.97 ± 7.54*	13.08 ± 8.15
<b>Eotaxin</b>	539.42	836.39 ± 229.64	3974.88 ± 894.88**	743.67 ± 187.39
<b>G-CSF</b>	94.72 ± 46.39	302.85 ± 56.98	156212.26 ± 59031.70**	300.03 ± 38.42
GM-CSF	15.06	<i>bd</i>	216.35 ± 16.78	<i>bd</i>
IFN- $\gamma$	<i>bd</i>	<i>bd</i>	17.10 ± 4.60	<i>bd</i>
<b>KC</b>	5.61 ± 6.84	43.02 ± 11.94	1159.46 ± 523.33*	61.28 ± 57.88
<b>MCP-1</b>	<i>bd</i>	169.58 ± 12.19	55001.74 ± 19457.26**	327.11 ± 38.26
<b>MIP-1<math>\alpha</math></b>	2.45	12.85 ± 8.24	303.94 ± 27.35**	14.24 ± 9.31
<b>MIP-1<math>\beta</math></b>	39.55 ± 50.19	40.73 ± 0.69	1291.42 ± 360.00**	92.01 ± 73.37
<b>RANTES</b>	11.5 ± 4.33	53.69 ± 3.49	3657.80 ± 1455.71**	68.55 ± 14.17
IL-12(p70)	7.19 ± 4.39	6.45 ± 5.43	90.28 ± 6.22	8.95 ± 9.74

**Table 3. Cytokine and chemokine secretion of mice infected with Ad5 vectors after 24 hours.** Mice were infected IV with either Ad5-Null (n=2), Ad5-VCA0956 (n=3), or Ad5-VCA0956\* (n=3). Values indicate the mean pg / mL ± standard deviation. Asterisks (\*) indicate a statistically significant difference between Ad5-VCA0956 and Ad5-VCA0956\*, which was determined using a two-way ANOVA test combined with a Bonferroni posttest (\* p < 0.05; \*\* p < 0.01).

Gram-positive spore-forming anaerobic bacteria, is the leading causative agent of nosocomial infections leading to diarrheal disease in the developed world. *C. difficile* associated diarrhea (CDAD) represents nearly 1% of all hospital stays in the United States and can lead to septicemia, renal failure, and toxic megacolon [181].

Incidents and mortality of *C. difficile* infections are rising in the U.S., and the economic burden on the health care system is reported to be in the billions of dollars [181-185]. Furthermore, to date there are no approved effective vaccine treatments available for CDAD treatment or prevention [186].

A previously developed adenovirus vector that expresses the immunogenic portion of the *C. difficile* toxin A (Ad5-TA) protects mice from a toxin challenge by generating a humoral and T-cell response specific to toxin A in a murine model system [170]. I hypothesized that supplementing this vaccine with the Ad5-VCA0956 adjuvant would enhance this humoral and T-cell response due to the strong pro-inflammatory innate response it generates. I therefore vaccinated mice by IM injection with varying concentrations of the Ad5-TA vector in combination with the Ad5-VCA0956 vector in equal ratio ranging from  $1 \times 10^6$  to  $5 \times 10^9$  viral particles (vp). After two weeks, I assessed TA specific T-cell responses in the spleens of the naive and vaccinated animals using an IFN $\gamma$  ELISpot assay, utilizing the 15-mer peptide (VNGSRYYFDTDTAIA) that has been previously shown to elicit the secretion of IFN $\gamma$  in splenocytes of mice immunized with the Ad5-TA vector [170]. I found that co-injection of equal amounts of the Ad5-TA and the mutant DGC allele vector Ad5-VCA0956\* produced no induction of IFN $\gamma$  secreting T-cells over that of

naïve splenocytes at viral doses of  $1 \times 10^6$  and  $1 \times 10^7$ , but did generate significant IFN $\gamma$  producing T-cells at  $1 \times 10^8$  and  $5 \times 10^9$  (Fig. 29, white squares). Although co-injection of  $1 \times 10^6$  Ad5-TA with Ad5-VCA0956 did not produce increased IFN $\gamma$  levels, I observed significantly increased ( $p < 0.05$ ) IFN $\gamma$  producing T-cells at a dose of  $1 \times 10^7$ , as compared to cells derived from the DGC mutant treated control (Fig. 29, black squares). No c-di-GMP was detected in the liver of mice infected with Ad5-VCA0956 at the  $5 \times 10^9$  dose after 14 days, suggesting that even at high doses, IM administration of Ad5-VCA0956 does not lead to long-lasting c-di-GMP production at distal sites (data not shown). Thus, I conclude that c-di-GMP synthesized by Ad5-VCA0956 lowers the effective dose to generate an adaptive response to Ad5-TA.

*Ad5-VCA0956 does not significantly enhance protection of Ad-TA against C. difficile*

To determine if the Ad5-VCA0956 construct increases the efficacy of the Ad5-TA vaccine *in vivo*, I decided to test the adjuvant-vaccine combination in a cefoperazone-treated mouse *C. difficile* challenge model [173, 174]. I first sought to determine the optimum dose of *C. difficile* to administer to effectively challenge the mice. Naïve mice were administered cefoperazone (0.5 mg/mL in drinking water) for 10 days, followed by a two day rest period. Mice were then administered varying doses ranging from  $5 \times 10^3$  to  $5 \times 10^6$  of hyperinfectious *C. difficile* CD2015 (NAP-1, 027 ribotype [187]) spores by oral gavage. The strain of *C. difficile* used is a clinically isolated strain from a hospital in Southeast Michigan (unpublished). Weights of the mice were monitored for a four day period. Mice were sacrificed upon

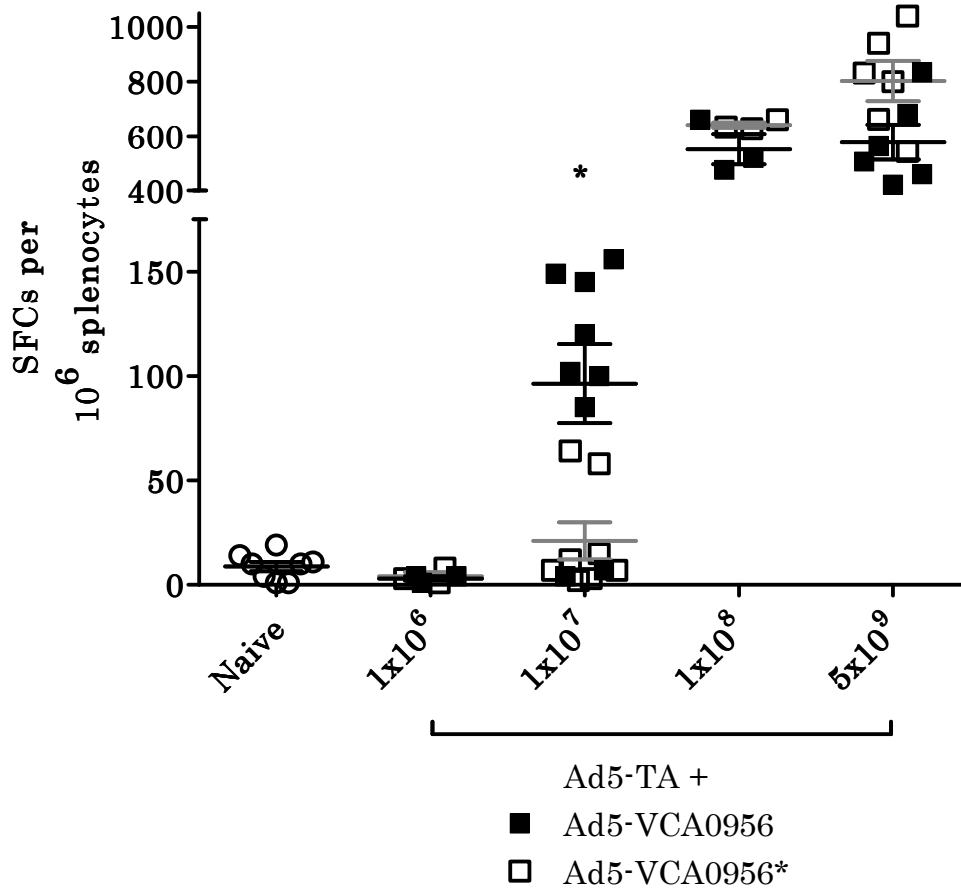


**Figure 29. IFN $\gamma$  ELISPOT analysis of mice vaccinated with Ad5-TA and Ad5 vectors.** Mice were administered IM varying doses of both Ad-TA and either Ad-VCA0956 (black) or Ad-VCA0956\* (grey). After 14 days, splenocytes were *ex vivo* stimulated with a *C. difficile* specific peptide and the number of IFN $\gamma$  secreting splenocytes was determined using ELISPOT. Each point represents an individual animal. Lines indicate the mean of the replicates, and error bars indicate standard error. \* indicates statistical significance using a two-way ANOVA test combined with a Bonferroni posttest ( $P < 0.05$ ).

losing >20% of their initial body weight. I found that none of the mice administered the lowest dose lost >20% of their initial body weight (Fig. 30 A and B). However, when the dose was increased, I observed significantly more weight loss. The

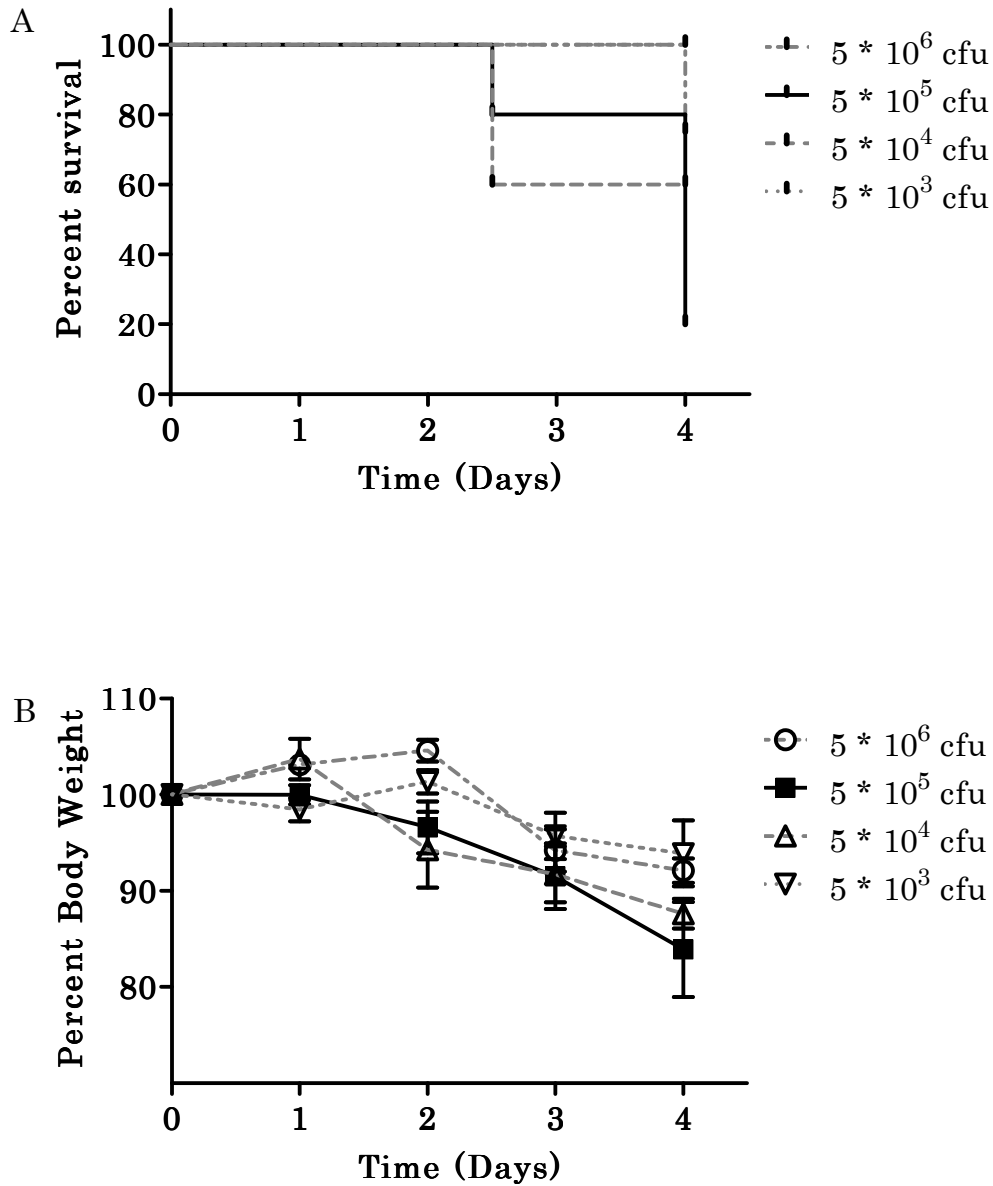


**Figure 30. *C. difficile* challenge of BALB/c mice.** Mice were challenged with varying doses of *C. difficile* CD2015 spores. (A) Survival of mice challenged with varying doses of *C. difficile*. Mice were sacrificed after losing > 20% of their initial body weight. (B) Weight loss of mice challenged with *C. difficile*. Each point represents the mean of 5 replicates. Error bars indicate standard error.

greatest weight loss was observed in the  $5 \times 10^5$  dose of *C. difficile*, resulting in 80% mortality by day 4 of the challenge.

To determine how effective my Ad5-VCA0956 adjuvant was at increasing the protective properties of Ad5-TA, I vaccinated mice with  $1 \times 10^7$  vp of both the Ad5-TA vaccine antigen and the Ad5-VCA0956 adjuvant vector; this dose was selected as it produced a significant difference in the ELISPOT analysis (Fig. 29). As controls, I also vaccinated mice with equal doses of the Ad5-TA vaccine with the Ad5-VCA0956\* and Ad5-Null vectors. After 10 weeks, mice were administered cefoperazone for 10 days, followed by a 2-day rest. Mice were then challenged with  $5 \times 10^5$  *C. difficile* spores. I found that both the mortality and weight loss of all mice treated with the Ad5-TA was less than the naïve mice (Fig. 31). However, I did not observe any significant differences between the mice that received the Ad5-VCA0956 treatment compared to either the Ad5-VCA0956\* or the Ad5-Null treatments. And while the average weight loss at the end of the challenge was lowest in the Ad5-VCA0956 treated mice, this difference was not statistically significant from that of the Ad5-VCA0956\* or Ad5-Null treated mice. Thus, I conclude from this experiment that in the conditions examined here, the Ad5-VCA0956 does not contribute to the effectiveness of the Ad5-TA vaccine.

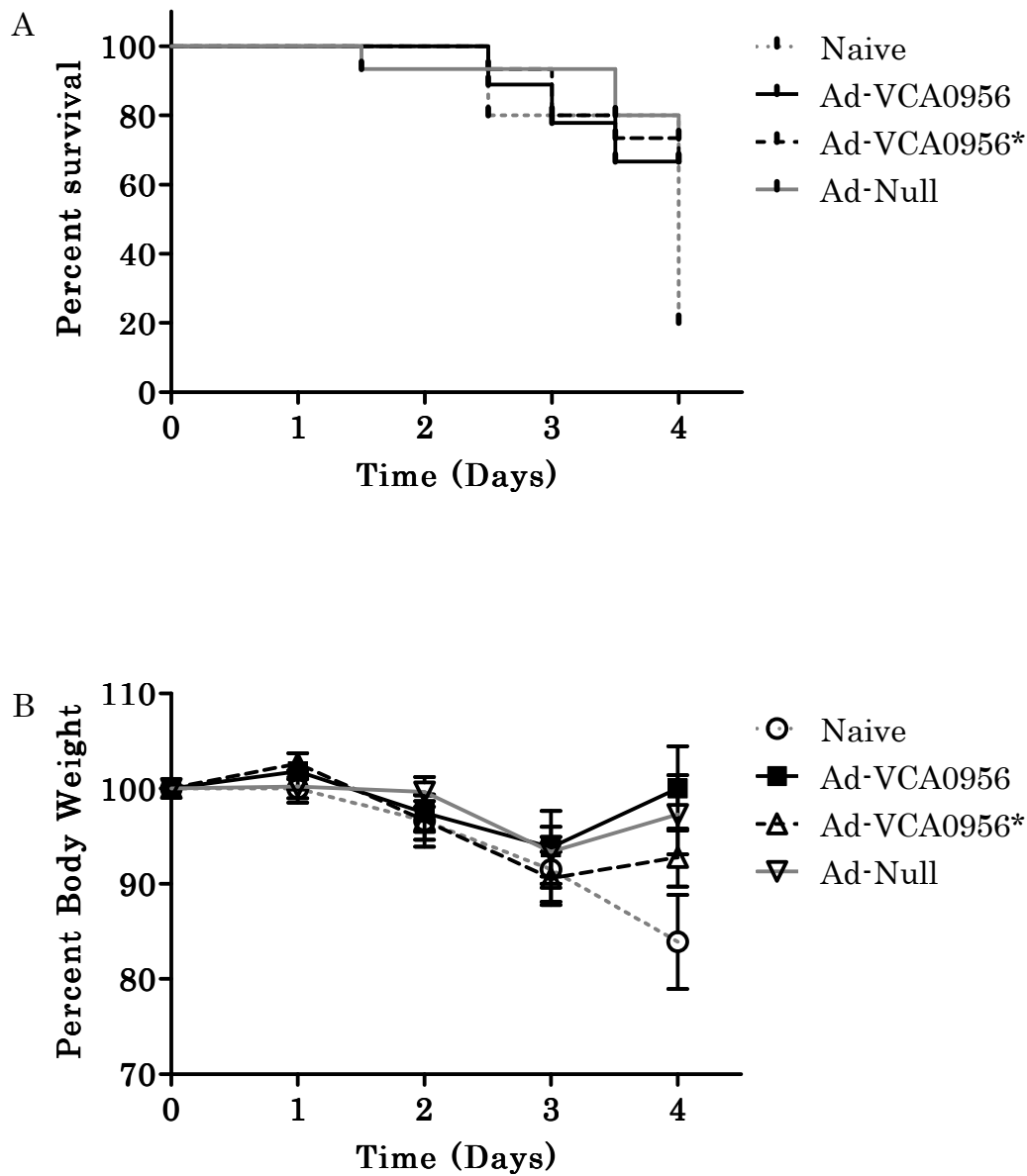


**Figure 31. *C. difficile* challenge of BALB/c mice vaccinated with Ad5-TA and Ad5-VCA0956.** Mice were treated with equal doses of Ad5-TA and either Ad5-VCA0956 (squares), Ad5-VCA0956\* (up-triangles), or Ad5-Null (down-triangles). (A) Survival of mice challenged with *C. difficile*. Mice were sacrificed after losing > 20% of their initial body weight. (B) Weight loss of mice challenged with *C. difficile*. Naïve: N=5, Ad5-VCA0956: N=9, Ad5-VCA0956\* and Ad5-Null: N=15. Error bars indicate standard error.

## *Discussion*

With a current demand for novel vaccines that target difficult-to-treat diseases, it is crucial to have adjuvants to pair with these vaccines to optimize efficacy. Currently, there are a limited number of adjuvants available for clinical use, and there is a need for new adjuvants which can enhance the efficacy of vaccines to improve immunological protection [61, 188]. Numerous studies have implicated c-di-GMP as a promising novel adjuvant. Indeed, this second messenger molecule has been shown to stimulate a robust type I interferon response and increase the secretion of numerous cytokines and chemokines to initiate a balanced Th1/Th2 response, as well as stimulate the inflammasome pathway and immune cell activation/recruitment [49-57]. My approach to utilize c-di-GMP as an adjuvant is novel in that it utilizes an adenovirus vector to deliver c-di-GMP producing enzyme DNA into cells, thereby synthesizing the adjuvant *in vivo* and circumventing the inefficient delivery of IM or IV administration of chemically synthesized c-di-GMP. Adenovirus vectors are promising in that they are cost-efficient to produce and can efficiently deliver specific antigens or adjuvants into cells for *in vivo* production, greatly reducing the cost of using c-di-GMP as an adjuvant.

I have demonstrated that an adenovirus vector carrying a bacterial DGC is capable of synthesizing c-di-GMP in both human and mouse model systems. Consistent with other reports utilizing c-di-GMP, synthesis of c-di-GMP by virally mediated transduction of the DGC gene *in vivo* increases the secretion of numerous

cytokines and chemokines [50, 52-57]. These induced cytokines and chemokines include signals characteristic of both Th1 (Table 2 and 3, IFN $\gamma$ , IL-12) and Th2 (Table 2 and 3, IL-4, IL-6) type responses. Additionally, c-di-GMP production from Ad5-VCA0956 enhances activation of the innate immune system by activating TLR signaling (Fig. 28, TLR2, MyD88). It appears however that c-di-GMP synthesized *in vivo* negatively regulates the expression of inflammasome-dependent pathways in hepatocytes (Fig. 28, IL-1 $\beta$ , IL-18). The significance of this finding is unclear, especially as it has been reported that c-di-GMP activates the NLRP3 inflammasome pathway [51]. Importantly, I observed no signs of poor cell physiology or health in my cell cultures and animal models. Furthermore, my data indicate that the c-di-GMP synthesized by the Ad5-VCA0956 vector is transient, and thus should enhance antigen recognition and response while minimizing any potentially unwanted long term effects associated with administration, such as autoimmune activation [189].

I have also shown that c-di-GMP synthesized *in vivo* reduces the effective antigen dose of Ad5-TA, a vaccine antigen which targets the toxin of the human pathogen *C. difficile*. Reducing the dose required to initiate an adaptive immune response is of particular significance as high viral particle doses can lead to global toxicities, endothelial cell activation, and liver damage [171, 177, 190-192]. C-di-GMP has been shown to enhance protection against other pathogens including *S. aureus*, *K. pneumoniae*, and *S. pneumoniae* [53-55, 58], indicating that c-di-GMP has broad antigen-adjuvant synergy. Although I have only demonstrated an

enhanced adaptive response to *C. difficile in vitro*, Ad5-VCA0956 can be coupled with other vaccines to enhance antigen recognition efficacy. While c-di-GMP is a bacteria-specific second messenger, the Ad5-VCA0956 stimulated c-di-GMP innate immune response could enhance protection in viral or cancer vaccine systems as well.

I believe that the approach of synthesizing c-di-GMP *in vivo* offers numerous advantages over directly administering c-di-GMP as a mucosal, intramuscular, or intravenous adjuvant; these include lower cost, more efficient adjuvant delivery, and a more robust innate immune response. Furthermore, adjustments can be made to alter and optimize the Ad5-VCA0956 for clinical use. *V. cholerae* contains 40 predicted DGC alleles within its genome, and it has been shown that ectopic expression of these different DGCs results in different intracellular c-di-GMP concentrations [79]. Hence intracellular expression of other DGCs could produce different amounts of c-di-GMP in eukaryotic cells, increasing the efficiency of this adjuvant. Alternatively, other types of second messengers could be used to stimulate innate immunity. One example would be to express a diadenylate cyclase to synthesize the related bacterial second messenger cyclic di-AMP *in vivo*. Cyclic di-AMP has similarly been shown to induce a robust innate immune response through STING mediated recognition [193, 194]. Additionally, different promoters could be used in lieu of the CMV promoter to produce localized or temporally controlled c-di-GMP production in the body.

### *Future directions*

With a current demand for development of vaccines for otherwise difficult to treat infectious diseases, vaccine adjuvant development has been proposed as a promising research avenue. I have shown that an adenovirus vector harboring a DGC gene results in c-di-GMP synthesis in eukaryotic cells, leading to robust stimulation of the innate immune system. In this study, I identified two DGCs that produced c-di-GMP upon transfection into HeLa cells (Fig. 26A). The DGC VCA0848 produced significantly more c-di-GMP upon transfection than the VCA0956 strain. As my data indicate that this DGC is more efficient at synthesizing c-di-GMP in the eukaryotic cell environment, I hypothesize that an Ad5 construct harboring this DGC will produce more intracellular c-di-GMP than the Ad5-VCA0956 vector *in vivo*. This is significant, as less adenovirus would be required to stimulate innate immunity and thus would increase the effect of c-di-GMP specific innate immune activation compared to Ad5-stimulated innate immunity. Furthermore, reducing the dosage of Ad5 required to initiate an innate immune response would reduce the adverse effects associated with Ad5 treatment [171, 177, 190-192]. I propose creating an Ad5-VCA0848 construct and determining its effect on innate and adaptive immunity as described in Chapter 4.

Previous studies demonstrated that administration of purified c-di-GMP leads to an innate immune response that conveys protection against *S. pneumonia*, *K. pneumonia*, and *S. aureus* [53, 54, 58]. As the Ad5-VCA0956 is able to synthesize c-di-GMP *in vivo*, I hypothesize that the Ad5-VCA0956 produces a more efficient

stimulation of innate immunity and thus leads to a more robust response. I propose to test the Ad5-VCA0956 in a *S. pneumonia* challenge model to see if the vector is capable of protecting animals against acute bacterial infection [58]. As a control, the Ad5-VCA0956\* and the Ad5-Null vectors should be included to account for any protection granted by the vector or expressing a bacterial protein in an animal. Additionally, purified c-di-GMP should be administered intranasally as a control to determine if the Ad5-VCA0956 is more effective than c-di-GMP.

The Ad5-VCA0956 construct is able to increase the adaptive response of Ad5-TA at lower doses (Table 2 and 3, Fig. 29). However, treatment of mice with Ad5-VCA0956 in combination with Ad5-TA did not increase protection in a *C. difficile* mouse challenge model compared with Ad5-VCA0956\* or the empty Ad5-Null vector. The dose I utilized in this challenge was the dose that increased IFN $\gamma$  production of splenocytes compared to the negative controls (Fig. 29). It is possible that this dose is not sufficient to produce other cytokines or chemokines important for enhancing an adaptive immune response. I postulate that the Ad5-VCA0956 vector could increase the protection of Ad5-TA at higher doses. I propose repeating this challenge with different doses of the Ad5-VCA0956 while maintaining the Ad5-TA dose. Additionally, this experiment should be repeated with the Ad5-VCA0848 to determine if increased Ad5 mediated c-di-GMP production can improve protection.

## CHAPTER 6 – Conclusions

While there are numerous studies describing the role c-di-GMP plays in regulating the physiology of many bacteria, the regulatory inputs to this almost ubiquitously utilized second messenger are currently under-characterized. I have demonstrated that the growth environment effects intracellular c-di-GMP concentrations in *V. cholerae*, and that these differences can be as great as 20-fold (Fig. 5). Furthermore, I have developed a novel method to differentiate the impact of c-di-GMP synthesis and hydrolysis on overall intracellular c-di-GMP. This method can be applied to other bacterial systems to determine the effects of specific environmental factors on c-di-GMP, the effects of deleting DGCs and PDEs, and differences in c-di-GMP synthesis and hydrolysis between different organisms.

The intestinal environment is a tropism for many human pathogens. To efficiently cause disease, pathogens recognize specific host-derived cues and subsequently produce virulence factors. It has been proposed that the intracellular c-di-GMP of *V. cholerae* is elevated in the marine environment, and reduced in the human host. In contrast, my research suggests that the regulation of intracellular c-di-GMP in *V. cholerae* in the human host is more complex than previously appreciated. I have demonstrated that bile and bicarbonate inversely modulate intracellular c-di-GMP, where bile increases c-di-GMP approximately 4-fold and bicarbonate quenches this induction (Fig. 8, 18). As c-di-GMP signaling is widely distributed amongst bacteria, it is possible that other enteric bacteria employ similar responses as *V. cholerae* to bile and bicarbonate in order to adapt to

different microenvironments within the small intestine. Thus, this study may provide insights about the role c-di-GMP plays in the biology of both human pathogens and normal members of the human intestinal microbiota.

Growth rate regulation of bacteria has been a focus of study for the last 50 years, and yet there are still many questions regarding how cell division is governed. I have demonstrated that intracellular c-di-GMP concentration and growth rate are negatively correlated in *V. cholerae* (Fig. 20, 21, 22). I have also shown that rRNA is decreased upon ectopic DGC expression (Fig. 25). Determining the mechanism governing the c-di-GMP mediated growth rate inhibition is important, as this phenotype could have large implications in core bacterial processes. Understanding the relationship between growth rate regulation and c-di-GMP is also informative for drug discovery studies targeting compounds that effect c-di-GMP synthesis and hydrolysis, as these compounds may have unanticipated effects on bacterial growth rate.

As new and re-emerging infectious diseases continue to take a toll on our population and burden our healthcare system, vaccine and adjuvant development offer promising solutions to combat this problem. I have shown that a DGC delivered into the cytoplasm of a eukaryotic cell can synthesize c-di-GMP and activate innate immunity by inducing the production of 15 cytokines and chemokines (Fig. 26, 27; Table 2, 3). Furthermore, I have provided evidence that using adenovirus to deliver a DGC gene can be utilized as a vaccine adjuvant to enhance an adaptive immune response (Fig. 29). As c-di-GMP initiates a potent

innate response, our novel adenovirus construct is a promising candidate for clinical applications to enhance the efficacy of existing vaccine antigens. Additionally, the Ad5-VCA0956 vector is capable of efficiently producing high levels of c-di-GMP in eukaryotic cells, and thus can be used as a tool elucidate the different c-di-GMP response mechanisms of various eukaryotic cell types.

There are still many questions regarding regulatory inputs to c-di-GMP signaling networks, as well as what behaviors c-di-GMP regulates in response to these inputs. Discerning how bacteria interact with and perceive their changing environments is paramount to understanding the ecology and behaviors of these organisms, as well as developing new clinical applications to protect ourselves against devastating human pathogens. I have demonstrated here that the role of c-di-GMP as a second messenger is to translate environmental signals into physiological changes that allow *V. cholerae* to adapt and persist in various niches. As c-di-GMP is ubiquitously utilized amongst bacteria, we are only beginning to appreciate the role this molecule plays in enabling bacteria to transition between different lifestyles, the physiological changes associated with different levels of intracellular c-di-GMP, and the subsequent impact on the pathogenesis of bacteria.

## **APPENDICES**

Strain	Genotype	Reference
<i>Escherichia coli</i> DH10B		Invitrogen
<i>Escherichia coli</i> S17		[103]
<i>Vibrio cholerae</i> C6706	WT	[78]
<i>Vibrio cholerae</i> $\Delta vpsL$	VC0934 ( <i>vpsL</i> ) knockout mutant	[72]
<i>Vibrio cholerae</i> $\Delta hapR$	<i>hapR</i> knockout mutant	[67]
<i>Vibrio cholerae</i> $\Delta luxO$	VC1021 ( <i>luxO</i> ) knockout mutant	[68]
<i>Vibrio cholerae</i> $\Delta cdgA$	VCA0074 knockout mutant	Chapter 2
<i>Vibrio cholerae</i> $\Delta toxR$	VC0984 ( <i>toxR</i> ) knockout mutant	Chapter 3
<i>Vibrio cholerae</i> $\Delta toxT$	VC0838 ( <i>toxT</i> ) knockout mutant	Chapter 3
<i>Vibrio cholerae</i> $\Delta VC1372$	VC1372 knockout mutant	Chapter 3
<i>Vibrio cholerae</i> $\Delta VC1376$	VC1376 knockout mutant	Chapter 3
<i>Vibrio cholerae</i> $\Delta VC1067$	VC1067 knockout mutant	Chapter 3
<i>Vibrio cholerae</i> $\Delta VC1372 \Delta VC1376$	VC1372, VC1376 double knockout mutant	Chapter 3
<i>Vibrio cholerae</i> $\Delta VC1372 \Delta VC1376$ $\Delta VC1067$	VC1067, VC1372, VC1376 triple knockout mutant	Chapter 3
<i>Vibrio cholerae</i> $\Delta VC1295$	VC1295 knockout mutant	Chapter 3
<i>Vibrio cholerae</i> $\Delta VC1295 \Delta VC1372$ $\Delta VC1376 \Delta VC1067$	VC1295, VC1067, VC1372, VC1376 quadruple knockout mutant	Chapter 3
<i>Clostridium difficile</i> CD2015	NAP-1, Ribotype 027	Unpublished

**Table A1. Bacteria strain list.** All bacteria strains used in this dissertation, and their references.

<i>Plasmid Name</i>	<i>Description</i>	<i>Reference</i>
pTL17	Inducible FLP recombinase vector	[86]
pKD3	Contains <i>cat</i> flanked by FRT sites	[84]
pEVS141	Backbone for DGC expression plasmids, vector control	[195]
pVCA0956	IPTG inducible VCA0956 GGDEF expression vector	[79]
pCMW121	IPTG inducible VC1086 EAL expression vector	[72]
pBBRlux	Backbone for luminescence reporter plasmids	[69]
6:C9- <i>lux</i>	VC1673 – c-d-GMP inducible <i>lux</i> reporter vector	[107]
<i>vpsT-lux</i>	VC2647 - c-d-GMP inducible <i>lux</i> reporter vector	[196]
pBRP2	<i>qrgB</i> expression plasmid, pMMB67eh backbone (Pursley, B.R.)	Chapter 3
pCMW75	IPTG inducible <i>qrgB</i> expression vector	[72]
pCMW98	IPTG inducible <i>qrgB</i> * active site mutant expression vector	[72]
pANDA2	IPTG inducible VC1153 ( <i>tfoX</i> ) expression plasmid (Chan, C.)	Chapter 3
pVC0900	IPTG inducible VC0900 GGDEF expression vector	[79]
pVC1029	IPTG inducible VC1029 GGDEF expression vector	[79]
pVC1067	IPTG inducible VC1067 GGDEF expression vector	[79]
pVC1104	IPTG inducible VC1104 GGDEF expression vector	[79]
pVC1185	IPTG inducible VC1185 GGDEF expression vector	[79]
pVC1216	IPTG inducible VC1216 GGDEF expression vector	[79]
pVC1353	IPTG inducible VC1353 GGDEF expression vector	[79]
pVC1367	IPTG inducible VC1367 GGDEF expression vector	[79]
pVC1370	IPTG inducible VC1370 GGDEF expression vector	[79]
pVC1372	IPTG inducible VC1372 GGDEF expression vector	[79]
pVC1376	IPTG inducible VC1376 GGDEF expression vector	[79]
pVC1593	IPTG inducible VC1593 GGDEF expression vector	[79]
pVC1599	IPTG inducible VC1599 GGDEF expression vector	[79]
pVC2224	IPTG inducible VC2224 GGDEF expression vector	[79]
pVC2285	IPTG inducible VC2285 GGDEF expression vector	[79]
pVC2454	IPTG inducible VC2454 GGDEF expression vector	[79]
pVC2697	IPTG inducible VC2697 GGDEF expression vector	[79]
pVCA0049	IPTG inducible VCA0049 GGDEF expression vector	[79]
pVCA0074	IPTG inducible VCA0074 GGDEF expression vector	[79]
pVCA0165	IPTG inducible VCA0165 GGDEF expression vector	[79]
pVCA0217	IPTG inducible VCA0217 GGDEF expression vector	[79]
VCA0557	IPTG inducible VCA0557 GGDEF expression vector	[79]
pVCA0560	IPTG inducible VCA0560 GGDEF expression vector	[79]
pVCA0697	IPTG inducible VCA0697 GGDEF expression vector	[79]
pVCA0848	IPTG inducible VCA0848 GGDEF expression vector	[79]
pVCA0939	IPTG inducible VCA0939 GGDEF expression vector	[79]

**Table A2. Plasmid list.** All plasmids used in this dissertation, and their references.

<b>Table A2 (cont'd)</b>		
pVCA0960	IPTG inducible VCA0960 GGDEF expression vector	[79]
pVCA0965	IPTG inducible VCA0965 GGDEF expression vector	[79]
pVCA1082	IPTG inducible VCA1082 GGDEF expression vector	[79]
pVC0072	IPTG inducible VC0072 GGDEF/EAL expression vector	[79]
pVC0130	IPTG inducible VC0130 GGDEF/EAL expression vector	[79]
pVC0398	IPTG inducible VC0398 GGDEF/EAL expression vector	[79]
pVC0653	IPTG inducible VC0653 GGDEF/EAL expression vector	[79]
pVC0658	IPTG inducible VC0658 GGDEF/EAL expression vector	[79]
pVC0703	IPTG inducible VC0703 GGDEF/EAL expression vector	[79]
pVC1934	IPTG inducible VC1934 GGDEF/EAL expression vector	[79]
pVC2750	IPTG inducible VC2750 GGDEF/EAL expression vector	[79]
pVCA0080	IPTG inducible VCA0080 GGDEF/EAL expression vector	[79]
pVCA0785	IPTG inducible VCA0785 GGDEF/EAL expression vector	[79]
pVC1652	IPTG inducible VC1652 EAL expression vector	[79]
pVCA1083	IPTG inducible VCA1083 EAL expression vector	[79]
pBK34	IPTG inducible VC1087 HD-GYP expression vector	Chapter 3
pBK35	IPTG inducible VC1295 HD-GYP expression vector	Chapter 3
pBK36	IPTG inducible VC1348 HD-GYP expression vector	Chapter 3
pBK37	IPTG inducible VC2340 HD-GYP expression vector	Chapter 3
pBK38	IPTG inducible VC2497 HD-GYP expression vector	Chapter 3
pBK39	IPTG inducible VCA0210 HD-GYP expression vector	Chapter 3
pBK40	IPTG inducible VCA0681 HD-GYP expression vector	Chapter 3
pBK41	IPTG inducible VCA0895 HD-GYP expression vector	Chapter 3
pBK42	IPTG inducible VCA0931 HD-GYP expression vector	Chapter 3
pBK43	IPTG inducible VC0137 EAL expression vector	Chapter 3
pBK45	IPTG inducible VC1592 EAL expression vector	Chapter 3
pBK46	IPTG inducible VC1851 EAL expression vector	Chapter 3
pBK47	IPTG inducible VCA0101 EAL expression vector	Chapter 3
pBK48	IPTG inducible VCA0536 EAL expression vector	Chapter 3
pCMW122	IPTG inducible VC1211 EAL expression vector	[72]
pCMW123	IPTG inducible VC1641 EAL expression vector	[72]
pCMW124	IPTG inducible VC1710 EAL expression vector	[72]

Table A2 (cont'd)		
pVC1372*	IPTG inducible VC1372* active site mutant expression vector	Chapter 3
pVC1376*	IPTG inducible VC1376* active site mutant expression vector	Chapter 3
pVC1067*	IPTG inducible VC1067* active site mutant expression vector	[79]
pBK51	<i>toxT</i> knockout vector, pKAS32 backbone	Chapter 3
pCMW27	VC0072- <i>gfp</i> transcriptional fusion	[72]
pCMW28	VC0653- <i>gfp</i> transcriptional fusion	[72]
pCMW33	VC0130- <i>gfp</i> transcriptional fusion	[72]
pCMW34	VC0900- <i>gfp</i> transcriptional fusion	[72]
pCWM35	VC1029- <i>gfp</i> transcriptional fusion	[72]
pCMW36	VC1104- <i>gfp</i> transcriptional fusion	[72]
pCMW37	VC1185- <i>gfp</i> transcriptional fusion	[72]
pCMW38	VC1216- <i>gfp</i> transcriptional fusion	[72]
pCMW39	VC1353- <i>gfp</i> transcriptional fusion	[72]
pCMW40	VC1367- <i>gfp</i> transcriptional fusion	[72]
pCMW41	VC1372- <i>gfp</i> transcriptional fusion	[72]
pCMW42	VCA0074- <i>gfp</i> transcriptional fusion	[72]
pCMW47	VC1370- <i>gfp</i> transcriptional fusion	[72]
pCMW48	VC1376- <i>gfp</i> transcriptional fusion	[72]
pCMW49	VC1593- <i>gfp</i> transcriptional fusion	[72]
pCMW50	VC1599- <i>gfp</i> transcriptional fusion	[72]
pCMW51	VC1934- <i>gfp</i> transcriptional fusion	[72]
pCMW52	VC2224- <i>gfp</i> transcriptional fusion	[72]
pCMW53	VC2285- <i>gfp</i> transcriptional fusion	[72]
pCMW54	VC2370- <i>gfp</i> transcriptional fusion	[72]
pCMW55	VC2454- <i>gfp</i> transcriptional fusion	[72]
pCMW56	VC2697- <i>gfp</i> transcriptional fusion	[72]
pCMW57	VC2750- <i>gfp</i> transcriptional fusion	[72]
pCMW58	VCA0049- <i>gfp</i> transcriptional fusion	[72]
pCMW59	VCA0080- <i>gfp</i> transcriptional fusion	[72]
pCMW60	VCA0165- <i>gfp</i> transcriptional fusion	[72]
pCMW61	VCA0217- <i>gfp</i> transcriptional fusion	[72]
pCMW62	VCA0557- <i>gfp</i> transcriptional fusion	[72]
pCMW63	VCA0560- <i>gfp</i> transcriptional fusion	[72]
pCMW64	VCA0697- <i>gfp</i> transcriptional fusion	[72]
pCMW65	VCA0785- <i>gfp</i> transcriptional fusion	[72]
pCMW66	VCA0848- <i>gfp</i> transcriptional fusion	[72]
pCMW67	VCA0939- <i>gfp</i> transcriptional fusion	[72]
pCMW68	VCA0956- <i>gfp</i> transcriptional fusion	[72]
pCMW69	VCA0960- <i>gfp</i> transcriptional fusion	[72]

Table A2 (cont'd)		
pCMW70	VCA0965- <i>gfp</i> transcriptional fusion	[72]
pCMW71	VC0658- <i>gfp</i> transcriptional fusion	[72]
pCMW72	VC1067- <i>gfp</i> transcriptional fusion	[72]
pCMW73	VC0703- <i>gfp</i> transcriptional fusion	[72]
pCMW78	VCA1082- <i>gfp</i> transcriptional fusion	[72]
pCMW79	VC0398- <i>gfp</i> transcriptional fusion	[72]
pCMW80	VC0137- <i>gfp</i> transcriptional fusion	[72]
pCMW81	VC0515- <i>gfp</i> transcriptional fusion	[72]
pCMW82	VC1086- <i>gfp</i> transcriptional fusion	[72]
pCMW83	VC1211- <i>gfp</i> transcriptional fusion	[72]
pCMW84	VC1592- <i>gfp</i> transcriptional fusion	[72]
pCMW85	VC1641- <i>gfp</i> transcriptional fusion	[72]
pCMW86	VC1652- <i>gfp</i> transcriptional fusion	[72]
pCMW87	VC1710- <i>gfp</i> transcriptional fusion	[72]
pCMW88	VC1851- <i>gfp</i> transcriptional fusion	[72]
pCMW89	VCA0101- <i>gfp</i> transcriptional fusion	[72]
pCMW90	VCA0536- <i>gfp</i> transcriptional fusion	[72]
pBBRlux- VC1295	VC1295- <i>lux</i> transcriptional fusion	[66]
pBBRLux- VC1348	VC1348- <i>lux</i> transcriptional fusion	[66]
pBBRlux- VC2340	VC2340- <i>lux</i> transcriptional fusion	[66]
pBBRlux- VC2497	VC2497- <i>lux</i> transcriptional fusion	Chapter 3
pBBRlux- VCA0210	VCA0210- <i>lux</i> transcriptional fusion	[66]
pBBRlux- VCA0681	VCA0681- <i>lux</i> transcriptional fusion	[66]
pBBRlux- VCA0895	VCA0895- <i>lux</i> transcriptional fusion	[66]
pBBRlux- VCA0931	VCA0931- <i>lux</i> transcriptional fusion	[66]
pShuttle-CMV	Backbone for DGC eukaryote expression vectors	[165]
pShuttleCMV- <i>qrgB</i>	<i>qrgB</i> expression vector under CMV control	Chapter 5
pShuttleCMV- <i>qrgB*</i>	<i>qrgB*</i> active site mutant expression vector under CMV control	Chapter 5
pShuttleCMV- VCA0848	VCA0848 expression vector under CMV control	Chapter 5
pShuttleCMV- VCA0848*	VCA0848* active site mutant expression vector under CMV control	Chapter 5

<b>Table A2 (cont'd)</b>		
pShuttleCMV- VCA0956	VCA0956 expression vector under CMV control	Chapter 5
pShuttleCMV- VCA0956*	VCA0956* active site mutant expression vector under CMV control	Chapter 5

Primer Name	Description	Sequence	Restriction Site
VCA0074KO-1	For $\Delta cdgA$ strain	TCGATGTGTCTGATCTGCGTATCCGCGTTGGTAT	
VCA0074KO-2	For $\Delta cdgA$ strain	GAAGCAGCTCCAGCCTACACGGGGCAAAGTTTACCAT	
VCA0074KO-3	For $\Delta cdgA$ strain	TAAGGAGGATATTCATATGGGGCTTCTTATGAATCAAAAT	
VCA0074KO-4	For $\Delta cdgA$ strain	GGTTGAGAAGTAGAACACAATCGATATCCACACG	
342-us.2-ecoR1	For pBRP2	ATAGAATTCCTCTGCGCTCCTCATA TTCT	EcoRI
342-ds.2-bamH1	For pBRP2	ATAGGATCCGACAGAGAAAGTTAAGAAAC	BamHI
VC1087fw-ecoR1	For pBK34	ATAGAATTCAGGAGCTAAGGAAGCTAAAATGCCAATGGATAACAT	EcoRI
VC1087rv-bamh1	For pBK34	ATAGGATCCTTATCCTATATAAACGGGATCGGC	BamHI
VC1295fw-ecoR1	For pBK35	ATAGAATTCAGGAGCTAAGGAAGCTAAATTGACCATTTGGGTTCT	EcoRI
VC1295rv-bamh1	For pBK35	ATAGGATCCTTATGCGGCATCTTTAAAGTGTGCT	BamHI
VC1348fw-ecoR1	For pBK36	ATAGAATTCAGGAGCTAAGGAAGCTAAAATGGCAACCGCCAATAT	EcoRI
VC1348rv-bamh1	For pBK36	ATAGGATCCTCAGCCTGACGCTTGT TGAC	BamHI
VC2340fw-ecoR1	For pBK37	ATAGAATTCAGGAGCTAAGGAAGCTAAAATGCAGATGCAACCCAA	EcoRI
VC2340rv-bamh1	For pBK37	ATAGGATCCTCAGTGGGTGATTCCC TGGTC	BamHI
VC2497fw-ecoR1	For pBK38	ATAGAATTCAGGAGCTAAGGAAGCTAAAGTGGCAAGCATTAATAAT	EcoRI
VC2497rv-bamh1	For pBK38	ATAGGATCCTTACTCTTCGCTGTCAAAGAAGTATG	BamHI
VCA0210fw-ecoR1	For pBK39	ATAGAATTCAGGAGCTAAGGAAGCTAAATTGAAGTGGTTTAAATA	EcoRI
VCA0210rv-bamh1	For pBK39	ATAGGATCCCTAGTCAGGCAGCGAAGCAC	BamHI
VCA0681fw-ecoR1	For pBK40	ATAGAATTCAGGAGCTAAGGAAGCTAAAATGAGATGGTCAGAAAT	EcoRI
VCA0681rv-bamh1	For pBK40	ATAGGATCCTTATGCCCATTCGGTTGGGCTTT	BamHI

**Table A3. Primer list.** All primers used in this dissertation and their sequence, and any restriction sites included for cloning applications.

Table A3 (cont'd)			
VCA0895fw-mfeI	For pBK41	ATACAATTGAGGAGCTAAGGAAGCT AAATTGCAACCTAGCCAAGA	MfeI
VCA0895rv-bglII	For pBK41	ATAAGATCTCTAGTAATCTTCCCGT AAATACGCC	BglII
VCA0931fw-ecoRI	For pBK42	ATAGAATTCAGGAGCTAAGGAAGCT AAAATGAGTGTTGCACAAAA	EcoRI
VCA0931rv-bamHI	For pBK42	ATAGGATCCTTAGGTCTTATCTGAA GAGTGTGGTA	BamHI
VC0137fw-ecoRI	For pBK43	ATAGAATTCAGGAGCTAAGGAAGCT AAATTGGTTCGATGTTTATG	EcoRI
VC0137rv-bamHI	For pBK43	ATAGGATCCCTAAATTAATCGATTG ATGTCCTGGC	BamHI
VC0515fw-ecoRI	For pBK44	ATAGAATTCAGGAGCTAAGGAAGCT AAAATGGATAGTTTCATAGC	EcoRI
VC0515rv-bamHI	For pBK44	ATAGGATCCCTATTTAACTTCTTTC ATTAAAGTTCGAC	BamHI
VC1592fw-ecoRI	For pBK45	ATAGAATTCAGGAGCTAAGGAAGCT AAAATGAATCACATCCACCC	EcoRI
VC1592rv-bamHI	For pBK45	ATAGGATCCCTATAACGCAGACATA CGTGGAG	BamHI
VC1851fw-ecoRI	For pBK46	ATAGAATTCAGGAGCTAAGGAAGCT AAATTGAAGTACTCGTATGT	EcoRI
VC1851rv-bamHI	For pBK46	ATAGGATCCTTAGGTTTGTACACCA AGAAGATCG	BamHI
VCA0101fw-ecoRI	For pBK47	ATAGAATTCAGGAGCTAAGGAAGCT AAAATGGCTAAGGAAAAGAC	EcoRI
VCA0101rv-bglII	For pBK47	ATAAGATCTTTATATTTTGCTTGTG GCAAAGTTTAATG	BglII
VCA0536fw-ecoRI	For pBK48	ATAGAATTCAGGAGCTAAGGAAGCT AAAATGGCGTGCGTCAAAAG	EcoRI
VCA0536rv-bamHI	For pBK48	ATAGGATCCTTAGTTAGCATTGCT ACCTTAGCG	BamHI
CMW464	For pANDA2	GAATTCGGGGAACGTGATTAAAGG	EcoRI
CMW465	For pANDA2	GGATCCACGCTGCTGACAACTTCT AAC	BamHI
VC1372-ASM	For pVC1372*	TCGCGAACTCTTCAGCGGCATATCG AGCGACC	
VC1376-ASM	For pVC1376*	ATATTTTTCGCCGTTTCGCCGCTGA TGAGTTTGCCATCTT	
VC1067-ASM	For pVC1067*	GGGCGCAGCTATCGGATTGCTGCG G	
2497-fw-SacI	For pBBRlux-2497	GAGCTC TCTTGGTACTTGAAAGAGGCC	SacI

Table A3 (cont'd)			
2497-rv- BamHI	For pBBRlux- 2497	GGATCC AATCTTAATTACATCTGAGTGAATA ACC	BamHI
VC1372KO-1	For $\Delta$ VC1372 strain	CGTCTTGTTGATATTGATGATTGCG TGCGACCAGT	
VC1372KO-2	For $\Delta$ VC1372 strain	GAAGCAGCTCCAGCCTACACGCTTG GTCGTCCTGAATGCACAAA	
VC1372KO-3	For $\Delta$ VC1372 strain	TAAGGAGGATATTCATATGGCTCAG ATTGTTTATAGGATGGGAGC	
VC1372KO-4	For $\Delta$ VC1372 strain	CATTTACAGGTGGAAGACAAAACCTC TACTCGCCAC	
VC1376KO-1	For $\Delta$ VC1376 strain	GCGCTTGGCCAGTCACTTGACCGGT TAG	
VC1376KO-2	For $\Delta$ VC1376 strain	GAAGCAGCTCCAGCCTACACGAAAA ATCATGATGAAG	
VC1376KO-3	For $\Delta$ VC1376 strain	TAAGGAGGATATTCATATGAATCGA ATTATGCCTTCAA	
VC1376KO-4	For $\Delta$ VC1376 strain	CCAACGCGGATGGCACGATTGATCC GC	
VC1067KO-1	For $\Delta$ VC1067 strain	GGCCATTTTGGCGATAGCGCCGTAA GTCG	
VC1067KO-2	For $\Delta$ VC1067 strain	GAAGCAGCTCCAGCCTACACAGAC GTTGAATAATGGTATG	
VC1067KO-3	For $\Delta$ VC1067 strain	TAAGGAGGATATTCATATGTCAAAC TGGTGAAATGC	
VC1067KO-4	For $\Delta$ VC1067 strain	CCCTTCCCAACTAAGCAGCCATCGT GGC	
VC1295KO-1	For $\Delta$ VC1295 strain	GCCAGCGGCATTGAACACACC	
VC1295KO-2	For $\Delta$ VC1295 strain	GAAGCAGCTCCAGCCTACAC TTGCAGCACACTTTAAAGATGC	
VC1295KO-3	For $\Delta$ VC1295 strain	TAAGGAGGATATTCATATG TAAGTTACGGCTAGTTAAGTAT	
VC1295KO-4	For $\Delta$ VC1295 strain	GCTCCTGTGAAAACAGGAACTGATC	
toxRKO-1	For $\Delta$ toxR strain	CTAAAGTTCGACATCCCCTTGC	
toxRKO-2	For $\Delta$ toxR strain	GAAGCAGCTCCAGCCTACACGATCT TGCTATGCAAATAGACACA	
toxRKO-3	For $\Delta$ toxR strain	TAAGGAGGATATTCATATGCTAATG TCCAGTATCTCCCTG	
toxRKO-4	For $\Delta$ toxR strain	GTTGAGCGGCAGATCGTTTGAG	

Table A3 (cont'd)			
toxTpkas1-pBK51	For $\Delta$ <i>toxT</i> strain	ATAGAGCTCCCTCATATCAAAGTTT ATGAAGGGAC	SacI
toxTpkas2-pBK51	For $\Delta$ <i>toxT</i> strain	ATAGCGGCCGCTGCGTTCTACTCTG AAGATATATAAATAA	NotI
toxTpkas3-pBK51	For $\Delta$ <i>toxT</i> strain	ATAGCGGCCGCGCATGGAATACGTTTA CTTGATCCTATTTTC	NotI
toxTpkas4-pBK51	For $\Delta$ <i>toxT</i> strain	ATAGGTACCCAAAGAGTCTAGCGTT TCAGAAATAG	KpnI
<i>qrgB</i> -CMV-fw	For pShuttleCMV- <i>qrgB</i>	ATACTCGAGTTAAGAAACCTTTTGG ATTCTTAAGTTG	KpnI
<i>qrgB</i> -CMV-rv	For pShuttleCMV- <i>qrgB</i>	ATACTCGAGTTAAGAAACCTTTTGG ATTCTTAAGTTG	XhoI
VCA0848-CMV-fw	For pShuttleCMV-VCA0848	ATAGGTACCCCACCATGAATGACAA AGTGCT	KpnI
VCA0848-CMV-rv	For pShuttleCMV-VCA0848	ATACTCGAGTTAGAAAAGTTCAACG TCATCAGAA	XhoI
VCA0848-ASM	For pShuttleCMV-VCA0848*	GTCTTCTCAACTATTTTCGCTTTGCT GCTGAAGAGTTCGTGATTATTTTTT	
VCA0956-CMV-fw	For pShuttleCMV-VCA0956	ATAGGTACCCCACCGTGATGACAAC TGAAGATTTCA	KpnI
VCA0956-CMV-rv	For pShuttleCMV-VCA0956	ATACTCGAGTTAGAGCGGCATGACT CGAT	XhoI
VCA0956-ASM	For pShuttleCMV-VCA0956*	TGACAGCTTATCGTTATGCCGCTGA AGAGTTTGCACTGAT	

## REFERENCES

## REFERENCES

1. Ross, P., et al., *Regulation of cellulose synthesis in Acetobacter xylinum by cyclic diguanylic acid*. Nature, 1987. **325**(6101): p. 279-281.
2. Seshasayee, A.S.N., G.M. Fraser, and N.M. Luscombe, *Comparative genomics of cyclic-di-GMP signaling in bacteria: post-translational regulation and catalytic activity*. Nucleic Acids Research, 2010. **38**(18): p. 5970-5981.
3. Ausmees, N., et al., *Genetic data indicate that proteins containing the GGDEF domain possess diguanylate cyclase activity*. Fems Microbiology Letters, 2001. **204**(1): p. 163-167.
4. Ryjenkov, D.A., et al., *Cyclic diguanylate is a ubiquitous signaling molecule in bacteria: Insights into biochemistry of the GGDEF protein domain*. Journal of Bacteriology, 2005. **187**(5): p. 1792-1798.
5. Galperin, M.Y., *Bacterial signal transduction network in a genomic perspective*. Environmental Microbiology, 2004. **6**(6): p. 552-567.
6. Ryan, R.P., et al., *Cyclic di-GMP signaling in bacteria: Recent advances and new puzzles*. Journal of Bacteriology, 2006. **188**(24): p. 8327-8334.
7. Schmidt, A.J., D.A. Ryjenkov, and M. Gomelsky, *The ubiquitous protein domain EAL is a cyclic diguanylate-specific phosphodiesterase: Enzymatically active and inactive EAL domains*. Journal of Bacteriology, 2005. **187**(14): p. 4774-4781.
8. Ryan, R.P., et al., *Cell-cell signaling in Xanthomonas campestris involves an HD-GYP domain protein that functions in cyclic di-GMP turnover*. Proceedings of the National Academy of Sciences of the United States of America, 2006. **103**(17): p. 6712-6717.
9. Romling, U., M.Y. Galperin, and M. Gomelsky, *Cyclic di-GMP: the First 25 Years of a Universal Bacterial Second Messenger*. Microbiology and Molecular Biology Reviews, 2013. **77**(1): p. 1-52.

10. Christen, B., et al., *Allosteric control of cyclic di-GMP signaling*. Journal of Biological Chemistry, 2006. **281**(42): p. 32015-32024.
11. Simm, R., et al., *GGDEF and EAL domains inversely regulate cyclic di-GMP levels and transition from sessility to motility*. Molecular Microbiology, 2004. **53**(4): p. 1123-1134.
12. Fang, X. and M. Gomelsky, *A post-translational, c-di-GMP-dependent mechanism regulating flagellar motility*. Molecular Microbiology, 2010. **76**(5): p. 1295-1305.
13. Boehm, A., et al., *Second messenger-mediated adjustment of bacterial swimming velocity*. Cell, 2010. **141**(1): p. 107-116.
14. Cheng, K.J., R.P. McCowan, and J.W. Costerton, *Adherent epithelial bacteria in ruminants and their roles in digestive-tract function*. American Journal of Clinical Nutrition, 1979. **32**(1): p. 139-148.
15. Costerton, J.W., P.S. Stewart, and E.P. Greenberg, *Bacterial biofilms: A common cause of persistent infections*. Science, 1999. **284**(5418): p. 1318-1322.
16. Tischler, A.D. and A. Camilli, *Cyclic diguanylate (c-di-GMP) regulates Vibrio cholerae biofilm formation*. Molecular Microbiology, 2004. **53**(3): p. 857-869.
17. Galperin, M.Y., A.N. Nikolskaya, and E.V. Koonin, *Novel domains of the prokaryotic two-component signal transduction systems*. Fems Microbiology Letters, 2001. **203**(1): p. 11-21.
18. Zähringer, F., et al., *Structure and signaling mechanism of a zinc-sensory diguanylate cyclase*. Structure, 2013: p. In press.
19. Bernier, S.P., et al., *Modulation of Pseudomonas aeruginosa surface-associated group behaviors by individual amino acids through c-di-GMP signaling*. Research in Microbiology, 2011. **162**(7): p. 680-688.

20. Carlson, H.K., R.E. Vance, and M.A. Marletta, *H-NOX regulation of c-di-GMP metabolism and biofilm formation in Legionella pneumophila*. *Molecular Microbiology*, 2010. **77**(4): p. 930-942.
21. Karatan, E., T.R. Duncan, and P.I. Watnick, *NspS, a predicted polyamine sensor, mediates activation of Vibrio cholerae biofilm formation by norspermidine*. *Journal of Bacteriology*, 2005. **187**(21): p. 7434-7443.
22. Wan, X.H., et al., *Globins synthesize the second messenger bis-(3'-5')-cyclic diguanosine monophosphate in bacteria*. *Journal of Molecular Biology*, 2009. **388**(2): p. 262-270.
23. Tuckerman, J.R., et al., *An oxygen-sensing diguanylate cyclase and phosphodiesterase couple for c-di-GMP control*. *Biochemistry*, 2009. **48**(41): p. 9764-9774.
24. Kanazawa, T., et al., *Biochemical and physiological characterization of a BLUF protein-EAL protein complex involved in blue light-dependent degradation of cyclic diguanylate in the purple bacterium Rhodospseudomonas palustris*. *Biochemistry*, 2010. **49**(50): p. 10647-10655.
25. Agostoni, M., et al., *Occurrence of Cyclic di-GMP-Modulating Output Domains in Cyanobacteria: an Illuminating Perspective*. *mBio*, 2013. **4**(4).
26. Ryan, R.P., et al., *Cell-cell signal-dependent dynamic interactions between HD-GYP and GGDEF domain proteins mediate virulence in Xanthomonas campestris*. *Proceedings of the National Academy of Sciences of the United States of America*, 2010. **107**(13): p. 5989-5994.
27. Trimble, M.J. and L.L. McCarter, *Bis-(3'-5')-cyclic dimeric GMP-linked quorum sensing controls swarming in Vibrio parahaemolyticus*. *Proceedings of the National Academy of Sciences of the United States of America*, 2011. **108**(44): p. 18079-18084.
28. Huq, A., et al., *Ecological relationships between Vibrio cholerae and planktonic crustacean copepods*. *Applied and Environmental Microbiology*, 1983. **45**(1): p. 275-283.

29. Tamplin, M.L., et al., *Attachment of Vibrio cholerae serogroup-O1 to zooplankton and phytoplankton of Bangladesh waters*. Applied and Environmental Microbiology, 1990. **56**(6): p. 1977-1980.
30. Halpern, M., et al., *Chironomid egg masses as a natural reservoir of Vibrio cholerae non-O1 and non-O139 in freshwater habitats*. Microbial Ecology, 2004. **47**(4): p. 341-349.
31. Faruque, S.M., M.J. Albert, and J.J. Mekalanos, *Epidemiology, genetics, and ecology of toxigenic Vibrio cholerae*. Microbiology and Molecular Biology Reviews, 1998. **62**(4): p. 1301-+.
32. DiRita, V.J., *Co-ordinate expression of virulence genes by ToxR in Vibrio cholerae*. Molecular Microbiology, 1992. **6**(4): p. 451-458.
33. Bina, J., et al., *ToxR regulon of Vibrio cholerae and its expression in vibrios shed by cholera patients*. Proceedings of the National Academy of Sciences, 2003. **100**(5): p. 2801-2806.
34. Tischler, A.D. and A. Camilli, *Cyclic diguanylate regulates Vibrio cholerae virulence gene expression*. Infection and Immunity, 2005. **73**(9): p. 5873-5882.
35. Tamayo, R., et al., *Role of cyclic di-GMP during El tor biotype Vibrio cholerae infection: Characterization of the in vivo-induced cyclic di-GMP phosphodiesterase CdpA*. Infection and Immunity, 2008. **76**(4): p. 1617-1627.
36. Martinez-Wilson, H.F., et al., *The Vibrio cholerae hybrid sensor kinase VieS contributes to motility and biofilm regulation by altering the cyclic diguanylate level*. Journal of Bacteriology, 2008. **190**(19): p. 6439-6447.
37. Dawson, P.A., *Bile Secretion and the Enterohepatic Circulation*, in *Sleisenger and Fordtran's Gastrointestinal and Liver Disease (9th)*, M. Feldman, L.S. Friedman, and L.J. Brandt, Editors. 2010, W.B. Saunders: Philadelphia, PA. p. 1075-1088.
38. O'Connor, C.J. and R.G. Wallace, *Physicochemical behavior of bile-salts*. Advances in Colloid and Interface Science, 1985. **22**(1): p. 1-111.

39. Begley, M., C.G.M. Gahan, and C. Hill, *The interaction between bacteria and bile*. Fems Microbiology Reviews, 2005. **29**(4): p. 625-651.
40. Bernstein, C., et al., *Bile salt activation of stress response promoters in Escherichia coli*. Current Microbiology, 1999. **39**(2): p. 68-72.
41. Schubert, R. and K.H. Schmidt, *Structural changes in vesicle membranes and mixed micelles of various lipid compositions after binding of different bile salts*. Biochemistry, 1988. **27**(24): p. 8787-8794.
42. Cabral, D.J., et al., *Transbilayer movement of bile-acids in model membranes*. Biochemistry, 1987. **26**(7): p. 1801-1804.
43. Provenzano, D., et al., *The virulence regulatory protein ToxR mediates enhanced bile resistance in Vibrio cholerae and other pathogenic Vibrio species*. Infection and Immunity, 2000. **68**(3): p. 1491-1497.
44. Colmer, J.A., J.A. Fralick, and A.N. Hamood, *Isolation and characterization of a putative multidrug resistance pump from Vibrio cholerae*. Molecular Microbiology, 1998. **27**(1): p. 63-72.
45. Bina, J.E. and J.J. Mekalanos, *Vibrio cholerae tolC is required for bile resistance and colonization*. Infection and Immunity, 2001. **69**(7): p. 4681-4685.
46. Bina, X.R., et al., *Vibrio cholerae RND family efflux systems are required for antimicrobial resistance, optimal virulence factor production, and colonization of the infant mouse small intestine*. Infection and Immunity, 2008. **76**(8): p. 3595-3605.
47. Hung, D.T., et al., *Bile acids stimulate biofilm formation in Vibrio cholerae*. Molecular Microbiology, 2006. **59**(1): p. 193-201.
48. McWhirter, S.M., et al., *A host type I interferon response is induced by cytosolic sensing of the bacterial second messenger cyclic-di-GMP*. Journal of Experimental Medicine, 2009. **206**(9): p. 1899-1911.

49. Sauer, J.D., et al., *The N-Ethyl-N-Nitrosourea-Induced Goldenticket Mouse Mutant Reveals an Essential Function of Sting in the In Vivo Interferon Response to Listeria monocytogenes and Cyclic Dinucleotides*. Infection and Immunity, 2011. **79**(2): p. 688-694.
50. Ebensen, T., et al., *The bacterial second messenger cyclic diGMP exhibits potent adjuvant properties*. Vaccine, 2007. **25**(8): p. 1464-1469.
51. Abdul-Sater, A.A., et al., *Cyclic-di-GMP and cyclic-di-AMP activate the NLRP3 inflammasome*. EMBO reports, 2013. **14**(10): p. 900-906.
52. Ebensen, T., et al., *The bacterial second messenger cdiGMP exhibits promising activity as a mucosal adjuvant*. Clinical and Vaccine Immunology, 2007. **14**(8): p. 952-958.
53. Karaolis, D.K.R., et al., *Bacterial c-di-GMP is an immunostimulatory molecule*. Journal of Immunology, 2007. **178**(4): p. 2171-2181.
54. Karaolis, D.K.R., et al., *Cyclic Di-GMP stimulates protective innate immunity in bacterial pneumonia*. Infection and Immunity, 2007. **75**(10): p. 4942-4950.
55. Yan, H.B., et al., *3',5'-Cyclic diguanylic acid elicits mucosal immunity against bacterial infection*. Biochemical and Biophysical Research Communications, 2009. **387**(3): p. 581-584.
56. Gray, P.M., et al., *Evidence for cyclic diguanylate as a vaccine adjuvant with novel immunostimulatory activities*. Cellular Immunology, 2012. **278**(1-2): p. 113-119.
57. Blaauboer, S.M., V.D. Gabrielle, and L. Jin, *MPYS/STING-Mediated TNF- $\alpha$ , Not Type I IFN, Is Essential for the Mucosal Adjuvant Activity of (3'-5')-Cyclic-Di-Guanosine-Monophosphate In Vivo*. Journal of Immunology, 2014. **192**(1): p. 492-502.
58. Ogunniyi, A.D., et al., *C-di-GMP is an effective immunomodulator and vaccine adjuvant against pneumococcal infection*. Vaccine, 2008. **26**(36): p. 4676-4685.

59. Chen, W.X., R. KuoLee, and H.B. Yan, *The potential of 3',5'-cyclic diguanylic acid (c-di-GMP) as an effective vaccine adjuvant*. *Vaccine*, 2010. **28**(18): p. 3080-3085.
60. Mosca, F., et al., *Molecular and cellular signatures of human vaccine adjuvants*. *Proceedings of the National Academy of Sciences*, 2008. **105**(30): p. 10501-10506.
61. Coffman, R.L., A. Sher, and R.A. Seder, *Vaccine Adjuvants: Putting Innate Immunity to Work*. *Immunity*, 2010. **33**(4): p. 492-503.
62. Gupta, R.K., *Aluminum compounds as vaccine adjuvants*. *Advanced Drug Delivery Reviews*, 1998. **32**(3): p. 155-172.
63. Meibom, K.L., et al., *Chitin induces natural competence in *Vibrio cholerae**. *Science*, 2005. **310**(5755): p. 1824-1827.
64. Atkinson, S., et al., *A hierarchical quorum-sensing system in *Yersinia pseudotuberculosis* is involved in the regulation of motility and clumping*. *Molecular Microbiology*, 1999. **33**(6): p. 1267-1277.
65. Hammer, B.K. and B.L. Bassler, *Quorum sensing controls biofilm formation in *Vibrio cholerae**. *Molecular Microbiology*, 2003. **50**(1): p. 101-114.
66. Hammer, B.K. and B.L. Bassler, *Distinct sensory pathways in *Vibrio cholerae* El Tor and Classical biotypes modulate cyclic dimeric GMP levels to control biofilm formation*. *Journal of Bacteriology*, 2009. **191**(1): p. 169-177.
67. Miller, M.B., et al., *Parallel quorum sensing systems converge to regulate virulence in *Vibrio cholerae**. *Cell*, 2002. **110**(3): p. 303-314.
68. Zhu, J., et al., *Quorum-sensing regulators control virulence gene expression in *Vibrio cholerae**. *Proceedings of the National Academy of Sciences of the United States of America*, 2002. **99**(5): p. 3129-3134.
69. Lenz, D.H., et al., *The Small RNA Chaperone Hfq and Multiple Small RNAs Control Quorum Sensing in *Vibrio harveyi* and *Vibrio cholerae**. *Cell*, 2004. **118**(1): p. 69-82.

70. Hammer, B.K. and B.L. Bassler, *Regulatory small RNAs circumvent the conventional quorum sensing pathway in pandemic Vibrio cholerae*. Proceedings of the National Academy of Sciences of the United States of America, 2007. **104**(27): p. 11145-11149.
71. Freeman, J.A. and B.L. Bassler, *A genetic analysis of the function of LuxO, a two-component response regulator involved in quorum sensing in Vibrio harveyi*. Molecular Microbiology, 1999. **31**(2): p. 665-677.
72. Waters, C.M., et al., *Quorum sensing controls biofilm formation in Vibrio cholerae through modulation of cyclic di-GMP levels and repression of vpsT*. Journal of Bacteriology, 2008. **190**(7): p. 2527-2536.
73. Srivastava, D. and C.M. Waters, *A tangled web: Regulatory connections between quorum sensing and cyclic di-GMP*. Journal of Bacteriology, 2012. **194**(17): p. 4485-4493.
74. Yildiz, F.H., et al., *Molecular analysis of rugosity in a Vibrio cholerae O1 El Tor phase variant*. Molecular Microbiology, 2004. **53**(2): p. 497-515.
75. Zhu, J. and J.J. Mekalanos, *Quorum sensing-dependent biofilms enhance colonization in Vibrio cholerae*. Developmental Cell, 2003. **5**(4): p. 647-656.
76. Lim, B., et al., *Cyclic-diGMP signal transduction systems in Vibrio cholerae: modulation of rugosity and biofilm formation*. Molecular Microbiology, 2006. **60**(2): p. 331-348.
77. Koestler, B.J. and C.M. Waters, *Exploring Environmental Control of Cyclic di-GMP Signaling in Vibrio cholerae by Using the Ex Vivo Lysate Cyclic di-GMP Assay (TELCA)*. Applied and Environmental Microbiology, 2013. **79**(17): p. 5233-41.
78. Thelin, K.H. and R.K. Taylor, *Toxin-coregulated pilus, but not mannose-sensitive hemagglutinin, is required for colonization by Vibrio cholerae O1 El Tor biotype and O139 strains*. Infection and Immunity, 1996. **64**(7): p. 2853-6.

79. Massie, J.P., et al., *Quantification of high-specificity cyclic diguanylate signaling*. Proceedings of the National Academy of Sciences of the United States of America, 2012. **109**(31): p. 12746-12751.
80. Iwanaga, M. and K. Yamamoto, *New medium for the production of cholera toxin by Vibrio cholerae 01 biotype El Tor*. Journal of Clinical Microbiology, 1985. **22**(3): p. 405-408.
81. Clark, D.J. and O. Maaløe, *DNA replication and the division cycle in Escherichia coli*. Journal of Molecular Biology, 1967. **23**(1): p. 99-112.
82. Sambrook, J., Russell, D.W., *Molecular Cloning - A Laboratory Manual*. 3rd ed. 2001, Cold Spring Harbor, NY: Cold Spring Harbor Laboratory Press.
83. Svitil, A.L., et al., *Chitin degradation proteins produced by the marine bacterium Vibrio harveyi growing on different forms of chitin*. Applied and Environmental Microbiology, 1997. **63**(2): p. 408-413.
84. Datsenko, K.A. and B.L. Wanner, *One-step inactivation of chromosomal genes in Escherichia coli K-12 using PCR products*. Proceedings of the National Academy of Sciences of the United States of America, 2000. **97**(12): p. 6640-6645.
85. Marvig, R.L. and M. Blokesch, *Natural transformation of Vibrio cholerae as a tool - Optimizing the procedure*. BMC Microbiology, 2010. **10**.
86. Long, T., et al., *Quantifying the integration of quorum-sensing signals with single-cell resolution*. Plos Biology, 2009. **7**(3): p. 640-649.
87. Sambanthamoorthy, K., et al., *Identification of Small Molecules That Antagonize Diguanylate Cyclase Enzymes To Inhibit Biofilm Formation*. Antimicrobial Agents and Chemotherapy, 2012. **56**(10): p. 5202-5211.
88. Bennett, B.D., et al., *Absolute metabolite concentrations and implied enzyme active site occupancy in Escherichia coli*. Nature Chemical Biology, 2009. **5**(8): p. 593-599.

89. Bobrov, A.G., et al., *Systematic analysis of cyclic di-GMP signalling enzymes and their role in biofilm formation and virulence in Yersinia pestis*. Molecular Microbiology, 2011. **79**(2): p. 533-551.
90. Bellows, L.E., et al., *Hfq-dependent, co-ordinate control of cyclic diguanylate synthesis and catabolism in the plague pathogen Yersinia pestis*. Molecular Microbiology, 2012. **86**(3): p. 661-674.
91. Newell, P.D., et al., *Systematic Analysis of Diguanylate Cyclases That Promote Biofilm Formation by Pseudomonas fluorescens Pf0-1*. Journal of Bacteriology, 2011. **193**(18): p. 4685-4698.
92. Christen, M., et al., *Asymmetrical Distribution of the Second Messenger c-di-GMP upon Bacterial Cell Division*. Science, 2010. **328**(5983): p. 1295-1297.
93. Romling, U., M. Gomelsky, and M.Y. Galperin, *C-di-GMP: the dawning of a novel bacterial signaling system*. Molecular Microbiology, 2005. **57**(3): p. 629-639.
94. Beyhan, S., L.S. Odell, and F.H. Yildiz, *Identification and characterization of cyclic diguanylate signaling systems controlling rugosity in Vibrio cholerae*. Journal of Bacteriology, 2008. **190**(22): p. 7392-7405.
95. Fong, J.C.N. and F.H. Yildiz, *Interplay between cyclic AMP-Cyclic AMP receptor protein and cyclic di-GMP signaling in Vibrio cholerae biofilm formation*. Journal of Bacteriology, 2008. **190**(20): p. 6646-6659.
96. Mueller, R.S., et al., *Indole acts as an extracellular cue regulating gene expression in Vibrio cholerae*. Journal of Bacteriology, 2009. **191**(11): p. 3504-3516.
97. Shikuma, N.J., J.C.N. Fong, and F.H. Yildiz, *Cellular levels and binding of c-di-GMP control subcellular localization and activity of the Vibrio cholerae transcriptional regulator VpsT*. Plos Pathogens, 2012. **8**(5).
98. Kulasakara, H., et al., *Analysis of Pseudomonas aeruginosa diguanylate cyclases and phosphodiesterases reveals a role for bis-(3'-5')-cyclic-GMP in*

- virulence*. Proceedings of the National Academy of Sciences of the United States of America, 2006. **103**(8): p. 2839-44.
99. Hecht, G.B. and A. Newton, *Identification of a novel response regulator required for the swarmer-to-stalked-cell transition in Caulobacter crescentus*. Journal of Bacteriology, 1995. **177**(21): p. 6223-6229.
  100. Aldridge, P., et al., *Role of the GGDEF regulator PleD in polar development of Caulobacter crescentus*. Molecular Microbiology, 2003. **47**(6): p. 1695-1708.
  101. Edmunds, A.C., et al., *Cyclic di-GMP Modulates the Disease Progression of Erwinia amylovora*. Journal of Bacteriology, 2013. **195**(10): p. 2155-65.
  102. Beyhan, S., et al., *Regulation of rugosity and biofilm formation in Vibrio cholerae: Comparison of VpsT and VpsR regulons and epistasis analysis of vpsT, vpsR, and hapR*. Journal of Bacteriology, 2007. **189**(2): p. 388-402.
  103. de Lorenzo, V. and K.N. Timmis, *Analysis and construction of stable phenotypes in Gram-negative bacteria with Tn5-derived and Tn10-derived minitransposons*. Bacterial Pathogenesis, Pt A, 1994. **235**: p. 386-405.
  104. Graham, D.Y. and M.S. Osato, *H. pylori in the pathogenesis of duodenal ulcer: Interaction between duodenal acid load, bile, and H. pylori*. American Journal of Gastroenterology, 2000. **95**(1): p. 87-91.
  105. Northfield, T.C. and I. McColl, *Postprandial concentrations of free and conjugated bile acids down the length of the normal human small intestine*. Gut, 1973. **14**(7): p. 513-518.
  106. Sambrook, J., E. F. Fritsch, and T. Maniatis., *Molecular Cloning - A Laboratory Manual, 2nd Edition*. 2 ed. 1989, Cold Spring Harbor, NY: Cold Spring Harbor Laboratory Press.
  107. Srivastava, D., R.C. Harris, and C.M. Waters, *Integration of cyclic di-GMP and quorum sensing in the control of vpsT and aphA in Vibrio cholerae*. Journal of Bacteriology, 2011. **193**(22): p. 6331-6341.

108. Skorupski, K. and R.K. Taylor, *Positive selection vectors for allelic exchange*. Gene, 1996. **169**(1): p. 47-52.
109. Fürste, J.P., et al., *Molecular cloning of the plasmid RP4 primase region in a multi-host-range tacP expression vector*. Gene, 1986. **48**(1): p. 119-131.
110. Hofmann, A.F., *The continuing importance of bile acids in liver and intestinal disease*. Archives of Internal Medicine, 1999. **159**(22): p. 2647-2658.
111. Claros, M.G. and G. Vonheijne, *TOPPRED-II - an improved software for membrane-protein structure predictions*. Computer Applications in the Biosciences, 1994. **10**(6): p. 685-686.
112. Neron, B., et al., *MobyLe: a new full web bioinformatics framework*. Bioinformatics, 2009. **25**(22): p. 3005-3011.
113. Schultz, J., et al., *SMART: a web-based tool for the study of genetically mobile domains*. Nucleic Acids Research, 2000. **28**(1): p. 231-234.
114. Goss, T.J., et al., *ToxR recognizes a direct repeat element in the toxT, ompU, ompT and ctxA promoters of Vibrio cholerae to regulate transcription*. Infection and Immunity, 2013. **81**(3): p. 884-95.
115. Abuaita, B.H. and J.H. Withey, *Termination of Vibrio cholerae virulence gene expression is mediated by proteolysis of the major virulence activator, ToxT*. Molecular Microbiology, 2011. **81**(6): p. 1640-1653.
116. Provenzano, D. and K.E. Klose, *Altered expression of the ToxR-regulated porins OmpU and OmpT diminishes Vibrio cholerae bile resistance, virulence factor expression, and intestinal colonization*. Proceedings of the National Academy of Sciences of the United States of America, 2000. **97**(18): p. 10220-10224.
117. Hung, D.T. and J.J. Mekalanos, *Bile acids induce cholera toxin expression in Vibrio cholerae in a ToxT-independent manner*. Proceedings of the National Academy of Sciences of the United States of America, 2005. **102**(8): p. 3028-3033.

118. Seidler, U. and M. Sjöblom, *Gastroduodenal Bicarbonate Secretion*, in *Physiology of the Gastrointestinal Tract*, L.R. Johnson, Editor. 2012, Elsevier: San Diego. p. 1311-1339.
119. Hogan, D.L., M.A. Ainsworth, and J.I. Isenberg, *Gastroduodenal bicarbonate secretion*. *Alimentary Pharmacology & Therapeutics*, 1994. **8**(5): p. 475-488.
120. Abuaita, B.H. and J.H. Withey, *Bicarbonate induces Vibrio cholerae virulence gene expression by enhancing ToxT activity*. *Infection and Immunity*, 2009. **77**(9): p. 4111-4120.
121. Schuhmacher, D.A. and K.E. Klose, *Environmental signals modulate ToxT-dependent virulence factor expression in Vibrio cholerae*. *Journal of Bacteriology*, 1999. **181**(5): p. 1508-1514.
122. Yang, M.H., et al., *Bile salt-induced intermolecular disulfide bond formation activates Vibrio cholerae virulence*. *Proceedings of the National Academy of Sciences of the United States of America*, 2013. **110**(6): p. 2348-2353.
123. Hunter, J.L., et al., *The Vibrio cholerae diguanylate cyclase VCA0965 has an AGDEF active site and synthesizes cyclic di-GMP*. *Bmc Microbiology*, 2014. **14**(1): p. 22.
124. Gu, J.Y., et al., *Genomic and systems evolution in Vibrionaceae species*. *Bmc Genomics*, 2009. **10**: p. 13.
125. Begley, M., C.G.M. Gahan, and C. Hill, *Bile stress response in Listeria monocytogenes LO28: Adaptation, cross-protection, and identification of genetic loci involved in bile resistance*. *Applied and Environmental Microbiology*, 2002. **68**(12): p. 6005-6012.
126. Tamayo, R., B. Patimalla, and A. Camilli, *Growth in a Biofilm Induces a Hyperinfectious Phenotype in Vibrio cholerae*. *Infection and Immunity*, 2010. **78**(8): p. 3560-3569.
127. Quigley, E.M.M. and L.A. Turnberg, *pH of the microclimate lining human gastric and duodenal mucosa in vivo*. *Gastroenterology*, 1987. **92**(6): p. 1876-1884.

128. Prouty, A.M. and J.S. Gunn, *Salmonella enterica serovar typhimurium invasion is repressed in the presence of bile*. Infection and Immunity, 2000. **68**(12): p. 6763-6769.
129. Krukonis, E.S. and V.J. DiRita, *From motility to virulence: sensing and responding to environmental signals in Vibrio cholerae*. Current Opinion in Microbiology, 2003. **6**(2): p. 186-190.
130. Cybulski, L.E., et al., *Membrane Thickness Cue for Cold Sensing in a Bacterium*. Current Biology, 2010. **20**(17): p. 1539-1544.
131. Mansilla, M.C., et al., *Control of membrane lipid fluidity by molecular thermosensors*. Journal of Bacteriology, 2004. **186**(20): p. 6681-6688.
132. Kingston, A.W., et al., *A sigma(W)-dependent stress response in Bacillus subtilis that reduces membrane fluidity*. Molecular Microbiology, 2011. **81**(1): p. 69-79.
133. Taranto, M.P., et al., *Bile salts and cholesterol induce changes in the lipid cell membrane of Lactobacillus reuteri*. Journal of Applied Microbiology, 2003. **95**(1): p. 86-91.
134. Choi, K.-H., R.J. Heath, and C.O. Rock,  *$\beta$ -Ketoacyl-Acyl Carrier Protein Synthase III (FabH) Is a Determining Factor in Branched-Chain Fatty Acid Biosynthesis*. Journal of Bacteriology, 2000. **182**(2): p. 365-370.
135. Cerda-Maira, F.A., C.S. Ringelberg, and R.K. Taylor, *The Bile Response Repressor BreR Regulates Expression of the Vibrio cholerae breAB Efflux System Operon*. Journal of Bacteriology, 2008. **190**(22): p. 7441-7452.
136. Wibbenmeyer, J.A., et al., *Vibrio cholerae OmpU and OmpT porins are differentially affected by bile*. Infection and Immunity, 2002. **70**(1): p. 121-126.
137. Oude Elferink, R.P., et al., *Regulation of biliary lipid secretion by mdr2 P-glycoprotein in the mouse*. The Journal of Clinical Investigation, 1995. **95**(1): p. 31-38.

138. Klappenbach, J.A., J.M. Dunbar, and T.M. Schmidt, *rRNA Operon Copy Number Reflects Ecological Strategies of Bacteria*. Applied and Environmental Microbiology, 2000. **66**(4): p. 1328-1333.
139. Miura, A., et al., *Growth-rate-dependent regulation of ribosome synthesis in E. coli: Expression of the lacZ and galK genes fused to ribosomal promoters*. Cell, 1981. **25**(3): p. 773-782.
140. Sarmientos, P. and M. Cashel, *Carbon starvation and growth rate-dependent regulation of the Escherichia coli ribosomal RNA promoters: differential control of dual promoters*. Proceedings of the National Academy of Sciences, 1983. **80**(22): p. 7010-7013.
141. Nomura, M., R. Gourse, and G. Baughman, *Regulation of the Synthesis of Ribosomes and Ribosomal Components*. Annual Review of Biochemistry, 1984. **53**(1): p. 75-117.
142. Gourse, R.L., H.A. de Boer, and M. Nomura, *DNA determinants of rRNA synthesis in E. coli: Growth rate dependent regulation, feedback inhibition, upstream activation, antitermination*. Cell, 1986. **44**(1): p. 197-205.
143. Condon, C., C. Squires, and C.L. Squires, *Control of ribosomal-RNA Transcription in Escherichia coli*. Microbiological Reviews, 1995. **59**(4): p. 623-&.
144. Gourse, R.L., et al., *Rrna transcription and growth rate-dependent regulation of ribosome synthesis in Escherichia coli*. Annual Review of Microbiology, 1996. **50**: p. 645-677.
145. Schneider, D.A., W. Ross, and R.L. Gourse, *Control of rRNA expression in Escherichia coli*. Current Opinion in Microbiology, 2003. **6**(2): p. 151-156.
146. Jin, D.J., C. Cagliero, and Y.N. Zhou, *Growth rate regulation in Escherichia coli*. Fems Microbiology Reviews, 2012. **36**(2): p. 269-287.
147. Svitil, A.L., M. Cashel, and J.W. Zyskind, *Guanosine tetraphosphate inhibits protein synthesis in vivo. A possible protective mechanism for starvation*

- stress in Escherichia coli*. Journal of Biological Chemistry, 1993. **268**(4): p. 2307-11.
148. Traxler, M.F., et al., *The global, ppGpp-mediated stringent response to amino acid starvation in Escherichia coli*. Molecular Microbiology, 2008. **68**(5): p. 1128-1148.
  149. Potrykus, K. and M. Cashel, *(p)ppGpp: Still Magical?* Annual Review of Microbiology, 2008. **62**: p. 35-51.
  150. Srivatsan, A. and J.D. Wang, *Control of bacterial transcription, translation and replication by (p)ppGpp*. Current Opinion in Microbiology, 2008. **11**(2): p. 100-105.
  151. Kriel, A., et al., *Direct Regulation of GTP Homeostasis by (p)ppGpp: A Critical Component of Viability and Stress Resistance*. Molecular Cell, 2012. **48**(2): p. 231-241.
  152. Kahm, M., et al., *grofit: Fitting Biological Growth Curves with R*. Journal of Statistical Software, 2010. **33**(7): p. 1-21.
  153. R Development Core Team, *R: A language and environment for statistical computing*. 2008, R Foundation for Statistical Computing Vienna, Austria.
  154. Stokke, C., T. Waldminghaus, and K. Skarstad, *Replication patterns and organization of replication forks in Vibrio cholerae*. Microbiology, 2011. **157**(3): p. 695-708.
  155. Merritt, J.H., et al., *Specific Control of Pseudomonas aeruginosa Surface-Associated Behaviors by Two c-di-GMP Diguanylate Cyclases*. mBio, 2010. **1**(4).
  156. Kader, A., et al., *Hierarchical involvement of various GGDEF domain proteins in rdar morphotype development of Salmonella enterica serovar Typhimurium*. Molecular Microbiology, 2006. **60**(3): p. 602-616.

157. Stevenson, B.S. and T.M. Schmidt, *Life History Implications of rRNA Gene Copy Number in Escherichia coli*. Applied and Environmental Microbiology, 2004. **70**(11): p. 6670-6677.
158. Ross, W., et al., *The Magic Spot: A ppGpp Binding Site on E. coli RNA Polymerase Responsible for Regulation of Transcription Initiation*. Molecular Cell, 2013. **50**(3): p. 420-429.
159. Krásný, L. and R. Gourse, *An alternative strategy for bacterial ribosome synthesis: Bacillus subtilis rRNA transcription regulation*. The EMBO Journal, 2004. **23**(22): p. 4473-83.
160. Anderson, J.D., et al., *Role of bacterial growth rates in the epidemiology and pathogenesis of urinary infections in women*. Journal of Clinical Microbiology, 1979. **10**(6): p. 766-771.
161. Klumpp, S., Z.G. Zhang, and T. Hwa, *Growth Rate-Dependent Global Effects on Gene Expression in Bacteria*. Cell, 2009. **139**(7): p. 1366-1375.
162. Hartman, Z.C., D.M. Appledorn, and A. Amalfitano, *Adenovirus vector induced innate immune responses: Impact upon efficacy and toxicity in gene therapy and vaccine applications*. Virus Research, 2008. **132**(1-2): p. 1-14.
163. Aldhamen, Y.A., S.S. Seregin, and A. Amalfitano, *Immune recognition of gene transfer vectors: focus on adenovirus as a paradigm*. Frontiers in immunology, 2011. **2**(40): p. 1-12.
164. Fukazawa, T., et al., *Adenovirus-mediated cancer gene therapy and virotherapy (Review)*. International Journal of Molecular Medicine, 2010. **25**(1): p. 3-10.
165. Seregin, S.S., et al., *Use of DAF-Displaying Adenovirus Vectors Reduces Induction of Transgene- and Vector-Specific Adaptive Immune Responses in Mice*. Human Gene Therapy, 2010. **22**(9): p. 1083-1094.
166. Seregin, S.S., et al., *CR1/2 is an important suppressor of Adenovirus-induced innate immune responses and is required for induction of neutralizing antibodies*. Gene Therapy, 2009. **16**(10): p. 1245-1259.

167. Seregin, S.S., et al., *Adenovirus capsid-display of the retro-oriented human complement inhibitor DAF reduces Ad vector-triggered immune responses in vitro and in vivo*. *Blood*, 2010. **116**(10): p. 1669-1677.
168. Amalfitano, A., et al., *Production and Characterization of Improved Adenovirus Vectors with the E1, E2b, and E3 Genes Deleted*. *Journal of Virology*, 1998. **72**(2): p. 926-933.
169. Morgan, J., P. Ng, and F. Graham, *Construction of First-Generation Adenoviral Vectors*, in *Gene Therapy Protocols*. 2002, Springer New York. p. 389-414.
170. Seregin, S.S., et al., *Adenovirus-based vaccination against Clostridium difficile toxin A allows for rapid humoral immunity and complete protection from toxin A lethal challenge in mice*. *Vaccine*, 2012. **30**(8): p. 1492-1501.
171. Seregin, S.S., et al., *Transient Pretreatment With Glucocorticoid Ablates Innate Toxicity of Systemically Delivered Adenoviral Vectors Without Reducing Efficacy*. *Molecular Therapy*, 2009. **17**(4): p. 685-696.
172. Appledorn, D.M., et al., *Wild-type adenoviruses from groups A-F evoke unique innate immune responses, of which HAd3 and SAd23 are partially complement dependent*. *Gene Therapy*, 2008. **15**(12): p. 885-901.
173. Theriot, C.M., et al., *Cefoperazone-treated mice as an experimental platform to assess differential virulence of Clostridium difficile strains*. *Gut Microbes*, 2011. **2**(6): p. 326-334.
174. Reeves, A.E., et al., *The interplay between microbiome dynamics and pathogen dynamics in a murine model of Clostridium difficile Infection*. *Gut Microbes*, 2011. **2**(3): p. 145-158.
175. Nakhamchik, A., C. Wilde, and D.A. Rowe-Magnus, *Cyclic-di-GMP regulates extracellular polysaccharide production, biofilm formation, and rugose colony development by Vibrio vulnificus*. *Applied and Environmental Microbiology*, 2008. **74**(13): p. 4199-4209.

176. Thormann, K.M., et al., *Control of formation and cellular detachment from Shewanella oneidensis MR-1 biofilms by cyclic di-GMP*. Journal of Bacteriology, 2006. **188**(7): p. 2681-2691.
177. Everett, R.S., et al., *Liver Toxicities typically induced by first-generation adenoviral vectors can be reduced by use of E1, E2b-deleted adenoviral vectors*. Human Gene Therapy, 2003. **14**(18): p. 1715-1726.
178. Nakamura, T., K. Sato, and H. Hamada, *Reduction of natural adenovirus tropism to the liver by both ablation of fiber-coxsackievirus and adenovirus receptor interaction and use of replaceable short fiber*. Journal of Virology, 2003. **77**(4): p. 2512-2521.
179. Tanaka, Y. and Z.J. Chen, *STING Specifies IRF3 Phosphorylation by TBK1 in the Cytosolic DNA Signaling Pathway*. Science Signaling, 2012. **5**(214): p. ra20-.
180. de Almeida, L.A., et al., *MyD88 and STING Signaling Pathways Are Required for IRF3-Mediated IFN- $\alpha$  Induction in Response to Brucella abortus Infection*. PLoS ONE, 2011. **6**(8): p. e23135.
181. Lucado, J., C. Gould, and A. Elixhauser, *Clostridium difficile Infections (CDI) in Hospital Stays, 2009*, in *HCUP Statistical Brief*. 2012, Agency for Healthcare Research and Quality: Rockville, MD.
182. Morris, A.M., et al., *Clostridium difficile colitis: An increasingly aggressive iatrogenic disease?* Archives of Surgery, 2002. **137**(10): p. 1096-1100.
183. Redelings, M.D., F. Sorvillo, and L. Mascola, *Increase in Clostridium difficile-related mortality rates, United States, 1999-2004*. 2007, Emerg Infect Dis.
184. Kyne, L., et al., *Health Care Costs and Mortality Associated with Nosocomial Diarrhea Due to Clostridium difficile*. Clinical Infectious Diseases, 2002. **34**(3): p. 346-353.

185. Dubberke, E.R. and A.I. Wertheimer, *Review of Current Literature on the Economic Burden of Clostridium difficile Infection*. Infection Control and Hospital Epidemiology, 2009. **30**(1): p. 57-66.
186. Aslam, S., R.J. Hamill, and D.M. Musher, *Treatment of Clostridium difficile-associated disease: old therapies and new strategies*. The Lancet Infectious Diseases, 2005. **5**(9): p. 549-557.
187. Cartman, S.T., et al., *The emergence of 'hypervirulence' in Clostridium difficile*. International Journal of Medical Microbiology, 2010. **300**(6): p. 387-395.
188. Reed, S.G., et al., *New horizons in adjuvants for vaccine development*. Trends in Immunology, 2009. **30**(1): p. 23-32.
189. Zandman-Goddard, G. and Y. Shoenfeld, *Infections and SLE*. Autoimmunity, 2005. **38**(7): p. 473-485.
190. Wolins, N., et al., *Intravenous administration of replication-incompetent adenovirus to rhesus monkeys induces thrombocytopenia by increasing in vivo platelet clearance*. British Journal of Haematology, 2003. **123**(5): p. 903-905.
191. Appledorn, D.M., et al., *Complex interactions with several arms of the complement system dictate innate and humoral immunity to adenoviral vectors*. Gene Therapy, 2008. **15**(24): p. 1606-1617.
192. Schiedner, G., S. Hertel, and S. Kochanek, *Efficient transformation of primary human amniocytes by E1 functions of Ad5: Generation of new cell lines for adenoviral vector production*. Human Gene Therapy, 2000. **11**(15): p. 2105-2116.
193. Barker, J.R., et al., *STING-Dependent Recognition of Cyclic di-AMP Mediates Type I Interferon Responses during Chlamydia trachomatis Infection*. mBio, 2013. **4**(3).

194. Woodward, J.J., A.T. Iavarone, and D.A. Portnoy, *c-di-AMP Secreted by Intracellular Listeria monocytogenes Activates a Host Type I Interferon Response*. *Science*, 2010. **328**(5986): p. 1703-1705.
195. Dunn, A.K., et al., *New rfp- and pES213-derived tools for analyzing symbiotic Vibrio fischeri reveal patterns of infection and lux expression in situ*. *Applied and Environmental Microbiology*, 2006. **72**(1): p. 802-810.
196. Lenz, D.H., et al., *CsrA and three redundant small RNAs regulate quorum sensing in Vibrio cholerae*. *Molecular Microbiology*, 2005. **58**(4): p. 1186-1202.